UNIVERSITY OF CINCINNATI

May 25 , 20 01

I, William A. Fladung, Jr. **,**

hereby submit this as part of the requirements for the degree of:

Doctorate of Philosophy

in:

Mechanical Engineering

It is entitled:

A GENERALIZED RESIDUALS MODEL FOR THE UNIFIED MATRIX POLYNOMIAL APPROACH TO FREQUENCY DOMAIN MODAL PARAMETER ESTIMATION

Approved by:

Robert W. Rost, Ph.D.

Randall J. Allemang, Ph.D.

David L. Brown, Ph.D.

Allyn W. Phillips, Ph.D.

A GENERALIZED RESIDUALS MODEL FOR THE UNIFIED MATRIX POLYNOMIAL APPROACH TO FREQUENCY DOMAIN MODAL PARAMETER ESTIMATION

A dissertation submitted to the

Division of Research and Advanced Studies
of the University of Cincinnati

in partial fulfillment of the
requirements for the degree of

DOCTORATE OF PHILOSOPHY

in the Department of Mechanical, Industrial and Nuclear Engineering
of the College of Engineering

2001

by

William A. Fladung, Jr.

B.S.M.E., University of Cincinnati, 1990
M.S., University of Cincinnati, 1994

Dr. Robert W. Rost, Committee Chair

ABSTRACT

The purpose of this dissertation is twofold: to generalize residuals for frequency domain modal parameter estimation and to introduce the notion of a consistency diagram for residuals. The frequency response of a system is the superposition of an infinite number of individual modes that have contribution at all frequency. Residuals are simplified expressions included in an FRF model to account for the influence of modes outside the frequency range of interest. The development of most frequency domain algorithms have had some consideration of residuals, but only as fixed set of terms. A consistency diagram, which is a widely popular technique in modal parameter estimation, has historically been generated by varying only the number of poles in the model. However, there are other conditions of the parameter estimation process, such as the residuals, that can be varied to produce consistent estimates of the system poles.

An overview of the residual models and applications of the past illustrates the sometimes conflicting opinions of residuals and the need for a more systematic approach. The limitations of the traditional, physical residual model are established, which verifies that a more generalized residual model is justified. A power polynomial of frequency, with both positive and negative orders, is proposed, developed and implemented as a generalized residual model for frequency domain modal parameter estimation. It is demonstrated that a polynomial function is able to sufficiently describe the off-resonance frequency response characteristics, and thus model the residual effects. The generalized residual

polynomial is then combined with the rational fraction polynomial FRF model to derive the frequency domain UMPA model with generalized residuals.

While most of the emphasis is on frequency domain pole estimation, algorithms for residue estimation with generalized residuals are also given. In addition, a method for determining the residues directly from the UMPA model poles and numerator polynomial coefficients is developed. A procedure is also derived to deconvolve the estimated denominator polynomial coefficients into their constituent parts.

The concept of a consistency diagram has been extended allowing other conditions of the parameter estimation process, namely the residuals, to be varied. In methods such as CMIF and EMIF, the model order is fixed, but a consistency diagram for residuals is implemented. For the general UMPA model, both the denominator and numerator model order is varied in different permutations to generate a consistency diagram and pole surface diagram. The ideas introduced in this dissertation should lead to further study of other variable conditions in the parameter estimation process.

THIS PAGE INTENTIONALLY LEFT BLANK

ACKNOWLEDGMENTS

At long last there is an answer to the question I have frequently been asked: “So, when are you going to be done?” To all of those whom may wonder why it took me so long to finish, all I can say is that I guess I’m just a slow-learner. That and possibly the many opportunities to do so many other things while at SDRL, such as, taking one more set of data on a test trip, writing papers and attending conferences, working on projects with people in industry, or traveling to far away and exotic, as well as nearer and not as exotic, places. The SDRL graduate experience is truly unique and rewarding. Because as it says on our coffee mugs: “It’s not just a degree, it’s an adventure.”

I would like to offer my gratitude to SDRL for all of the opportunities and experiences afforded me during my stay. I would also like to acknowledge the following people: my dissertation committee, Bob Rost, Randy Allemang, Dave Brown and Allyn Phillips, for all of their assistance and guidance in getting this thing done; Boeing and Manta for support on X-Modal II software development contracts; The Modal Shop for providing some consulting jobs so I could supplement my lavish graduate-student lifestyle; Rhonda Christman, who keeps the lab running; my fellow grad students in the lab who have become friends, in order of height: Dan Lazor, Jason Blough, Matt Witter, John Schultze, Tom Terrell, Jeremy Williams and Susan Dumbacher; and, of course, to my family for their continuing support, encouragement ... and patience, they stopped asking when I’d be done a while ago.

CONTENTS

List of Figures 3

List of Tables 8

Nomenclature 9

1 Introduction 15

1.1 Overview of the Frequency Domain Unified Matrix Polynomial Approach to Modal Parameter Estimation 16

1.2 Frequency Response Function Models 18

1.3 Literature Review 22

1.4 Objectives of Dissertation 33

2 Theory 34

2.1 Derivation and Limitation of the Physical Residual Model 35

2.2 Power Polynomial Residual Model 39

2.3 Rational Fraction Polynomial Model with Generalized Residuals 50

2.3.1 Defining the Orders of the Generalized Residual Polynomial 52

2.3.2 Deconvolving the Coefficients of the Numerator Polynomial 54

2.4 Frequency Domain UMPA Model with Generalized Residuals 56

2.5 Relationship of Zeros and Residuals 57

2.6 The Consistency Diagram 59

3 Applications 64
3.1 Single Degree-of-Freedom Parameter Estimation Methods 65
3.2 Complex Mode Indicator Function Parameter Estimation Method 74
3.3 Enhanced Mode Indicator Function Parameter Estimation Method 85
3.4 Unified Matrix Polynomial Approach Parameter Estimation Method 96
4 Conclusion 103
4.1 Summary of Dissertation 104
4.2 Recommendations for Future Work 109
References 112
A Residue Estimation 118
A.1 Residue Estimation from the Partial Fraction Model 119
A.2 Residue Estimation from the Rational Fraction Polynomial Model 122
A.3 Residue Estimation with Scaled Frequency 129
B Polynomial Curve-Fit Plots 130
C MATLAB Functions 138

LIST OF FIGURES

1-1 Superposition of SDOF modes to form an MDOF FRF. 20

2-1 Relationship of the residual modes and the in-band modes. 36

2-2(a) Limitations of the physical residual model assumptions. 37

2-2(b) Relative error of the SDOF FRF asymptote and upper residual. 38

2-2(c) Relative error of the SDOF FRF asymptote and lower residual. 39

2-3(a) Positive-order polynomial terms, evaluated for orders 0,1,2,3,4. 41

2-3(b) Negative-order polynomial terms, evaluated for orders 0,-1,-2,-3,-4. 41

2-4 Polynomial curve-fit with orders 0:4 of the upper residual segment of an FRF away from resonance. 44

2-5 Polynomial curve-fit with orders 0:12 of the upper residual segment of an FRF near resonance. 44

2-6 Polynomial curve-fit with orders -4:0 of the lower residual segment of an FRF away from resonance. 45

2-7 Polynomial curve-fit with orders -12:0 of the lower residual segment of an FRF near resonance. 45

2-8 Polynomial curve-fit with orders -4:4 of the FRF segment between two resonances without an antiresonance. 46

2-9 Polynomial curve-fit with orders -4:4 of the FRF segment between two resonances with an antiresonance. 46

2-10 Polynomial curve-fit with orders -4:4 of an FRF segment at a resonance. . . . 47

2-11 Summation of three SDOF modes (dotted lines) to form an MDOF FRF (solid line). 49

2-12 Polynomial curve-fit with orders -4:4 of residual contributions in the region around a single mode. 49

2-13 Consistency Diagram and Legend. 61

3-1(a) Comparison of a 3-DOF analytical FRF (dashed line) and the FRF synthesized from estimated polynomial coefficients (solid line), with no residuals. 68

3-2(a) Comparison of a 3-DOF analytical FRF (dashed line) and the FRF synthesized from estimated polynomial coefficients (solid line), with physical residuals. 68

3-2(b) Magnitude of residual polynomial coefficients for Figure 3-2(a). 69

3-3(a) Comparison of a 3-DOF analytical FRF (dashed line) and the FRF synthesized from estimated polynomial coefficients (solid line), with a generalized residual polynomial of orders -4:4. 69

3-3(b) Magnitude of residual polynomial coefficients for Figure 3-3(a). 69

3-3(c) Comparison of a 3-DOF analytical FRF (dashed line) and the FRF synthesized from estimated and deconvolved polynomial coefficients (solid line), with a generalized residual polynomial of orders -4:4. 70

3-3(d) Comparison of the generalized residual polynomial with orders -4:4 to the contribution of the residual modes. 70

3-4(a) Comparison of a 3-DOF analytical FRF (dashed line) and the FRF synthesized from estimated polynomial coefficients (solid line), with no residuals. 72

3-5(a) Comparison of a 3-DOF analytical FRF (dashed line) and the FRF synthesized from estimated polynomial coefficients (solid line), with physical residuals. 72

3-5(b). Magnitude of residual polynomial coefficients for Figure 3-5(a). 73

3-6(a) Comparison of a 3-DOF analytical FRF (dashed line) and the FRF synthesized from estimated polynomial coefficients (solid line), with a generalized residual polynomial of orders -12:12. 73

3-6(b) Magnitude of residual polynomial coefficients for Figure 3-6(a). 73

3-7 Complex mode indicator function of a measured FRF dataset. 76

3-8 Enhanced frequency response function for the mode at 125 Hz; generated from measured FRFs (dashed line) and synthesized from UMPA model (solid line). 78

3-9 Enhanced frequency response function for the mode at 97 Hz. 80

3-10(a) CMIF method consistency diagram of the mode at 97 Hz, for varying the lower order of the residual polynomial. 81

3-10(b) CMIF method consistency diagram of the mode at 97 Hz, for varying the upper order of the residual polynomial. 81

3-10(c) CMIF method consistency diagram of the mode at 97 Hz, for varying the lower and upper orders of the residual polynomial. 82

3-11 Enhanced frequency response function for the mode at 97 Hz; generated from measured FRFs (solid line) and synthesized from UMPA model for all residual polynomials of the consistency diagram in Figure 3-10(c) (dashed lines). 83

3-12 Enhanced frequency response function for the mode at 97 Hz; generated from measured FRFs (dashed line) and synthesized from UMPA model variation 5 in Figure 3-10(c) (solid line). 83

3-13 CMIF method consistency diagram of the mode at 125 Hz. 84

3-14 Complex mode indicator function of a measured FRF dataset with a frequency band of interest. 89

3-15 EMIF method consistency diagram for the frequency band in Figure 3-14. . . . 89

3-16 Complex mode indicator function reconstructed from the EMIF model (solid lines) and of the measured FRF dataset (dashed lines). 91

3-17 Complex mode indicator function of a measured FRF dataset with a frequency band of interest. 93

3-18 EMIF method enhanced frequency response functions for condensation with two left singular vectors. 93

3-19 EMIF method consistency diagram for the frequency band in Figure 3-17 for condensation with two left singular vectors. 94

3-20 EMIF method enhanced frequency response functions for condensation with one left singular vector. 94

3-21 EMIF method consistency diagram for the frequency band in Figure 3-17 for condensation with one left singular vector. 95

3-22 Complex mode indicator function reconstructed from the EMIF model (solid line) and of the measured FRF dataset (dashed lines). 95

3-23 Consistency diagram of a low-order UMPA model, for varying the β-order. . . . 98

3-24 Consistency diagram of a high-order UMPA model, for varying the α-order, with no residuals. 99

3-25(a) Consistency diagram of a high-order UMPA model, for varying the β-order then the α-order. 99

3-25(b) Consistency diagram of a high-order UMPA model, for varying the α-order then the β-order. 100

3-25(c) Consistency diagram of a high-order UMPA model, for varying the α-order then the β-order, with resetting the consistency evaluation. 100

3-26(a) Pole surface consistency for the model variations of the consistency diagram in Figure 3-25(a). 101

3-26(a) Pole surface density for the high-order UMPA model variations in Figures 3-25(a-c). 102

B-1 Polynomial curve-fit with orders 0:4 of the upper residual segment of an FRF away from resonance, ref. Figure 2-4. 131

B-2 Polynomial curve-fit with orders 0:12 of the upper residual segment of an FRF near resonance, ref. Figure 2-5. 132

B-3 Polynomial curve-fit with orders -4:0 of the lower residual segment of an FRF away from resonance, ref. Figure 2-6. 133

B-4 Polynomial curve-fit with orders -12:0 of the lower residual segment of an FRF near resonance, ref. Figure 2-7. 134

B-5 Polynomial curve-fit with orders -4:4 of the FRF segment between two resonances without an antiresonance, ref. Figure 2-8. 135

B-6 Polynomial curve-fit with orders -4:4 of the FRF segment between two resonances with an antiresonance, ref. Figure 2-9. 136

B-7 Polynomial curve-fit with orders -4:4 of an FRF segment at a resonance, ref. Figure 2-10. 137

LIST OF TABLES

1-1 Matrix sizes of the UMPA model coefficients. 16

3-1 Estimated modal parameters of 3-DOF system. 71

3-2 Estimated modal parameters of 3-DOF system. 74

3-3 The lower and upper orders of the residual polynomial for the model variations of the consistency diagrams in Figures 3-10(a-c). 81

3-4 The estimated poles for the model variations of the consistency diagram in Figure 3-10(c). 82

3-5 The lower and upper orders of the residual polynomial and the estimated poles for the model variations of the consistency diagram in Figure 3-13. 84

3-6 The residual polynomial orders and estimated poles for the model variations of the consistency diagram in Figure 3-15. 90

3-7 The UMPA model denominator order and the generalized residual polynomial lower and upper orders for the model variations of the consistency diagrams in Figures 3-23 through 3-25. 97

NOMENCLATURE

Matrix and Operator Notation

$[\cdot\cdot]$	matrix enclosed by brackets
$[\cdot\cdot]_{(m\times n)}$ *or* $\underset{(m\times n)}{[\cdot\cdot]}$	size of a matrix (m rows by n columns)
$[\cdot\cdot]^T$	transpose of a matrix
$[\cdot\cdot]^H$	Hermitian, or conjugate transpose, of a matrix
$[\cdot\cdot]^{-1}$	inverse of a matrix
$[\cdot\cdot]^+$	pseudo-inverse of a matrix
$\lceil\cdot\cdot\rfloor$	diagonal matrix
$\{\cdot\cdot\}$	vector enclosed by braces
A^*	complex conjugate of A
$\sum_{k=a}^{b} A_k$	summation of A_k for $k=a$ to b
det$([\cdot\cdot])$	determinate of a matrix
adj$([\cdot\cdot])$	adjoint of a matrix
svd$([\cdot\cdot])$	singular value decomposition of a matrix

Roman Alphabet

A_{pqr}	residue for output DOF p, input DOF q, of mode r
A_r	residue of a SISO FRF of mode r
$A_r^{'}$	residue of mode r in the scaled-frequency domain

$[A_r]$	residue matrix of mode r
C	damping of single degree-of-freedom mode
$[C]$	companion matrix
$eH(\omega)$	enhanced frequency response function
$eH_s(\omega_k)$	enhanced frequency response function for mode s, at spectral line k
$[e\bar{H}(\omega_k)]$	enhanced frequency response function matrix, at spectral line k
$[H(\omega_k)]$	frequency response function matrix at spectral line k
$H_{pq}(\omega)$	frequency response function for output DOF p, input DOF q
$\{H_p(\omega)\}$	row of frequency response function matrix for output DOF p
$H(s)$	transfer function
$[I_n]$ *or* I_n	$n \times n$ identity matrix
j	$\sqrt{-1}$
K	stiffness of single degree-of-freedom mode
L_{qr}	modal participation factor for input DOF q, of mode r
$\{L_r\}$	vector of modal participation factors, of mode r
$[L]$	matrix of modal participation factors
M	mass of single degree-of-freedom mode
$\bar{\boldsymbol{m}}$	maximum index of denominator polynomial, for all system modes
m	maximum index of denominator polynomial, for in-band modes
n_l	lower index limit of the residual polynomial
n_u	upper index limit of the residual polynomial
$\bar{\boldsymbol{N}}$	total number of system modes
N	number of modes in the frequency range of interest

N_a	size of $[a_k]$ polynomial coefficient matrix
N_b	number of modes in EMIF frequency band
N_i	number of input DOFs
N_o	number of output DOFs
N_s	number of spectral lines
N_v	number of vectors in EMIF frequency band
p	output DOF (subscript)
q	input DOF (subscript)
r	mode number (subscript)
R_k	k^{th}-order generalized residual polynomial coefficient
R_{pqk}	k^{th}-order generalized residual polynomial coefficient for output DOF p, input DOF q
$\{R_{pk}\}$	k^{th}-order generalized residual polynomial coefficient vector for output DOF p
$[R_k]$	k^{th}-order generalized residual polynomial coefficient matrix
$[\hat{R}_k]$	k^{th}-order generalized residual polynomial coefficient matrix convolved with denominator polynomial
$[R_l(\omega)]$	lower residual function
$[R_u(\omega)]$	upper residual function
$[R_{l,k}]$	k^{th}-order lower residual polynomial coefficient matrix
$[R_{u,k}]$	k^{th}-order upper residual polynomial coefficient matrix
s	Laplace domain variable (*rad*/*sec*)
s'	Laplace scaled-frequency domain variable (*rad*/*sec*)
$[U]$	matrix of left singular vectors

$[U_b]$	matrix of left singular vectors for EMIF condensation
$[U_k]$	matrix of left singular vectors, at spectral line k
$\{U_s\}$	left singular vector for mode s
$[V]$	matrix of right singular vectors
$[V_k]$	matrix of right singular vectors, at spectral line k
$\{V_s\}$	right singular vector for mode s
$\{X_r\}$	eigenvector of companion matrix for mode r

Greek Alphabet

a_k	k^{th}-order denominator polynomial coefficient
$a_{r,k}$	k^{th}-order denominator polynomial coefficient, of mode r
$[a_k]$	k^{th}-order denominator polynomial coefficient matrix
β_k	k^{th}-order numerator polynomial coefficient
$\beta_{r,k}$	k^{th}-order numerator polynomial coefficient, of mode r
$[\beta_k]$	k^{th}-order numerator polynomial coefficient matrix
$[\hat{\beta}_k]$	k^{th}-order numerator polynomial coefficient matrix combined with generalized residual polynomial
$\hat{\beta}_k$	k^{th}-order numerator polynomial coefficient combined with generalized residual polynomial
$[\tilde{\beta}_k]$	k^{th}-order numerator polynomial coefficient, in Equations A-20 and A-22
λ_r	complex pole of mode r ; $\lambda_r = \sigma_r + j\omega_r$
λ_r'	complex pole of mode r in the scaled-frequency domain
$\lceil \Lambda_r \rfloor$	diagonal matrix of pole λ_r
$\lceil \bar{\Lambda}_i \rfloor^k$	diagonal matrix of permutations of k^{th}-products of poles, excluding λ_i

σ_r	damping factor of mode *r*
$\lceil\Sigma\rfloor$	matrix of singular values
$\lceil\Sigma_k\rfloor$	matrix of singular values, at spectral line*k*
ω	variable of frequency (*rad*/*sec*)
ω'	variable of scaled-frequency (*rad*/*sec*)
$\bar{\omega}$	scaling frequency (*rad*/*sec*)
ω_k	frequency at spectral line *k*
ω_r	damped natural frequency of mode *r*
ψ_{pr}	modal coefficient residue for output DOF *p* of mode *r*
$\{\psi_p\}$	vector of modal coefficients of all modes for output DOF *p*
$\{\psi_r\}$	modal vector of mode *r*
$\{\Psi_r\}$	modal vector or participation factor of UMPA modal for mode *r*

Abbreviations

α-order	the highest order of the UMPA model denominator polynomial
β-orders	the orders, from the lowest to the highest, of the UMPA model numerator polynomial which includes generalized residuals

Acronyms

CMIF	Complex Mode Indicator Function
DOF	Degree-of-Freedom
eFRF	Enhanced Frequency Response Function
EMIF	Enhanced Mode Indicator Function
FRF	Frequency Response Function

MAC	Modal Assurance Criteria
MDOF	Multiple Degree-of-Freedom
MIMO	Multiple-Input Multiple-Output
SDOF	Single Degree-of-Freedom
SISO	Single-Input Single-Output
SVD	Singular Value Decomposition
UMPA	Unified Matrix Polynomial Approach

CHAPTER ONE

1 Introduction

Many parameter estimation algorithms have been developed over the past two and a half decades: time and frequency domain algorithms, high- and low-order models, single and multiple degrees-of-freedom, single and multiple references, local and global methods, matrix and iterative solutions. Great effort has been put into the underlying, single most important problem in using any of the parameter estimation algorithms, determining the proper model order[1]. Almost all the emphasis has been in determining the order of the α-polynomial, which together with the size of the matrix coefficients determines the number of poles of the model. The α-polynomial is the denominator of the rational fraction model and forms the characteristic equation of the model. However, on the other side of the equation, the order of the β-polynomial has received only a cursory consideration. The β-side of the equation, that is, the numerator of the rational fraction model, describes the zeros of the model, which represent the residues and residuals, and is the primary focus of this dissertation.

1.1 Overview of the Frequency Domain Unified Matrix Polynomial Approach to Modal Parameter Estimation

The Unified Matrix Polynomial Approach[1] (UMPA) is a consolidated formulation of all of the time, frequency and spatial domain modal parameter estimation algorithms. The frequency domain UMPA model can be derived by rearranging the rational fraction polynomial model of a multiple-input, multiple-output (MIMO) frequency response function (FRF) matrix as

$$\sum_{k=0}^{m}\left[(j\omega)^k[a_k]\right][H(\omega)] = \sum_{k=0}^{m-2}(j\omega)^k[\beta_k] \tag{1-1}$$

Some of the fundamental properties of the frequency domain UMPA model are summarized below. A low-order model has $m = 2$, or $m = 1$ for the equivalent state-space formulation, and a high-order model has $m > 2$. A low-order model is typically used when the spatial information is complete and a high-order model is used when the spatial domain is undersampled.[1] If the FRF matrix $[H(\omega)]$ is $N_o \times N_i$, where N_o is the number of output DOFs and N_i is the number of input DOFs, the sizes of the low- and high-order UMPA model coefficient matrices are as given below in Table 1-1.

UMPA model	$N_i < N_o$	$[a_k]$	$[\beta_k]$	$N_i > N_o$	$[a_k]$	$[\beta_k]$
low-order	$[H(\omega_k)]$	$N_o \times N_o$	$N_o \times N_i$	$[H(\omega_k)]^T$	$N_i \times N_i$	$N_i \times N_o$
high-order	$[H(\omega_k)]^T$	$N_i \times N_i$	$N_i \times N_o$	$[H(\omega_k)]$	$N_o \times N_o$	$N_o \times N_i$

Table 1-1. *Matrix sizes of the UMPA model coefficients.*

Equation 1-1 is linear in the unknown $[a_k]$ and $[\beta_k]$ coefficient matrices, and since it is a homogeneous equation, any coefficient may be chosen arbitrarily. Letting $[a_m]$ be an identity matrix and rearranging yields a linear matrix equation

$$\sum_{k=0}^{m-1}\left[(j\omega)^k[a_k]\right][H(\omega)] - \sum_{k=0}^{m-2}(j\omega)^k[\beta_k] = -(j\omega)^m[H(\omega)] \tag{1-2}$$

or in matrix form

$$\begin{bmatrix} [a_0] & [a_1] & \cdots & [a_{m-1}] & [\beta_0] & \cdots & [\beta_{m-2}] \end{bmatrix} \begin{bmatrix} [H(\omega)] \\ j\omega[H(\omega)] \\ \vdots \\ (j\omega)^{m-1}[H(\omega)] \\ [I_\beta] \\ \vdots \\ -(j\omega)^{m-2}[I_\beta] \end{bmatrix} = -(j\omega)^m[H(\omega)] \tag{1-3}$$

Note that Equation 1-3 is actually the transpose of the more common $[A]\{x\} = \{b\}$ linear system of equations. To solve for the coefficient matrices, an overdetermined set of equations is generated by evaluating Equation 1-3 at a number of frequencies. The scaled identity matrix $[I_\beta]$ is $N_i \times N_i$ if $[\beta_k]$ is $N_o \times N_i$ or $N_o \times N_o$ if $[\beta_k]$ is $N_i \times N_o$. This matrix is typically scaled by the maximum of the FRF magnitudes contained in the set of equations to more equally weight the $[a_k]$ and $[\beta_k]$ coefficient matrices in the solution.[3] Positive and negative frequencies are included in the set of equations to estimate conjugate poles and the frequency values are typically scaled to improve the numerical conditioning of the solution.[3] The system poles are the eigenvalues of the companion matrix $[C]$ formed with the $[a_k]$ coefficient matrices.

$$[C] = \begin{bmatrix} -[a_{m-1}] & -[a_{m-2}] & -[a_{m-3}] & \cdots & \cdots & -[a_2] & -[a_1] & -[a_0] \\ [I] & [0] & [0] & \cdots & \cdots & [0] & [0] & [0] \\ [0] & [I] & [0] & \cdots & \cdots & [0] & [0] & [0] \\ [0] & [0] & [I] & \cdots & \cdots & [0] & [0] & [0] \\ \vdots & \vdots & \vdots & \vdots & \vdots & \vdots & \vdots & \vdots \\ [0] & [0] & [0] & \cdots & \cdots & [0] & [0] & [0] \\ [0] & [0] & [0] & \cdots & \cdots & [I] & [0] & [0] \\ [0] & [0] & [0] & \cdots & \cdots & [0] & [I] & [0] \end{bmatrix} \tag{1-4}$$

The eigenvector associated with eigenvalue r of the companion matrix has the form

$$\{X_r\} = \begin{Bmatrix} \lambda_r^{m-1}\{\Psi_r\} \\ \lambda_r^{m-2}\{\Psi_r\} \\ \vdots \\ \lambda_r\{\Psi_r\} \\ \{\Psi_r\} \end{Bmatrix} \tag{1-5}$$

where the length $\{\Psi_r\}$ is equal to the size of the $[a_k]$ coefficient matrices. For a low-order model $\{\Psi_r\}$ is a modal vector and for a high-order model $\{\Psi_r\}$ is a modal participation vector.

1.2 Frequency Response Function Models

Modal parameter estimation is defined in Ref. [1] as "a special case of system identification where the *a priori* model of the system is known to be in the form of modal parameters." The MIMO FRF model can be formulated as the partial fraction, or modal, model

$$[H(\omega)] = \sum_{r=1}^{\tilde{N}} \left(\frac{[A_r]}{j\omega - \lambda_r} + \frac{[A_r^*]}{j\omega - \lambda_r^*} \right) \tag{1-6}$$

which is nonlinear in the unknown parameters, the poles (λ_r) and the residues (A_r). The problem can also be approached in two linear stages as the rational fraction polynomial model

$$[H(\omega)] = \frac{\sum_{k=0}^{\bar{m}-2} (j\omega)^k [\beta_k]}{\sum_{k=0}^{\bar{m}} (j\omega)^k [a_k]} \text{ , where } \bar{m} \geq 2 \tag{1-7}$$

from which the poles are computed as the eigenvalues of the companion matrix formed with the $[a_k]$ coefficient matrices, as in Equation 1-4. Once the poles are known, the solution for the residues in Equation 1-6 is linear (see Appendix A for frequency domain residue estimation algorithms[2]).

The description of modal parameter estimation continues in Ref. [1] with: "The current approach in modal identification involves using numerical techniques to separate the contribution of individual modes of vibration in measurements such as frequency response functions. The concept involves estimation the individual single degree-of-freedom (SDOF) contributions to the multiple degree-of-freedom (MDOF) measurement." The summation of SDOF modes to form an MDOF FRF, which is stated mathematically in Equations 1-6 and 1-7, is depicted graphically in Figure 1-1, where the dotted lines are the SDOF modes and the solid line is the MDOF summation.

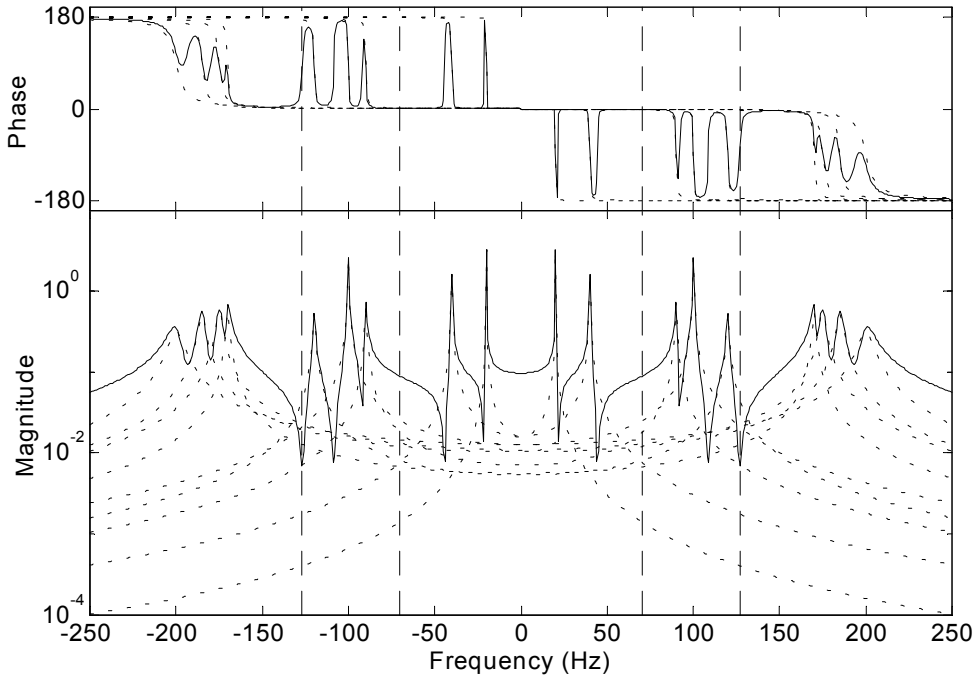

Figure 1-1. *Superposition of SDOF modes to form an MDOF FRF.*

In both forms of the MIMO FRF model in Equations 1-6 and 1-7 above, it is implicit that all modes are included, but in reality the FRFs are measured in some frequency range. In addition, the data is often processed in limited frequency bands of interest. This situation is also depicted in Figure 1, in which the vertical, dashed lines indicate the frequency range of interest. There are two sets of lines, one marking the positive-frequency band and the other marking the corresponding negative-frequency band, because the positive and negative frequency information is processed to estimate pairs of conjugate poles.[1]

The FRF models can be written in three frequency bands, with modes in the frequency range of interest and upper and lower out-of-band modes, in partial fraction form as

$$[H(\omega)] = \underbrace{\sum_r \frac{[A_r]}{j\omega - \lambda_r}}_{\text{lower out-of-band modes}} + \underbrace{\sum_r \frac{[A_r]}{j\omega - \lambda_r}}_{\text{in-band modes}} + \underbrace{\sum_r \frac{[A_r]}{j\omega - \lambda_r}}_{\text{upper out-of-band modes}} \tag{1-8}$$

or in rational fraction form as

$$[H(\omega)] = \underbrace{\frac{\sum_k (j\omega)^k [\beta_k]}{\sum_k (j\omega)^k [a_k]}}_{\text{lower out-of-band modes}} + \underbrace{\frac{\sum_k (j\omega)^k [\beta_k]}{\sum_k (j\omega)^k [a_k]}}_{\text{in-band modes}} + \underbrace{\frac{\sum_k (j\omega)^k [\beta_k]}{\sum_k (j\omega)^k [a_k]}}_{\text{upper out-of-band modes}} \tag{1-9}$$

With regards to the positive- and negative-frequency bands, the terms of upper and lower out-of-band modes should be considered in the absolute-value sense, while the in-band modes also include the contributions of the their conjugates. The lower and upper out-of-band modes are considered as *residuals* with respect to the frequency range of interest and are included in the models as simplified expressions.

$$[H(\omega)] = [R_l(\omega)] + \sum_{r=1}^{N} \left(\frac{[A_r]}{j\omega - \lambda_r} + \frac{[A_r^*]}{j\omega - \lambda_r^*} \right) + [R_u(\omega)] \tag{1-10}$$

and

$$[H(\omega)] = [R_l(\omega)] + \frac{\sum_{k=0}^{m-2} (j\omega)^k [\beta_k]}{\sum_{k=0}^{m} (j\omega)^k [a_k]} + [R_u(\omega)] \tag{1-11}$$

where $[R_l(\omega)]$ is the lower residual function and $[R_u(\omega)]$ is the upper residual function. Note that the N in Equation 1-10, the number of modes in the frequency range of interest, is different from the $\bar{N}$ in Equation 1-6, the total number of system modes, and that the m in Equation 1-11 is different from the $\bar{m}$ in Equation 1-7.

1.3 Literature Review

As indicated in Equations 1-8 through 1-11, residuals are terms included in the frequency response model to account for the contributions of modes that are above and below the frequency range of interest. Residuals are typically classified as lower residuals, which represent the contribution of the modes below the frequency range of interest, and as upper residuals, which represent the contribution of the modes above the frequency range of interest. The most commonly used, single-term expression for the lower residual is an inverse function of frequency squared $(1/\omega^2)$ and for the upper residual is a constant. Residuals have been included in algorithms that estimate poles, such as those developed in Refs. [4-28] and in algorithms that estimate residues or mode shapes, such as those in Refs. [14,16-18,21,25,29-32]. In addition, the residuals themselves have been estimated for use in system modeling application, such as in Refs. [33-39], or for Hilbert transform procedures, as in Ref. [40].

Some of the earliest developments of residuals in the modal area were by Klosterman[41] in 1971, followed by Van Loon[42] in 1974. Klosterman studied the use of experimentally determined modes for a building block approach to system analysis and concluded that a component can be modeled with fewer modes plus a "Residual Flexibility" which represents the flexibility of the other modes. Van Loon split the summation of modes into three partial sums, as in Equation 1-8, and stated that "in most practical cases the effect of lower modes can be suitably approximated by one term $-1/M_{ij}\omega^2$, called the inertia effect or lower mode admittance" and that "the influence of the higher modes ... can be suitably approximated by one term S_{ij} called the residual flexibility or higher mode admittance."

Van Loon concluded that "the effect of the lower and higher modes outside the frequency range of interest can have a significant influence and should be included in the analytical expression." Since then, the development of most frequency domain parameter estimation algorithms have included some consideration of residuals.

The use of residuals is generally restricted to frequency domain models because the effects of out-of-band modes are not readily described in the time domain. In the frequency domain, the contribution of the modes below, above and within the frequency range of interest can be naturally separated and simplified expressions for the residuals formulated. But in the time domain, both the modes of interest and the residual modes have response at all time points. That is, the response of in-band and out-of-band modes can not be separated into segments of the time response.

Although, Mergeay[43] did propose to use the inverse Fourier transforms of the $1/\omega^2$ lower residual and constant upper residual in the time domain, which yields a linear function of time and a delta function, but decided that including these two non-exponential terms in the impulse response function equation would complicate the mathematical solution. Instead, it was suggested that "the influence of lower and higher modes may also be adequately approximated by complex exponential terms having a damped resonant frequency at the lower frequency limit and the higher frequency limit of the concerned frequency range." However, these residuals terms were not included in the time domain algorithms presented elsewhere in this reference.

The more commonly accepted opinion is that it is difficult to formulate a reasonable mathematical model and solution for the general time domain algorithm that includes residuals.[44] Leuridan et al. examined the aliasing effect of the *z*-transform in relation to poles estimated from impulse response functions which were formed from a subband of a frequency response function and concluded that with time domain algorithms it is impossible to compensate for the influence of residual modes by increasing the model order because of the aliasing effect of frequencies.[24,30] Therefore, the discussion and developments contained herein concentrate solely on frequency domain algorithms.

Residuals and their effects have been viewed in a variety of ways, which has led to a variety of approaches to model them and applications that consider them. In the literature, residuals have been described as "asymptotic representations of other modes"[21] and as "correction" or "compensation" terms. Some have suggested to reduce computational modes with residuals, while others have suggested to compensate for residuals with out-of-band modes. There are a few prevalent residual models: physical models that express residuals as the low and high frequency behavior of an SDOF FRF, mathematical models that represent residuals with a frequency domain power polynomial, pseudo-modes of some variant and estimation out-of-band modes.

Some developments have been concerned with only upper residuals[5,31,34,37,39] and others have equated lower residuals with rigid-body modes[31,33]. In some cases it assumed that the lower residuals can be neglected because with baseband measurements there are no modes below the frequency range of interest[39], but this neglects analyzing some subsection of the measured frequency range. In other cases, when computing poles in

successive frequency ranges, the modes from the previous ranges are subtracted from the measurements to eliminate the need for lower residuals.[5] Ref. [31] develops a method for estimating mode shapes from quadrature response and proposes that the lower residual can be ignored if the rigid body modes are low relative to the elastic modes, otherwise the rigid body modes may need to be estimated and included in the residue calculation.

The physical residual model is based on the asymptotic behavior in the frequency range of interest of an out-of-band, single degree-of-freedom mode. Historically, the lower residual is a $1/\omega^2$ term and the upper residual is a constant term, such as in Refs. [5,6, 10,16-18,21,22,24,26,29,33,34,38,41-43,45]. This is equivalent to setting $R_l(\omega)$ to $R_{-2}\omega^{-2}$ and $R_u(\omega)$ to R_0 in Equations 1-10 and 1-11. The lower residual, which represents the inertia of the lower modes, is also known as inertia restraint, inertia constraint and residual inertia. The upper residual, which represents the flexibility of the upper modes, is also known as residual flexibility and residual compliance. The inertia and flexibility terminology of the lower and upper residuals stems from the original expressions for the residual terms, which will be made apparent in Section 2.1. The $1/\omega^2$ and constant term are for diplacement/force FRFs, for velocity/force FRFs these terms are multiplied by $j\omega$ and for acceleration/force FRFs these terms are multiplied by ω^2. A $1/j\omega$ term has also been added to the lower residual as a residual damping term[6] and the derivation of the Polyreference Frequency Domain algorithm in Ref. [27] has matrices for the residual effects of displacement, velocity and acceleration. These typical forms of the single-term residuals assume that the out-of-band modes are far below or far above the frequency range of interest and have diminishing validity when the out-of-band modes are not well

separated from the in-band modes. The limitations of this assumption of the physical residuals are explored in Section 2.1.

While the residual inertia and residual flexibility terms are based on a simplification of physical frequency response characteristics, "the residual effects of modes below and/or above the frequency range of interest cannot be completely represented by such simple relationships."[44] To overcome the limitations of the single-term, physical residuals, the upper and lower residual have also been modeled with multiple-term, purely mathematical expressions. As Allemang and Brown explain "the lower and upper residuals can have any mathematical form that is convenient as long as the lack of physical significance is understood. Power functions of frequency ... are commonly used with such a limitation."[46] It is these frequency domain power polynomials that are the basis of the generalized residual model developed and implemented in the following chapters.

The residual inertial of order -2 and residual flexibility of order 0 terms combine with the rational fraction FRF model to produce extra orders in the numerator polynomial. Some algorithms bypass the interpretation of physical residual models and simply add more orders in the numerator polynomial, such as in Refs. [4,8-11,13-15,19,20,23,25,28,31,32, 38] While some advise generally to just increase the order of numerator polynomial to include residuals, others use explicit power functions of frequency terms, such as orders of (-2,-1,0,1,2)[15], orders of (0,1,2) for an acceleration/force FRF model[13], orders of (0,1) for residual mass[20] and even, positive orders[39]. There have also been more elaborate models, such as $1/\omega^2$ and constant terms for the real part of the FRF and $1/j\omega$ and ω terms for the imaginary part of the FRF[19], the three highest terms of the numerator and

denominator polynomials of a mobility rational fraction FRF model as the lower residual and the three lowest terms for the upper residual[32] or a binomial expansion as an infinite series of odd order polynomial terms for the upper residual of the imaginary part of the FRF[31].

These extra orders have been referred to as "compensation" or "correction" terms in Refs. [4,7-9,14,16,25]. In most cases only the upper bound of the numerator polynomial order was increased, but the lower bound remained at zero. However, Van der Auweraer et al. recognized that adding positive order terms only models the effects of higher-frequency modes and suggested that lower-frequency modes can be modeled with negative order terms, but then claimed that "the inclusion of such lower frequency residual expression would complicate mathematics to great extent."[28] As will be shown in Section 2.2, positive orders to represent the upper residuals and negative orders to represent the lower residuals can both be used equally in a rational fraction polynomial frequency domain model.

It has been well established that out-of-band modes can be included in the parameter estimation by either increasing the order of the denominator polynomial, which adds computational poles to the model, or by including extra orders in the numerator polynomial, which adds residuals to the model. As Richardson and Formenti acknowledge "out-of-band effects can be approximated by specifying additional terms for either the numerator or the denominator polynomial."[4] Van der Auweraer suggested that instead of increasing the order of the denominator to account for out-of-band modes, to "approximate their influence by a simple, polynomial, relationship, obtained by

increasing the order of the numerator."[28] Leuridan et al. stated that: "By picking the order [of the denominator polynomial] sufficiently high, correct estimates may be found for poles outside the subband of analysis. The residual effect of modes outside the subband can also implicitly be accounted for by overspecifying the order of the $b_{ij}(s)$ [numerator] polynomials."[30] Finally, Braun and Ram concluded that in the frequency domain both the numerator and denominator can be overdetermined† and the amount of overdetermination can be different for poles and zeros.[23] In the parameter estimation methods developed in Chapter 3, the objective will to be to minimize or eliminate computational modes by including residuals in the numerator polynomial.

There have been contradictory viewpoints about the treatment of out-of-band modes and residuals. Some suggest to reduce computational modes with residuals, Refs. [5,9,11,14, 25], while others have suggested to compensate for residuals with out-of-band modes, Refs. [10,12,18,24,31,34-36,40,47]. Van der Auweraer and Leuridan suggested to "describe the effects of modes outside the frequency band of analysis by locating modes outside the band of analysis, by use of residual terms, or a combination of both".[24]

Shih et al. recommended that: "A larger order for the AR [denominator] part can be used for better estimation of modal parameters, but more computational modes will be introduced ... In considering the advantages of being able to compensate for the effect of residuals and the effects of bias noise, the order of the MA [numerator] polynomial can

---

† Here *overdetermination* means a higher than the minimal order polynomial, not a least-squares matrix solution with more equations than unknowns.

be higher than the AR polynomial."[25] Richardson and Formenti opined that: "Most other MDOF methods require that additional 'computational' modes be used in order to compensate for the residual effects of out-of-band mode in the curve fitting band ... The RFP [Rational Fraction Polynomial] method, on the other hand, allows the use of additional numerator polynomial terms as a means of compensating for the effects of out-of-band modes."[8] Richardson further claimed that: "The RFP method has the advantage that additional numerator polynomial terms can be added to compensate for out-of-band modes, thus avoiding the problem of computational modes."[9] The algorithm in Ref. [5] is the multi-matrix method for direct parameter extraction, in which: "Upper residuals appear explicitly in the matrix polynomial and are estimated from the measurements. Hence the need for 'computational' modes, that are introduced by many analysis procedures to describe residual effects implicitly, is reduced." The algorithm in Ref. [11] is an iterative solution of a set of nonlinear partial fraction expansion equations that uses a set of initial modal parameters for each mode estimated with an SDOF frequency domain method. Its benefits are purported to be that it "compensates for out-of-band modes by computing residual terms, rather than over-specifying the number of modes to be analyzed" and "produces only physical modes of vibration, thus eliminating annoying computational modes."

On the other side of the argument, it has been proposed to estimate more out-of-band modes to compensate for residuals[34,35] or to include a few modes above the frequency range of interest to account for the upper residuals[31]. The algorithm in Ref. [12] adds undamped out-of-band poles to the model, not just generic residual terms and claims:

"For practical applications, only a small number, say 2, of out-of-band modes, immediately below and above the frequency band of interest, are needed in the solution equations to compensate for the effects of all of the out-of-band modes." Similarly, Ref. [47] states: "The observed number of modes plus at least two to allow for contributions of modes whose natural frequencies lie outside the range yields the number of assumed modes *n* which are included in the effective set of dynamic equations."

Pseudo-modes have also been created for the upper residual, mostly in system modeling applications[37,39], but also for Hilbert transform procedures used to detect and quantify nonlinearities[40]. A pseudo-mode is a residual expression that is not just a series of power functions of frequency, but requires a value of the resonance frequency of a pole and possibly also the damping and residue. The modal parameter associated with residual modes have no physical significance.[46] Pseudo-modes are typically an overly complicated way to include residuals in an FRF model, as illustrated in the following examples.

Ref. [40] describes a method for removing the contribution of residual modes from measured FRFs so that the resulting functions contain a finite set of modes, which is a requirement of the Hilbert transform. A single mode, partial fraction form is separated into its real and imaginary parts and a simplified expression to approximate the behavior away from resonance is derived. The residual forms for all modes above and below modes of interest are then combined, but the poles and residues of residual modes are still unknown. Equations are developed for the upper and lower residual modes damped natural frequency and residues by making assumptions of dominant effects of out-of-band modes. In Ref. [18], the residual term is taken to be a simplified expression of the rational

fraction FRF model evaluated frequencies away from the poles. The lower residual has the form of $1/j\omega$ and the upper residual has polynomial orders (1,2,3) in the numerator and products of $(j\omega - \lambda)$ terms in the denominator, where the $\lambda's$ are determined by estimating the high-frequency poles. The lowest frequency pole included in the residuals is the first mode above the analysis frequency range and the highest frequency pole is approximately twice the maximum of the analysis frequency range.

The primary application of residuals is to compute better estimates of poles and residues. In other applications, the purpose is to estimate the residuals, such as in system modeling[33-39,41], where the residuals are included in the system model to better describe the system dynamics. In many of these methods, the residuals are estimated using some type of modal deflation.[10,18,32-39,41] That is, the FRFs of the in-band modes are synthesized and subtracted from the measurements, then the residuals are estimated from the remainder functions. For example, in Ref. [33] residual terms are estimated by subtracting a synthesized FRF with no residuals from the measured FRFs and in Ref [40] the residual parameters are estimated from off-resonance data. In Ref. [38], residuals are determined by subtracting synthesized from measured FRFs and estimating the lower residual from the remainder function at low frequency and the upper residual at high frequency. In Ref. [39] even order polynomial terms are estimated sequentially from the difference of the measured and the previous synthesized FRF at different frequencies. The approach in Ref. [34] is to "use the resulting stiffness line to estimate an additional set of modal parameters that approximate the higher frequency residual effects ... to find modes outside the analysis band or at least find a single frequency (and damping) that

approximate all the residual energy outside the analysis range." According to Ref. [36], which estimates a high-frequency pseudo-mode approximation for upper residuals: "The correct way of obtaining the residual terms' contribution from a modal analysis derived curve is to subtract from the measured (complete) FRF, the FRF regenerated using the modal parameters included in the frequency range of interest. From this difference, using a least-squares solution ..., one obtains the best estimate for the residual term."

Even in some parameter estimation algorithms[10], it has been proposed to estimate the residuals after the poles and residues are determined, that is, not to include the residuals in the parameter estimation process. A method for determining residues from mobility FRFs at a few discrete frequencies from off-resonance sine dwell is developed in Ref. [18] and in Ref. [32] with an improved residual model, in which the residual content is iteratively subtracted from the measurements to estimate the residues. The problem with these modal deflation schemes is that failure to include residuals when estimating the in-band modes degrades the estimation of the poles and residues, which in turn affects the synthesized functions that are subtracted from the measurements to create the remainder functions. The approach in the techniques developed in this dissertation will be to include the residuals in the parameter estimation process and treat the numerator polynomial coefficients equally with the denominator polynomials from which the poles are computed.

1.4 Objectives of Dissertation

Residuals have been included in all types of frequency domain algorithms for estimating poles and residues, but primarily as a byproduct or afterthought. In all of these published methods, the residuals are considered a fixed parameter in the model and the number of poles is the variable. The paradigm shift that will be proffered in this dissertation is considering the order of the numerator polynomial as a variable in the parameter estimation model, in addition to the order of the denominator polynomial, that can lead to consistent estimation of the system poles.

The focus of the work contained herein is to more fully explore the generalization of residuals in frequency domain modal parameter estimation algorithms. In particular, methods will be developed in which the number of poles is fixed and the residuals are varied to produce consistent poles. Chapter 2 describes the theory of generalized residuals and introduces the concept of a consistency diagram for residuals. Chapter 3 develops several applications of generalized residuals and Chapter 4 summarizes the conclusions and offers recommendations for further work in this area. Appendix A discusses topics related to frequency domain residue estimation with generalized residuals, Appendix B contains supplementary plots associated with several figures in Chapter 2 and Appendix C lists selected Matlab functions.

CHAPTER TWO

2 Theory

This chapter presents the theory of generalized residuals for frequency domain modal parameter estimation. An examination of the physical residual model leads to the realization that a more general, mathematical, residual model is needed to compensate for the effects of out-of-band modes. To meet this need, a power polynomial of frequency, with both positive and negative orders, is proposed as a generalized residual model. It is then shown that this residual polynomial can adequately represent the asymptotic behavior of residual modes. The generalized residual model is combined with the rational fraction polynomial FRF model to form the frequency domain UMPA model with generalized residuals. Then, the concept of a consistency diagram is broadened to incorporate the evaluation of an algorithm for a sequence of residual polynomials instead of the denominator polynomial model order. Some interesting observations are also cited about the relationship of the zeros of an FRF and residuals.

2.1 Derivation and Limitation of the Physical Residual Model

The physical residual model that has been used historically is a single, constant term for the upper residual and a single, $1/\omega^2$ term for the lower residual. This model is derived from the asymptotic behavior of an SDOF FRF away from the natural frequency of the mode. The low-frequency and high-frequency approximations of an SDOF FRF are

$$H(\omega) = \frac{1}{(j\omega)^2 M + j\omega C + K} \simeq \begin{cases} \dfrac{1}{K} & \text{for small } \omega \\ \dfrac{-1}{\omega^2 M} & \text{for large } \omega \end{cases} \tag{2-1}$$

As can be seen from Equation 2-1, the SDOF FRF is inversely proportional to the stiffness at low frequency, which is sometimes called the stiffness line of the FRF, and inversely proportional to the frequency squared times the mass at high frequency, which is sometimes called the mass line of the FRF. Figure 2-1 shows the residual relationship of the SDOF FRF asymptotes to the in-band modes, which are bounded by the vertical lines. The stiffness line of the mode above the frequency range of interest forms the upper residual, which gives the conventional name of residual flexibility for the upper residual. The mass line of the mode below the frequency range of interest forms the lower residual, which gives the conventional name of residual inertia for the lower residual.

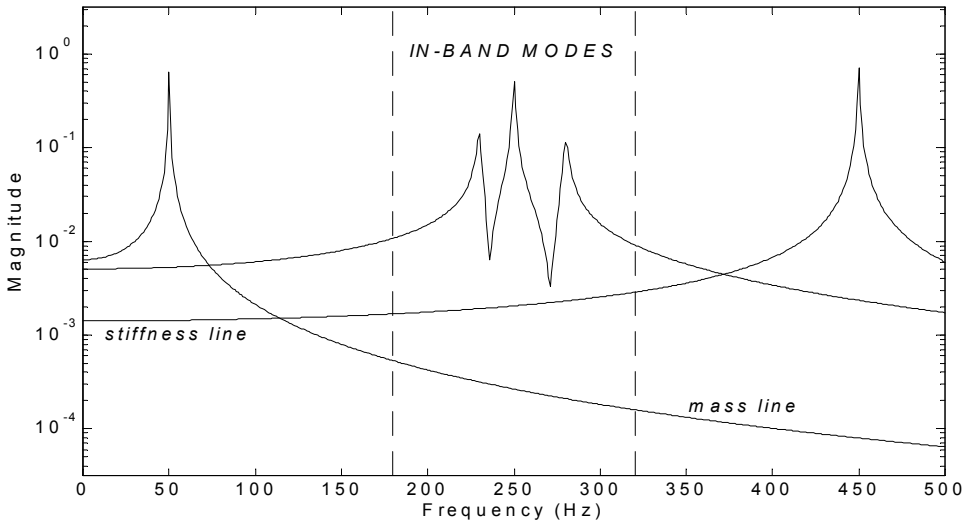

Figure 2-1. *Relationship of the residual modes and the in-band modes*.

These single-term, physical residuals are always implicitly used with the assumption that the out-of-band modes are far above and far below the frequency range of interest. For the upper residual, it is assumed that there is one mode far above the frequency band, and its residual flexibility effect in the frequency band can be approximated with a stiffness line or a constant term. For the lower residual, it is assumed that there is one mode far below the frequency band, and its residual inertia effect in the frequency band can be approximated with a mass line or a $1/\omega^2$ term. However, if the residual modes are not well separated from the in-band modes, this assumption has diminishing validity. To establish the limitations of this assumption, Figure 2-2(a) shows a normalized SDOF FRF plotted versus normalized frequency. Also plotted is a constant line representing the upper residual and a $1/\omega^2$ line representing the lower residual.

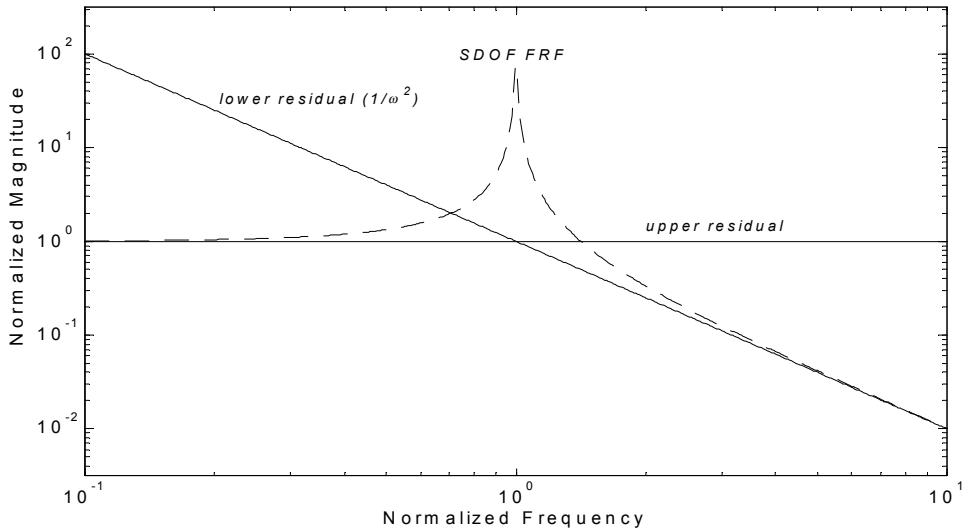

Figure 2-2(a). *Limitations of the physical residual model assumptions.*

The magnitude of the out-of-band SDOF FRF asymptotically approaches a constant value as the frequency decreases from the resonance, which forms the stiffness line that is physical upper residual. The relative error between the upper residual and the SDOF FRF versus log normalized frequency is shown in Figure 2-2(b), also plotted are the SDOF FRF and the upper residual. As can be seen from the plots, the relative error of the low-frequency asymptote is 0.1 at approximately 1/3 of the normalized resonant frequency and 0.01 at approximately 1/10 of the normalized resonant frequency. That is, the assumed natural frequencies of the upper residual modes must be at least 3 times the frequency of the in-band modes for the constant upper residual assumption to be valid within 10%, and 10 times for 1%. If the modes above the frequency range of interest are nearer to the in-band modes, then the constant upper residual does not accurately describe the effects of the upper residual modes in the frequency range of interest.

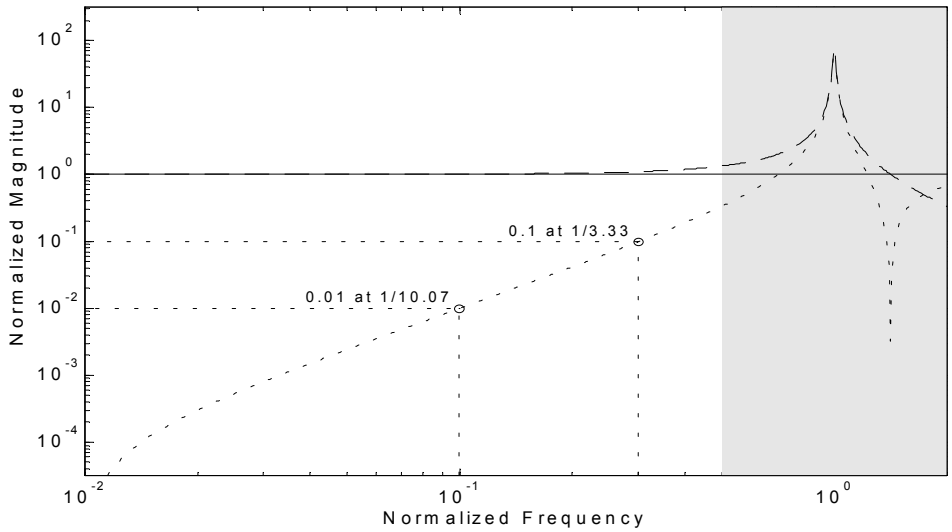

Figure 2-2(b). *Relative error of the SDOF FRF asymptote and upper residual.*

To evaluate the relative error of the lower residual, the SDOF FRF is multiplied by ω^2, which essentially makes it an acceleration/force FRF, and the lower residual becomes a constant. The magnitude of the out-of-band SDOF FRF asymptotically approaches a constant value as the frequency increases from the resonance, which forms the constant mass line that is physical lower residual. The relative error between the lower residual and the SDOF FRF versus log normalized frequency is shown in Figure 2-2(b), also plotted are the SDOF FRF and the lower residual. As can be seen from the plots, the relative error of the low-frequency asymptote is 0.1 at approximately 3 times the normalized resonant frequency and 0.01 at approximately 10 times the normalized resonant frequency. That is, the assumed natural frequencies of the upper residual modes must be at least 1/3 the frequency of the in-band modes for the $1/\omega^2$ lower residual assumption to be valid within 10%, and 1/10 times for 1%. If the modes below the frequency range of interest are nearer to the in-band modes, then the $1/\omega^2$ lower residual

does not accurately describe the effects of the lower residual modes in the frequency range of interest.

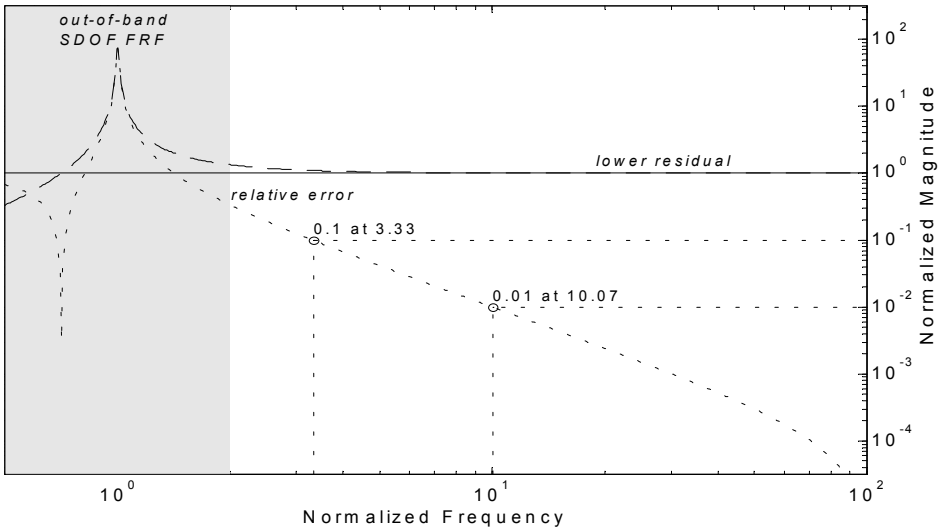

Figure 2-2(c). *Relative error of the SDOF FRF asymptote and lower residual.*

2.2 Power Polynomial Residual Model

If the out-of-band modes are not sufficiently separated from the in-band modes, the single-term, physical residual model is not adequate to describe the residual effects in the frequency range of interest. As was mentioned in Section 1.3, mathematical models of power polynomials of frequency have been used to represent residuals. To better model the asymptotic behavior of the residual modes, more polynomial terms can be used of the form $\sum_k (j\omega)^k R_k$. Since the $1/\omega^2$ term models the lower residuals, it is natural to use negative polynomial orders for the lower residual and similarly to use positive polynomial

orders for the upper residual.† In fact, as it will be shown below, a polynomial function can be fit to any segment of an FRF, or a superposition of FRFs, except at the resonance peaks.

Before proceeding, it is necessary to clarify the definition of some terminology. Juang defines *system identification* as "the process of developing or improving a mathematical representation of a physical system using experimental data."[48] In system identification, the form of the system model, as well as the values of its parameters, are not known. In *parameter estimation*, the form of the system model is known and the constants, or parameters, of the model are estimated from measured data.[49] As stated in the preceding chapter, *modal parameter estimation* is a special case in which the system is in the form of a modal model. The phrase *curve-fitting* has often been used interchangeably with all of the above three terms, but in the context of this dissertation, it will only refer to the fitting of a frequency domain polynomial to a segment of an FRF.

In Figure 2-3(a) some positive-order polynomial functions are compared to some SDOF FRFs. The polynomials were evaluated with frequency values scaled by the mean frequency.[3] The general shape of the polynomial functions matches the general shape of the FRFs below the natural frequencies, which form the asymptotic upper residual. Thus positive-order polynomials are an appropriate choice to model the upper residual. In Figure 2-3(b), some negative-order polynomial functions are compared to the SDOF

---

† Although zero is not strictly either positive or negative, the zeroth-order polynomial term is included in the upper residuals, with positive orders, because the constant term is the upper physical residual.

FRFs and a similar conclusion can be made for using negative-order polynomials to model the lower residual.

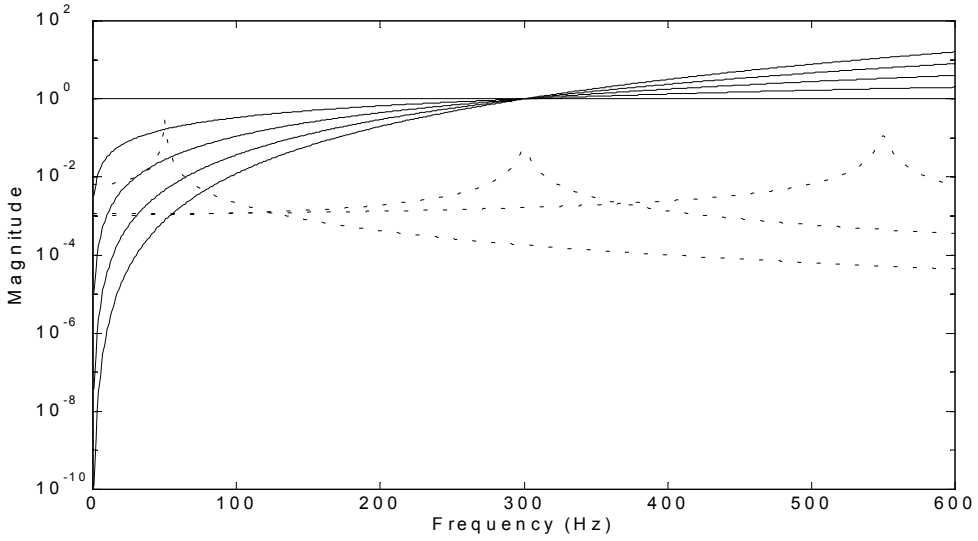

Figure 2-3(a). *Positive-order polynomial terms, evaluated for orders 0,1,2,3,4.*

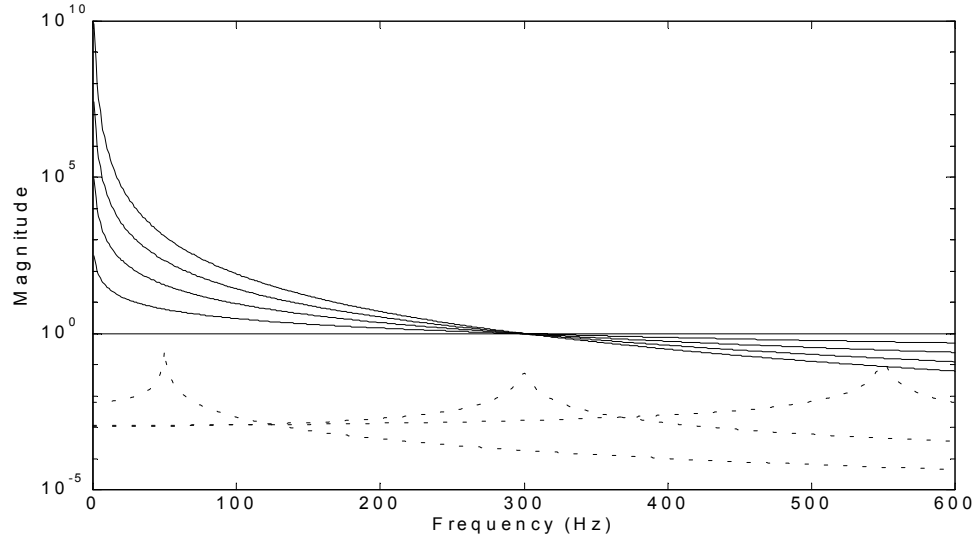

Figure 2-3(b). *Negative-order polynomial terms, evaluated for orders 0,-1,-2,-3,-4.*

Polynomial curve-fits of FRF segments are shown in Figures 2-4 through 2-10. The magnitude of the curve-fit polynomial function synthesized from the estimated coefficients (the solid line) is compared to the magnitude of a 3-DOF FRF (the dashed line). These same functions plotted in other formats and the values of the polynomial coefficients can be found in Appendix B. The relative error between the curve-fit polynomial and the FRF is shown in the inset plots for the region near the estimation interval. The polynomial coefficients are estimated by generating a system of linear equations from Equation 2-2 for a segment of the data and solving for the coefficients R_k.

$$H(\omega) = \sum_k (j\omega)^k R_k \tag{2-2}$$

The shaded region in the plots indicate the segment of data that was used in Equation 2-2 to estimate the polynomial coefficients. To improve the numerical conditioning of the solution, the frequency was scaled by the mean frequency of the segment, as recommended in Ref. [3]. Positive-order polynomial terms are used in the residual model for the upper residual segments of the FRF (i.e., the segment below the lowest mode) and negative-order polynomial terms are used in the residual model for the lower residual segments of the FRF (i.e., the segment above the highest mode). Both positive-order and negative-order polynomial terms are used for the segments of the FRF between resonances and at resonances.

The polynomial model fits upper and lower residual segments of the FRF sufficiently, as shown in Figures 2-4 through 2-7. That is, the summation of the polynomial functions synthesized from the estimated coefficients replicates the original data. The curve-fit will

typically match the data over the interval used to generate the equations from which the coefficients are estimated and for some region beyond this interval. However, the polynomial functions do tend to diverge greatly elsewhere and typically the divergence increases as more polynomial orders are included in the model. That the polynomial functions diverge outside the estimation interval is not of much concern since the purpose of the polynomial model is only to describe the residual effects in the frequency range of interest, that is, for interpolation, not extrapolation.

By using enough polynomial orders, the model can fit the FRF nearly to the resonant peak, as shown in Figure 2-5 and 2-7, but not at the resonant peaks, as shown in Figure 2-10. The polynomial curve-fit is unable to match the original data even in the estimation interval if that FRF segment contains a resonance, as detailed in the left inset plot of Figure 2-10. Here the polynomial model is not able to describe the resonant behavior of the$1/(j\omega - \lambda)$ SDOF functions in the modal model. Between two resonances, the polynomial model can adequately curve-fit the FRF without an antiresonance, as in Figure 2-8, and even with an antiresonance, as in Figure 2-9. This means that a polynomial model is able to represent the residuals effects in the frequency range of interest for data in which the residual modes are not well separated from the in-band modes.

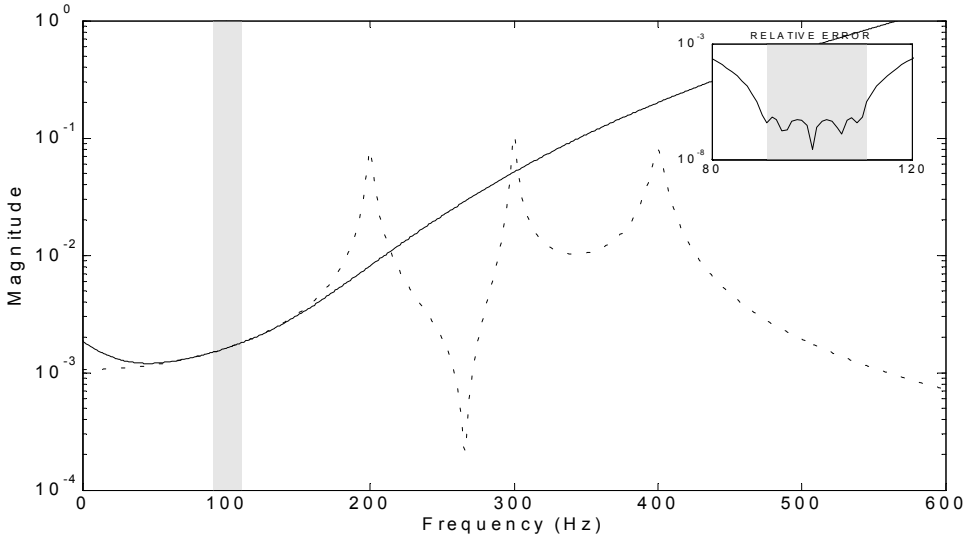

Figure 2-4. *Polynomial curve-fit with orders 0:4 of the upper residual segment of an FRF away from resonance.*

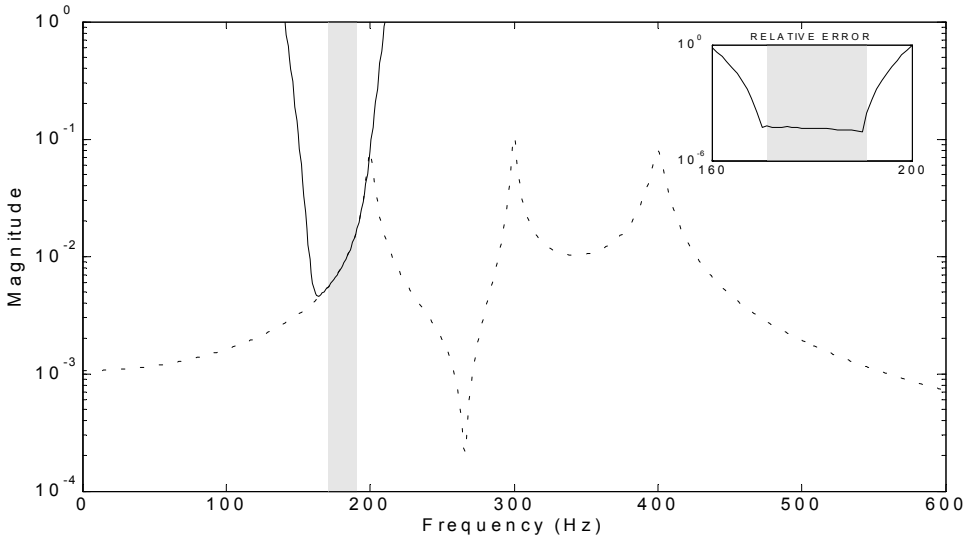

Figure 2-5. *Polynomial curve-fit with orders 0:12 of the upper residual segment of an FRF near resonance.*

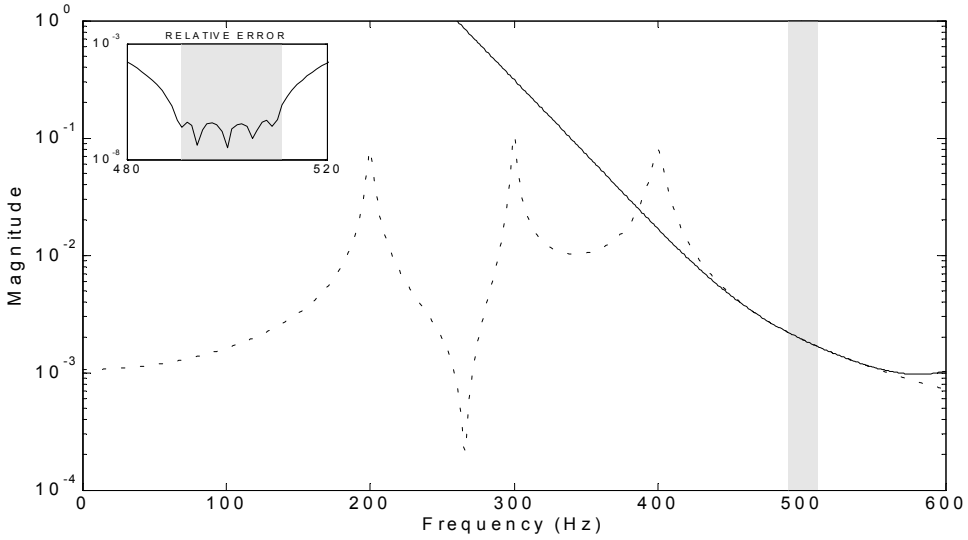

Figure 2-6. *Polynomial curve-fit with orders -4:0 of the lower residual segment of an FRF away from resonance.*

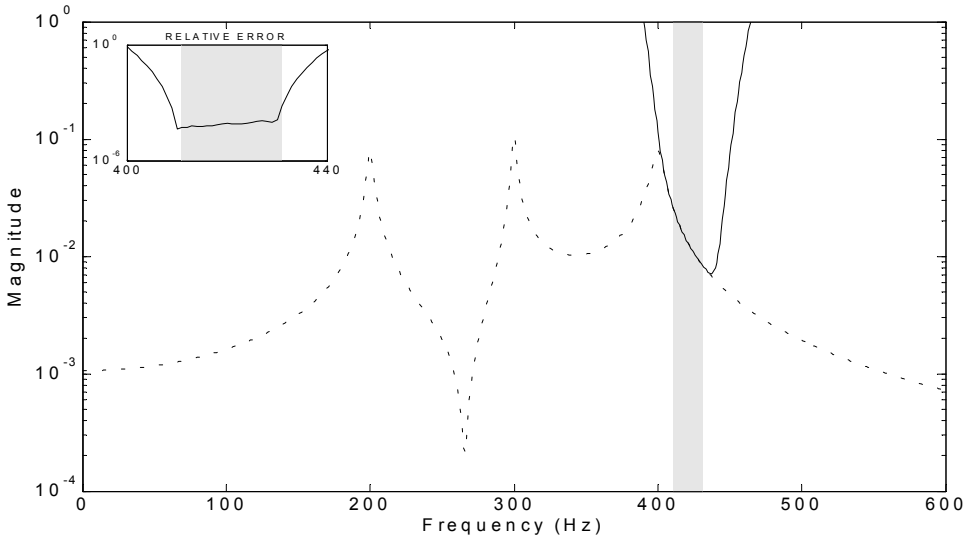

Figure 2-7. *Polynomial curve-fit with orders -12:0 of the lower residual segment of an FRF near resonance.*

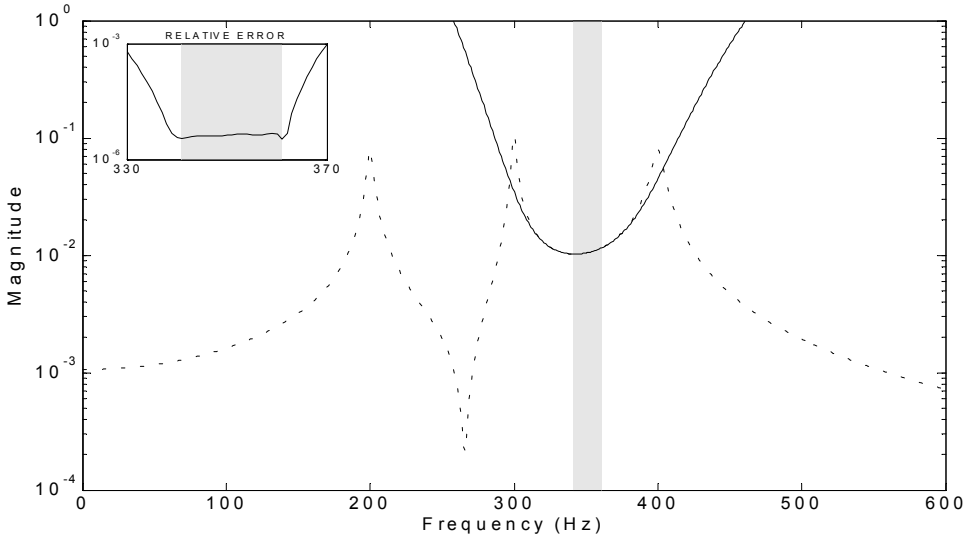

Figure 2-8. *Polynomial curve-fit with orders -4:4 of the FRF segment between two resonances without an antiresonance.*

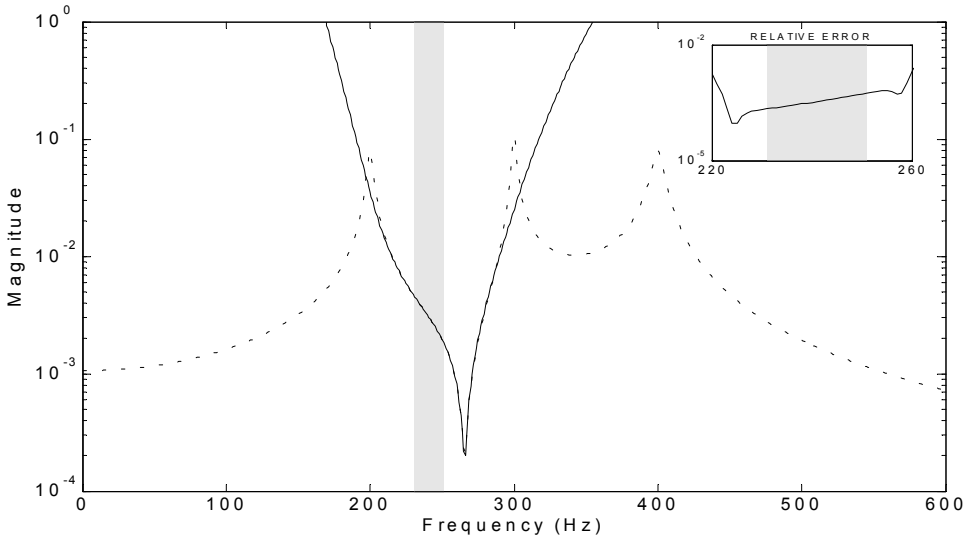

Figure 2-9. *Polynomial curve-fit with orders -4:4 of the FRF segment between two resonances with an antiresonance.*

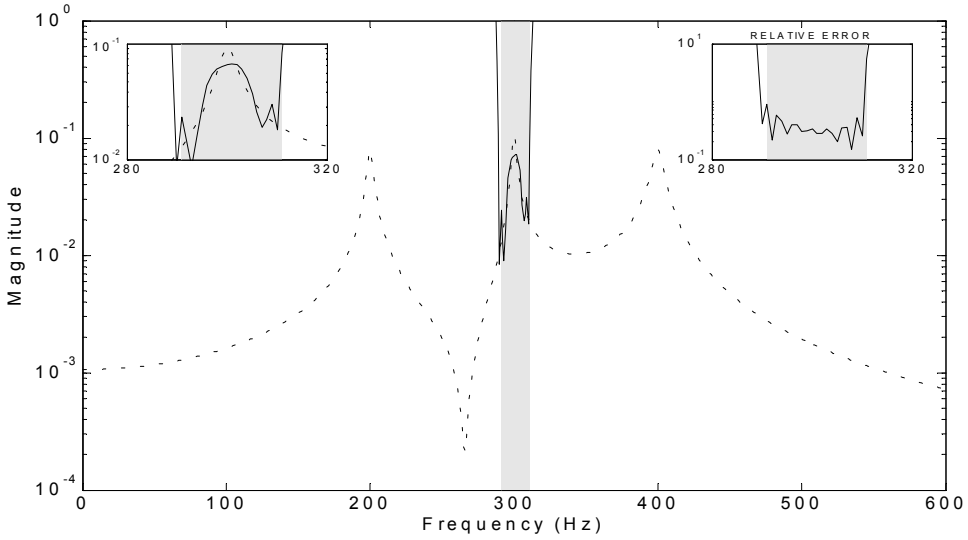

Figure 2-10. *Polynomial curve-fit with orders -4:4 of an FRF segment at a resonance.*

As has been demonstrated above, a frequency domain power polynomial can curve-fit any segment of an FRF except at a resonance and model the asymptotic behavior away from resonance, which are the residual effects. An MDOF FRF is a summation of SDOF modes, but with respect to any one mode, all other modes are residuals. For example, the 3-DOF FRF in Figure 2-11 in partial fraction form is

$$H(\omega_k) = \frac{A_1}{j\omega_k - \lambda_1} + \frac{A_1^*}{j\omega_k - \lambda_1^*} + \frac{A_2}{j\omega_k - \lambda_2} + \frac{A_2^*}{j\omega_k - \lambda_2^*} + \frac{A_3}{j\omega_k - \lambda_3} + \frac{A_3^*}{j\omega_k - \lambda_3^*} \tag{2-3}$$

and in rational fraction polynomial form is†

† For the coefficient notation in Equation 2-4, the first subscript refers to the mode number and the second subscript refers to the polynomial coefficient index (e.g., $\beta_{1,0}$ is the 0th-order numerator coefficient associated with mode 1, the first and second terms in Equation 2-3).

$$H(\omega) = \frac{\beta_{1,0}}{a_{1,0} + j\omega a_{1,1} - \omega^2 a_{1,2}} + \frac{\beta_{2,0}}{a_{2,0} + j\omega a_{2,1} - \omega^2 a_{2,2}} + \frac{\beta_{3,0}}{a_{3,0} + j\omega a_{3,1} - \omega^2 a_{3,2}} \qquad (2\text{-}4)$$

The $1/(j\omega - \lambda)$ SDOF functions describe the modal behavior for all frequency, but for a band around a particular mode, as indicated by the shaded region in Figures 2-11 and 2-12, the residual effects of the other modes can be approximated by a frequency domain power polynomial of the form in Equation 2-2, with $k \geq 0$ for the upper residual and $k < 0$ for the lower residual. Then, for mode 2, in partial fraction form

$$H(\omega) = \sum_{k<0} (j\omega)^k R_k + \frac{A_2}{j\omega - \lambda_2} + \frac{A_2^*}{j\omega - \lambda_2^*} + \sum_{k\geq 0} (j\omega)^k R_k \qquad (2\text{-}5)$$

and in rational fraction polynomial form

$$H(\omega) = \sum_{k\leq 0} (j\omega)^k R_k + \frac{\beta_{2,0}}{a_{2,0} + j\omega a_{2,1} - \omega_{2,2}^2 a} + \sum_{k\geq 0} (j\omega)^k R_k \qquad (2\text{-}6)$$

In Figure 2-12, mode 2 is the mode of interest and modes 1 and 3 are residuals in the frequency band around mode 2. The residual polynomial of orders (-4:4) is curve-fit to the modes 1+3 function in the 250-350 Hz frequency range. The second term in Equations 2-5 and 2-6 accounts for mode 2 and the residual polynomial accounts for the residual effects of modes 1 and 3 in this region. Together the modal model and residual model account for all of the contributions to the FRF in the frequency band.

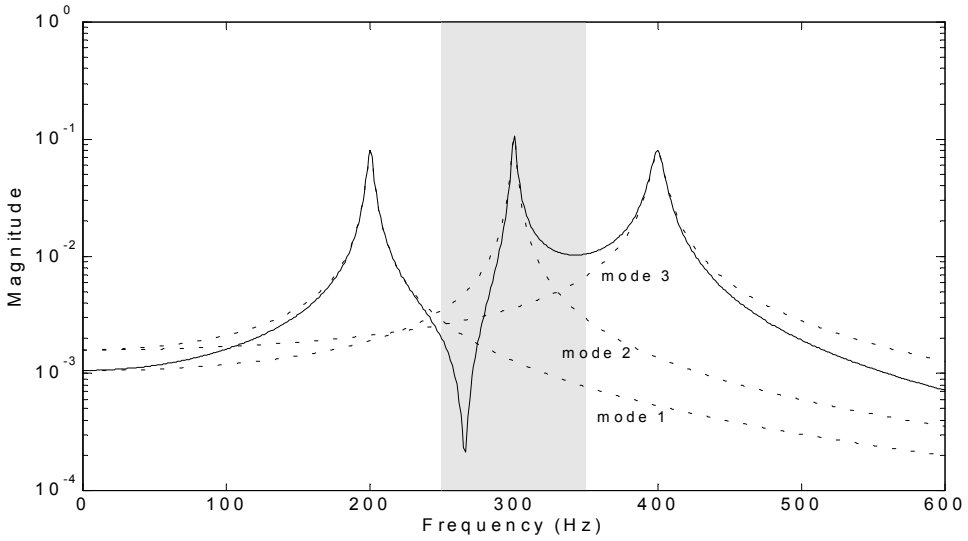

Figure 2-11. *Summation of three SDOF modes (dotted lines) to form an MDOF FRF (solid line).*

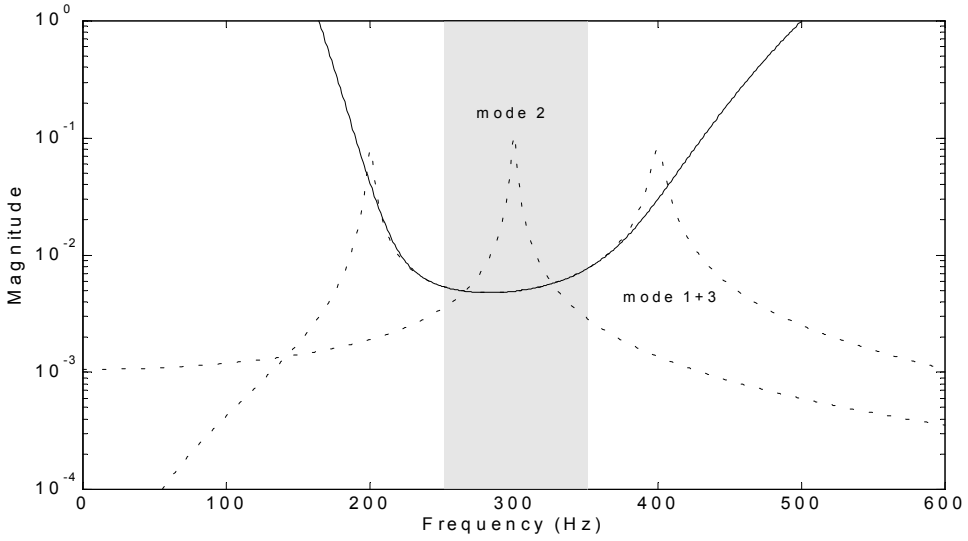

Figure 2-12. *Polynomial curve-fit with orders -4:4 of residual contributions in the region around a single mode.*

2.3 Rational Fraction Polynomial Model with Generalized Residuals

The power polynomial residual model is incorporated into the rational fraction polynomial FRF model of Equation 1-11 by letting the lower residual function $R_l(\omega)$ be a complete† polynomial with negative orders and the upper residual function $R_u(\omega)$ be a complete polynomial with positive orders, that is,

$$R_l(\omega) = \sum_{k=n_l}^{-1} (j\omega)^k [R_{l,k}] \text{ , where } n_l < 0 \text{ is the lower index limit of the residual polynomial} \tag{2-7}$$

$$R_u(\omega) = \sum_{k=0}^{n_u} (j\omega)^k [R_{u,k}] \text{ , where } n_u \geq 0 \text{ is the upper index limit of the residual polynomial}$$

Substituting these expressions for the residual functions into Equation 1-11,

$$[H(\omega)] = \sum_{k=n_l}^{-1} (j\omega)^k [R_{l,k}] + \frac{\sum_{k=0}^{m-2} (j\omega)^k [\beta_k]}{\sum_{k=0}^{m} (j\omega)^k [a_k]} + \sum_{k=0}^{n_u} (j\omega)^k [R_{u,k}] \tag{2-8}$$

and combining the upper and lower residual functions into a generalized residual polynomial that includes both the upper and lower residuals,

$$[H(\omega)] = \frac{\sum_{k=0}^{m-2} (j\omega)^k [\beta_k]}{\sum_{k=0}^{m} (j\omega)^k [a_k]} + \sum_{k=n_l}^{n_u} (j\omega)^k [R_k] \tag{2-9}$$

---

† By a *complete* polynomial it is meant that the orders of the polynomial are continuous and inclusive, that is, from a minimum order to a maximum order including all orders between.

The first term in Equation 2-9 is the rational fraction polynomial modal model and the second term is the generalized residual polynomial model. Multiplying the second term by a fractional identity to create a common denominator,

$$[H(\omega)] = \frac{\sum_{k=0}^{m-2}(j\omega)^k[\beta_k]}{\sum_{k=0}^{m}(j\omega)^k[a_k]} + \frac{\sum_{k=0}^{m}(j\omega)^k[a_k]\sum_{k=n_l}^{n_u}(j\omega)^k[R_k]}{\sum_{k=0}^{m}(j\omega)^k[a_k]} \tag{2-10}$$

The product of the polynomials in the numerator of the second term creates another polynomial. The coefficients of the new polynomial ($\hat{R}_k$) are linear combinations of the coefficients of the multiplied polynomials (a_k, R_k) and the indices of the new series are the sum of the indices of the multiplied series.

$$[H(\omega)] = \frac{\sum_{k=0}^{m-2}(j\omega)^k[\beta_k]}{\sum_{k=0}^{m}(j\omega)^k[a_k]} + \frac{\sum_{k=n_l}^{m+n_u}(j\omega)^k[\hat{R}_k]}{\sum_{k=0}^{m}(j\omega)^k[a_k]} \tag{2-11}$$

The range of the indices on the numerator series of the second term in Equation 2-11 is $k = n_l$ to $m + n_u$, which encompasses the range of the indices on the numerator series of the first term, $k = 0$ to $m - 2$. Combining these two numerator polynomials over the common denominator creates another numerator polynomial in which the $\hat{\beta}_k$ coefficients are a linear combination of the β_k and $\hat{R}_k$ coefficients,

$$[H(\omega)] = \frac{\sum_{k=n_l}^{m+n_u}(j\omega)^k[\hat{\beta}_k]}{\sum_{k=0}^{m}(j\omega)^k[a_k]} \tag{2-12}$$

to give the final form of the rational fraction polynomial model with generalized residuals. Note that by allowing n_l to be 0 and n_u to be –2, residuals are effectively eliminated from the general form of Equation 2-12, which reduces to the form of the rational fraction polynomial model without residuals in Equation 1-7.

2.3.1 Defining the Orders of the Generalized Residual Polynomial

Specifying the minimum and maximum of the orders indices, n_l and n_u, for the residual polynomial in Equation 2-9 is not the same as specifying the orders of the numerator polynomial in Equation 2-12. The convolution of the residual polynomial with the denominator polynomial determines the orders of the numerator polynomial. To illustrate this with an example, define a residual polynomial of orders (-2,-1,0) by letting $n_l = -2$ and $n_u = 0$ with $m = 4$ in Equation 2-9, replacing the variable $j\omega$ with s and omitting the matrix notation for brevity.

$$H(s) = \frac{\beta_0 + \beta_1 s + \beta_2 s^2}{\alpha_0 + \alpha_1 s + \alpha_2 s^2 + \alpha_3 s^3 + \alpha_4 s^4} + R_{-2}s^{-2} + R_{-1}s^{-1} + R_0$$

$$= \frac{\beta_0 + \beta_1 s + \beta_2 s^2}{\alpha_0 + \alpha_1 s + \alpha_2 s^2 + \alpha_3 s^3 + \alpha_4 s^4} + \frac{(\alpha_0 + \alpha_1 s + \alpha_2 s^2 + \alpha_3 s^3 + \alpha_4 s^4)(R_{-2}s^{-2} + +R_{-1}s^{-1} + R_0)}{\alpha_0 + \alpha_1 s + \alpha_2 s^2 + \alpha_3 s^3 + \alpha_4 s^4}$$

$$= \frac{B_0 + B_1 s + B_2 s^2}{\alpha_0 + \alpha_1 s + \alpha_2 s^2 + \alpha_3 s^3 + \alpha_4 s^4} + \frac{\begin{array}{l}\alpha_0 R_{-2}s^{-2} + (\alpha_1 R_{-2} + \alpha_0 R_{-1})s^{-1} + (\alpha_2 R_{-2} + \alpha_1 R_{-1} + \alpha_0 R_0)s^0 \\ +(\alpha_3 R_{-2} + \alpha_2 R_{-1} + \alpha_1 R_0)s + (\alpha_4 R_{-2} + \alpha_3 R_{-1} + \alpha_2 R_0)s^2 \\ +(\alpha_4 R_{-1} + \alpha_3 R_0)s^3 + \alpha_4 R_0 s^4\end{array}}{\alpha_0 + \alpha_1 s + \alpha_2 s^2 + \alpha_3 s^3 + \alpha_4 s^4}$$

$$= \frac{\begin{array}{l}\alpha_0 R_{-2}s^{-2} + (\alpha_1 R_{-2} + \alpha_0 R_{-1})s^{-1} + (\alpha_2 R_{-2} + \alpha_1 R_{-1} + \alpha_0 R_0 + \beta_0)s^0 \\ +(\alpha_3 R_{-2} + \alpha_2 R_{-1} + \alpha_1 R_0 + \beta_1)s + (\alpha_4 R_{-2} + \alpha_3 R_{-1} + \alpha_2 R_0 + \beta_2)s^2 \\ +(\alpha_4 R_{-1} + \alpha_3 R_0)s^3 + \alpha_4 R_0 s^4\end{array}}{\alpha_0 + \alpha_1 s + \alpha_2 s^2 + \alpha_3 s^3 + \alpha_4 s^4}$$

$$= \frac{\hat{\beta}_{-2}s^{-2} + \hat{\beta}_{-1}s^{-1} + \hat{\beta}_0 + \hat{\beta}_1 s + \hat{\beta}_2 s^2 + \hat{\beta}_3 s^3 + \hat{\beta}_4 s^4}{a_0 + a_1 s + a_2 s^2 + a_3 s^3 + a_4 s^4}$$

$$= \frac{\sum_{k=-2}^{4} s^k \hat{\beta}_k}{\sum_{k=0}^{4} s^k A_k} \tag{2-13}$$

The numerator polynomial has a minimum index of -2, which is equal to n_l, and a maximum index of 4, which is equal to $m + n_u$, as defined in Equation 2-12. The numerator polynomial is complete, containing all orders between -2 and 4. Including a lower residual of orders (-2,-1) adds these two terms to the numerator polynomial, but including an upper residual of order 0 adds two more positive-order terms, not just a 0 order term.

By relaxing the condition in Equation 2-7 that the residual polynomials be complete, the orders could be just the even orders, just the odd orders or any sequence of orders. Now if instead the residual polynomial of orders -2 and 0 is defined, which is the traditional, physical residual model, all terms containing R_{-1} in Equation 2-13 are deleted from the numerator polynomial. The term $(a_1 R_{-2} + a_0 R_{-1})s^{-1}$ now becomes $a_1 R_{-2} s^{-1}$, but the -1 order is still in the numerator polynomial even though the -1 order was not in the defined residual polynomial. It was produced by the convolution of the two numerator polynomials in the second line of Equation 2-13. This will typically happen and is why the residual model is usually defined as a complete polynomial, not as a spaced sequence of orders.

There can be atypical cases, however, when the spacing of the residual polynomial orders is much greater than the highest order of the denominator polynomial, in which the orders

of the resulting numerator polynomial are not complete. For example, define the residual polynomial of orders (-4,4), with $m = 4$ again.

$$
\begin{aligned}
H(s) &= \frac{\beta_0 + \beta_1 s + \beta_2 s^2}{\alpha_0 + \alpha_1 s + \alpha_2 s^2 + \alpha_3 s^3 + \alpha_4 s^4} + R_{-4} s^{-4} + R_4 s^4 \\
&= \frac{\begin{array}{l} \alpha_0 R_{-4} s^{-4} + \alpha_1 R_{-4} s^{-3} + \alpha_2 R_{-4} s^{-2} + \alpha_3 R_{-4} s^{-1} + (\alpha_4 R_{-4} + \beta_0) s^0 + \beta_1 s + \beta_2 s^2 \\ + \alpha_0 R_4 s^4 + \alpha_1 R_4 s^5 + \alpha_2 R_4 s^6 + \alpha_3 R_5 s^7 + \alpha_4 R_4 s^8 \end{array}}{\alpha_0 + \alpha_1 s + \alpha_2 s^2 + \alpha_3 s^3 + \alpha_4 s^4} \\
&= \frac{\hat{\beta}_{-4} s^{-4} + \hat{\beta}_{-3} s^{-3} + \hat{\beta}_{-2} s^{-2} + \hat{\beta}_{-1} s^{-1} + \hat{\beta}_0 + \hat{\beta}_1 s + \hat{\beta}_2 s^2 + \hat{\beta}_4 s^4 + \hat{\beta}_5 s^5 + \hat{\beta}_6 s^6 + \hat{\beta}_7 s^7 + \hat{\beta}_8 s^8}{\alpha_0 + \alpha_1 s + \alpha_2 s^2 + \alpha_3 s^3 + \alpha_4 s^4}
\end{aligned}
\tag{2-14}
$$

For this case, the convolution of the numerator polynomials creates the additional orders of (-3,-2,-1,0,5,6,7,8). Combining with the original numerator polynomial then adds the orders of (1,2), but the resulting numerator polynomial does not contain the order of 3. This is a contrived example to further illustrate that the orders of the residual polynomial are not the same as the orders of the numerator polynomial in Equation 2-12. Henceforth, the residuals included in the rational fraction polynomial model will be defined by specifying the values of n_l and n_u.

2.3.2 Deconvolving the Coefficients of the Numerator Polynomial

The numerator coefficients ($\hat{\beta}_k$) in Equation 2-12 are linear combinations of the original numerator polynomial coefficients (β_k), the denominator polynomial coefficients (α_k) and the generalized residual polynomial coefficients (R_k) in Equation 2-9. The $\hat{\beta}_k$ and α_k coefficients are estimated from the solution of the frequency domain UMPA model (see

Section 1.1). The β_k and R_k coefficients can be deconvolved by setting equal the like terms in the fourth and fifth lines of Equation 2-13 and arranging into a matrix equation.

$$\begin{bmatrix} \alpha_0 & 0 & 0 & 0 & 0 & 0 \\ \alpha_1 & \alpha_0 & 0 & 0 & 0 & 0 \\ \alpha_2 & \alpha_1 & \alpha_0 & I & 0 & 0 \\ \alpha_3 & \alpha_2 & \alpha_1 & 0 & I & 0 \\ \alpha_4 & \alpha_3 & \alpha_2 & 0 & 0 & I \\ 0 & \alpha_4 & \alpha_3 & 0 & 0 & 0 \\ 0 & 0 & \alpha_4 & 0 & 0 & 0 \end{bmatrix} \begin{Bmatrix} R_{-2} \\ R_{-1} \\ R_0 \\ \beta_0 \\ \beta_1 \\ \beta_2 \end{Bmatrix} = \begin{Bmatrix} \hat{\beta}_{-2} \\ \hat{\beta}_{-1} \\ \hat{\beta}_0 \\ \hat{\beta}_1 \\ \hat{\beta}_2 \\ \hat{\beta}_3 \\ \hat{\beta}_4 \end{Bmatrix} \tag{2-15}$$

Note that Equation 2-15 has seven equations, but only six unknown β_k and R_k coefficients. A linear system of equations with more equations than unknowns has no solution unless there are redundant equations, but there are no redundant equations in Equations 2-15. This condition can be rectified by recalling that the general expansion of a partial fraction model to a rational fraction polynomial model is

$$\sum_{r=1}^{m} \frac{A_r}{s-\lambda_r} = \frac{\sum_{k=0}^{m-1} \beta_k s^k}{\sum_{k=0}^{m} \alpha_k s^k}, \qquad \text{where } \beta_{m-1} = \sum_{r=1}^{m} A_r \tag{2-16}$$

The α_k coefficients are combinations of the poles (λ_r) and the β_k coefficients are combinations of the poles and residues (A_r), except β_{m-1}, which is equal to the summation of the residues. If the assumption is made that the system described by the partial fraction model in Equation 2-16 is causal, which is a standard assumption for the modal model, the β_{m-1} terms becomes zero. This is the reason that the numerator polynomial in Equations 1-7 and 2-8 are defined with a maximum order of $m-2$. If the $m-1$ term is

included in Equation 2-15, then there are as many unknowns as equations and the system of equations has a solution.

$$\begin{bmatrix} a_0 & 0 & 0 & 0 & 0 & 0 & 0 \\ a_1 & a_0 & 0 & 0 & 0 & 0 & 0 \\ a_2 & a_1 & a_0 & I & 0 & 0 & 0 \\ a_3 & a_2 & a_1 & 0 & I & 0 & 0 \\ a_4 & a_3 & a_2 & 0 & 0 & I & 0 \\ 0 & a_4 & a_3 & 0 & 0 & 0 & I \\ 0 & 0 & a_4 & 0 & 0 & 0 & 0 \end{bmatrix} \begin{Bmatrix} R_{-2} \\ R_{-1} \\ R_0 \\ \beta_0 \\ \beta_1 \\ \beta_2 \\ \beta_3 \end{Bmatrix} = \begin{Bmatrix} \hat{\beta}_{-2} \\ \hat{\beta}_{-1} \\ \hat{\beta}_0 \\ \hat{\beta}_1 \\ \hat{\beta}_2 \\ \hat{\beta}_3 \\ \hat{\beta}_4 \end{Bmatrix} \tag{2-17}$$

The β_3 coefficient computed from Equation 2-17 should be zero, or nearly zero relative to the other coefficients, if the assumptions on the FRF model are correct, which could be used as a numerical check on the UMPA model solution. Another reason that generalized residuals is conceptually defined as a complete polynomial is that if any of R_k coefficients are omitted, Equation 2-17 would not have a solution.

The matrix equation in Equation 2-17 is for the example used in the section above. The general form of the matrix equation to solve for the coefficients of the residual and original numerator polynomials can be determined by inspection. The first $n_u - n_l + 1$ columns are filled with a cyclic permutation of the denominator a_k coefficients and the rows corresponding to the $\hat{\beta}_0$, $\hat{\beta}_1$, ..., $\hat{\beta}_{m-1}$ coefficients in the last m columns are filled with an identity matrix.

2.4 Frequency Domain UMPA Model with Generalized Residuals

The frequency domain UMPA model that includes generalized residuals can be derived similarly to Equation 1-1 by rearranging Equation 2-12 as

$$\sum_{k=0}^{m}\left[(j\omega)^k[a_k]\right][H(\omega)] = \sum_{k=n_l}^{m+n_u}(j\omega)^k\left[\hat{\beta}_k\right] \tag{2-18}$$

Again, by letting $[a_m]$ be an identity matrix and rearranging, the linear matrix equation is

$$\sum_{k=0}^{m-1}\left[(j\omega)^k[a_k]\right][H(\omega)] - \sum_{k=n_l}^{m+n_u}(j\omega)^k\left[\hat{\beta}_k\right] = -(j\omega)^m[H(\omega)] \tag{2-19}$$

or in matrix form

$$\begin{bmatrix} [a_0] & [a_1] & \cdots & [a_{m-1}] & \left[\hat{\beta}_{n_l}\right] & \cdots & \left[\hat{\beta}_{m+n_u}\right] \end{bmatrix} \begin{bmatrix} [H(\omega)] \\ j\omega[H(\omega)] \\ \vdots \\ (j\omega)^{m-1}[H(\omega)] \\ -(j\omega)^{n_l}[I_\beta] \\ \vdots \\ -(j\omega)^{m+n_u}[I_\beta] \end{bmatrix} = -(j\omega)^m[H(\omega)] \tag{2-20}$$

Note that the only difference between the UMPA models in Equations 1-1 and 2-18 is the range of the indices on the right-hand side polynomial series. Thus, all of the developments related to the basic UMPA model in Equation 1-1 are also valid for the UMPA model that includes generalized residuals in Equation 2-18. The details of some of the fundamental properties of the frequency domain UMPA model, which were summarized in Section 1.1, will be expanded for the applications in Chapter 3. Frequency domain residue estimation algorithms are extended for the inclusion of generalized residuals in Appendix A.

2.5 Relationship of Zeros and Residuals

Some interesting observations about the numerator of the rational fraction polynomial model in relation to the zeros and residuals are made in Refs. [50] and [51]. These papers

consider the theoretical relationship between the zeros and residues for a lumped-mass, analytical system. For a system with a finite number of DOFs, the partial fraction model of an FRF in Equation 1-6, which is called a pole/residue model, and the rational fraction polynomial model of an FRF in Equation 1-7, which is called a pole/zero model, are equivalent if the model is complete. However, if modes are truncated from the model, the pole/zero and pole/residue representations of an FRF are not equivalent. When there is truncation, the pole/zero model can accurately define the zeros but the residues may be greatly distorted and the pole/residue model can describe the correct residues but the zeros will be shifted. The residue distortion in the pole/zero model and the zero shifts in the pole/residue model can be reduced by the addition of polynomial residual terms, which introduces "phantom zeros" in the FRF model.

The number of zeros of an FRF varies with the location of the output DOF relative to the input DOF. The number of zeros is greatest for coincident input and output DOFs (i.e., a driving point FRF) and becomes less when the input and output DOFs are separated (i.e., a cross FRF), which is mathematically caused by a banded dynamic stiffness matrix. A driving point FRF has almost the same number of zeros as poles and truncation effect is small because an equal number of alternate poles and zeros are truncated. For a cross FRF that has fewer antiresonances, more phantom zeros are required to compensate for the truncation effects because there is an imbalance in the number of numerator and denominator terms truncated.

The order of the numerator for a driving point FRF is $m-2$, where m is the order of the denominator, but the order of the numerator for a cross FRF is always less than $m-2$.

However, the order of the numerator of the rational fraction polynomial model is treated as a constant $m-2$ for all FRFs, which consequently introduces phantom zeros for cross FRFs. This is actually a beneficial circumstance since these phantom zeros have the ability to compensate for residuals and cross FRFs need more compensation than driving point FRFs. The meaning of these observations is that any numerator polynomial terms that are not necessary to describe the zeros of an FRF can be considered as residuals.

2.6 The Consistency Diagram

The number of poles computed by a frequency domain UMPA model is equal to the order of the denominator polynomial (m) times the size of the $[\alpha]$ coefficient matrices (N_i or N_o) . The size of the $[\alpha]$ coefficient matrices is determined by the algorithm, either high-order or low-order. Thus specifying m for any parameter estimation algorithm is based on determining the number of modes, including their conjugates, that are active in the analysis frequency range. A number of techniques have been developed over the years for estimating the model order, such as, error charts, rank estimation, measurement synthesis and comparison, mode indication functions and consistency diagrams (which have also been known as stability diagrams).[1] The two techniques that will be employed in the applications in Chapter 3 are mode indication functions, specifically the Complex Mode Indicator Function (CMIF), and the consistency diagram.

To generate a traditional consistency diagram, the UMPA model is sequentially evaluated from a minimum to a maximum model α-order†. The basic concept of a consistency diagram has been extended by allowing UMPA model conditions other than the α-order to vary. For instance, in the next generation of modal parameter estimation software being developed at the University of Cincinnati Structural Dynamics Research Lab, the consistency diagram is generated by varying the α-order and also the characteristic equation normalization. That is, for each α-order, the UMPA model is solved once by normalizing the $[a_o]$ coefficient matrix to an identity and again by normalizing the $[a_m]$ coefficient matrix to an identity, which produces two sets of estimates for each model α-order. As will be discussed below and demonstrated in the applications, the model β-orders, or residuals, is another UMPA model condition that can be varied to generate a consistency diagram.

The traditional consistency diagram is plotted with the model α-orders on the vertical axis and frequency on the horizontal axis, as in Figure 2-13. The current α-order is compared to the previous α-order to evaluate the consistency of the modes. A tolerance is typically defined for each parameter being evaluated for consistency. The frequency, or imaginary part of the complex pole, is evaluated first and usually has the smallest tolerance (e.g., 1%). The damping, or real part of the complex pole, is evaluated next and

---

† The term *model α-order* refers to the highest order of the denominator polynomial in the UMPA model. The term *model β-orders* refers to the orders, from the lowest to the highest, of the numerator polynomial which includes generalized residuals.

usually has a larger tolerance than the frequency (e.g., 5%). If both the frequency and damping are consistent, then the pole is consistent. The eigenvector is evaluated last and the comparison is based on the Modal Assurance Criteria (MAC), or dot-product, of the two vectors (e.g., 90%). If both the pole and vector are consistent, then the mode is consistent.

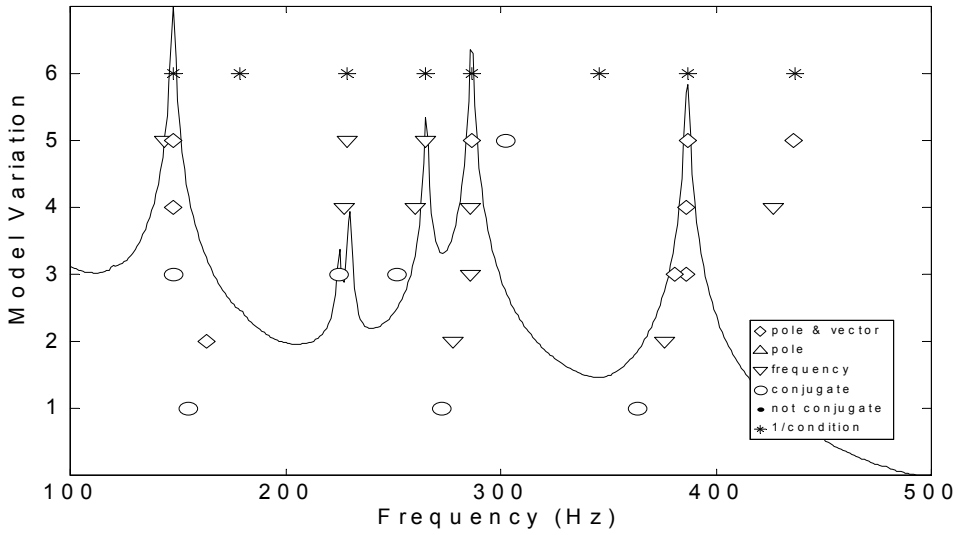

Figure 2-13. *Consistency Diagram and Legend.*

Auxiliary consistency criteria are the reciprocal condition number of the UMPA model solution and whether the poles occur in conjugate pairs. The tolerance for conjugates can be defined as either a percentage or an absolute value. The condition number applies to all poles computed by a particular UMPA model and indicates the numerical dynamic range of the solution. The accuracy or validity of the poles is suspect if the reciprocal condition number is too low. Using higher orders in the rational fraction polynomial model, actually larger absolute difference of orders when considering positive and negative orders in the generalized residual polynomial, generally leads to a lower

reciprocal condition number. Frequency and coefficient scaling improve the condition number of the UMPA model solution.[3] The tolerance on the reciprocal condition number is typically defined as an order of ten (e.g., 1e-10).

If the model α-order is too low, not all of the system poles are estimated. As the α-order is increased, more poles are estimated. Increasing the model α-order beyond the true system order produces nonphysical, or computational, poles. In time domain algorithms, the computational poles are typically located at the edges of the analysis frequency band. In frequency domain algorithms, the computational poles are spread throughout, as well as outside, the analysis frequency band. Even if the true number of system modes in the analysis frequency band is known, the residual effects of out-of-band modes affect the estimation of in-band modes. Often a much larger model α-order is needed to adequately compensate for residuals, which can clutter the consistency diagram.

A high level of user interaction is required in using consistency diagrams to sort the system poles from the computational poles. As model order increases, the system poles will hopefully become consistent, that is, consistent estimates of the system poles are computed for each successive model order. Well excited modes will tend to become consistent at lower model orders than poorly excited modes. Although, the poles do not have to be all selected from the same model order. The computational poles will typically not become consistent.

By including residuals in the parameter estimation algorithm, the model α-order does not have to be over-specified as much to compensate for out-of-band modes. In the currently

available implementations of consistency diagrams, residuals can be included as a polynomial, but with a fixed number of terms. Another way to generate a consistency diagram is to fix the α-order and evaluate the UMPA model for a sequence of residuals, or β-orders. Whereas the α-order is varied from a minimum to a maximum, the positive β-orders can be varied, or the negative β-orders, or a combination of both.

Consistency diagrams that vary the α-order have customarily been used only for high-order models since the model order for a low-order model is theoretically fixed at two or one. A consistency diagram that varies the β-order can now be used with a low-order algorithm the same as with a high-order algorithm. By further broadening the concept of a consistency diagram, one can be generated by varying the α-order, varying the β-orders, or a combination of both. This basic idea is implemented in the applications developed in Chapter 3.

CHAPTER THREE

3 Applications

This chapter describes applications of the generalized residual polynomial in frequency domain modal parameter estimation algorithms. The first application is an SDOF algorithm, which is included as a completion of some of the basic ideas of the generalized residual polynomial introduced in Section 2.2. The other three applications focus on generating consistency diagrams with variations of the residual polynomial orders (i.e., n_l and n_u, or the UMPA model β-order). The CMIF and EMIF methods rely on condensation of the FRF matrix and use a low-order UMPA model, in which case the α-order is fixed but the β-order is a variable parameter in the algorithm. A consistency diagram for these methods is generated by varying the β-order. Finally, for the general UMPA application, a consistency diagram is generated for a low-order model by varying the β-order and for a high-order model by varying both the α-order and the β-order with several different permutations. The examples for the first application use synthesized data and the examples for the other three applications use measured FRF datasets.

3.1 Single Degree-of-Freedom Parameter Estimation Methods

The simplest modal parameter estimation method is a single degree-of-freedom algorithm. For an SDOF algorithm, the frequency range of interest is a band around a resonance peak in an FRF, and only one mode (actually a pair of conjugate poles) is estimated from the FRF. With respect to any one mode, all other modes are considered residuals and their contribution in the frequency range of interest is included as a generalized residual polynomial. This SDOF algorithm deals with a single-input, single-output (SISO) measurement, which is equivalent to Equation 2-18 with $m = 2$ and scalar polynomial coefficients.

$$\sum_{k=0}^{2}\left[(j\omega)^k a_k\right]H(\omega) = \sum_{k=n_l}^{n_u+2}(j\omega)^k \hat{\beta}_k \tag{3-1}$$

Setting $a_2 = 1$ and rearranging into a linear matrix equation,

$$\begin{bmatrix} a_0 & a_1 & \hat{\beta}_{n_l} & \cdots & \hat{\beta}_{n_u+2} \end{bmatrix} \begin{bmatrix} H(\omega) \\ j\omega H(\omega) \\ -(j\omega)^{n_l} I_\beta \\ \vdots \\ -(j\omega)^{n_u+2} I_\beta \end{bmatrix} = -(j\omega)^2 H(\omega) \tag{3-2}$$

An overdetermined set of equations is generated by evaluating Equation 3-2 at a number of frequencies, N_s, (positive and negative) and augmenting the matrix equations.

$$\begin{bmatrix} a_0 & a_1 & \hat{\beta}_{n_l} & \cdots & \hat{\beta}_{n_u+2} \end{bmatrix} \begin{bmatrix} H(\omega_1) & \cdots & H(\omega_{N_s}) \\ j\omega H(\omega_1) & \cdots & j\omega H(\omega_{N_s}) \\ -(j\omega_1)^{n_l} I_\beta & \cdots & -(j\omega_{N_s})^{n_l} I_\beta \\ \vdots & & \vdots \\ -(j\omega_1)^{n_u+2} I_\beta & \cdots & -(j\omega_{N_s})^{n_u+2} I_\beta \end{bmatrix} = -\begin{bmatrix} (j\omega_1)^2 H(\omega_1) & \cdots & (j\omega_N)^2 H(\omega_{N_s}) \end{bmatrix} \tag{3-3}$$

The a_k and $\hat{\beta}_k$ coefficients are found by transposing Equation 3-3 and using a suitable pseudo-inverse numerical technique. The pair of conjugate poles is then computed as the eigenvalues of the companion matrix

$$[C] = \begin{bmatrix} -a_1 & -a_0 \\ 1 & 0 \end{bmatrix} \tag{3-4}$$

The $\hat{\beta}_k$ coefficients can be deconvolved into the coefficients of the original numerator polynomial without residuals (β_0) and of the residual polynomial ($R_{n_l}, ..., R_{n_u}$) with the algorithm developed in Section 2.3.2. The residue (A_1) can then be computed directly from Equation A-17.

As a completion of the 3-DOF example introduced in relation to Equations 2-3 through 2-6 and Figures 2-11 and 2-12, the modal parameters of the second mode are estimated with the SDOF frequency domain algorithm of Equation 3-1 for several residual polynomials. The FRF synthesized from Equation 2-12 with the estimated a_k and $\hat{\beta}_k$ coefficients is compared to the analytical function† in Figure 3-1(a) for no residuals (i.e., $n_l = 0$ and $n_u = -2$) , in Figure 3-2(b) for the physical residuals (i.e., $n_l = -2$ and $n_u = 0$) and in Figure 3-3(a) for a general residual polynomial ($n_l = -4$ and $n_u = 4$). The magnitudes of the residual polynomial coefficients are also plotted in Figures 3-2(b) and 3-3(b). The inset plot in the (a) figures details the comparison of the analytical and synthesized functions in the region near the resonance peak. In Figure 3-3(c) the FRF is synthesized

† The *analytical function* is the FRF synthesized from Equation 1-6 with the specified damped natural frequency, damping ratio and residue.

from Equation 2-9 using the coefficients of the original numerator polynomial without residuals (β_0) and of the residual polynomial ($R_{-4}, ..., R_4$), which were determined from Equation 3-5. This plot is included to show that the same FRF is synthesized from Equation 2-12 and 2-9 and to verify the deconvolution of the estimated numerator polynomial into the original numerator and residual polynomials. In Figure 3-3(d), the residual polynomial is synthesized and compared to the modes 1+3 function as in Figure 2-12 to illustrate that the residual polynomial does indeed account for the contributions of modes 1 and 3 in the frequency range of interest. The estimated modal parameters are listed in Table 3-1.

$$\begin{bmatrix} a_0 & 0 & 0 & 0 & 0 & 0 & 0 & 0 & 0 & 0 & 0 \\ a_1 & a_0 & 0 & 0 & 0 & 0 & 0 & 0 & 0 & 0 & 0 \\ a_2 & a_1 & a_0 & 0 & 0 & 0 & 0 & 0 & 0 & 0 & 0 \\ 0 & a_2 & a_1 & a_0 & 0 & 0 & 0 & 0 & 0 & 0 & 0 \\ 0 & 0 & a_2 & a_1 & a_0 & 0 & 0 & 0 & 0 & 1 & 0 \\ 0 & 0 & 0 & a_2 & a_1 & a_0 & 0 & 0 & 0 & 0 & 1 \\ 0 & 0 & 0 & 0 & a_2 & a_1 & a_0 & 0 & 0 & 0 & 0 \\ 0 & 0 & 0 & 0 & 0 & a_2 & a_1 & a_0 & 0 & 0 & 0 \\ 0 & 0 & 0 & 0 & 0 & 0 & a_2 & a_1 & a_0 & 0 & 0 \\ 0 & 0 & 0 & 0 & 0 & 0 & 0 & a_2 & a_1 & 0 & 0 \\ 0 & 0 & 0 & 0 & 0 & 0 & 0 & 0 & a_2 & 0 & 0 \end{bmatrix} \begin{Bmatrix} R_{-4} \\ R_{-3} \\ R_{-2} \\ R_{-1} \\ R_0 \\ R_1 \\ R_2 \\ R_3 \\ R_4 \\ \beta_0 \\ \beta_1 \end{Bmatrix} = \begin{Bmatrix} \hat{\beta}_{-4} \\ \hat{\beta}_{-3} \\ \hat{\beta}_{-2} \\ \hat{\beta}_{-1} \\ \hat{\beta}_0 \\ \hat{\beta}_1 \\ \hat{\beta}_2 \\ \hat{\beta}_3 \\ \hat{\beta}_3 \\ \hat{\beta}_5 \\ \hat{\beta}_6 \end{Bmatrix} \tag{3-5}$$

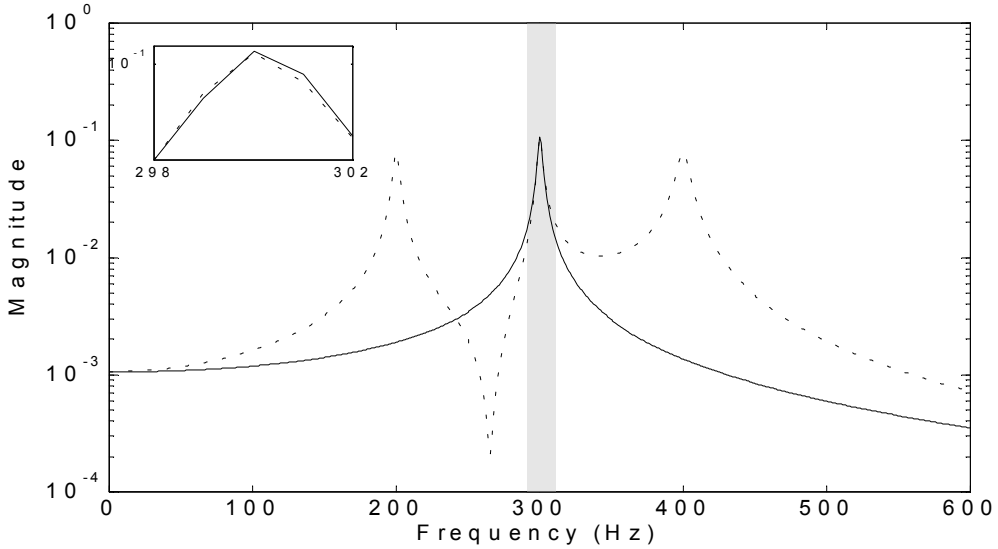

Figure 3-1(a). *Comparison of a 3-DOF analytical FRF (dashed line) and the FRF synthesized from estimated polynomial coefficients (solid line), with no residuals.*

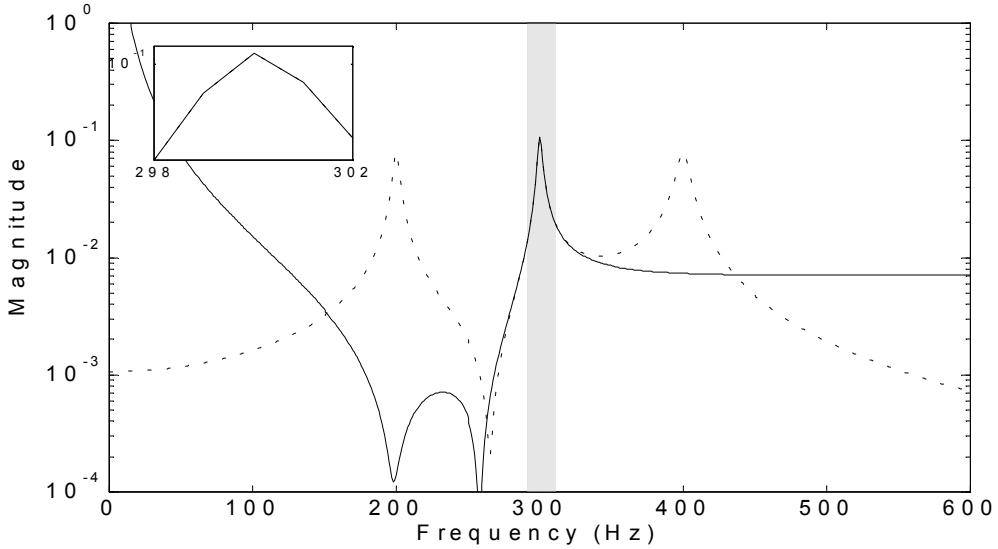

Figure 3-2(a). *Comparison of a 3-DOF analytical FRF (dashed line) and the FRF synthesized from estimated polynomial coefficients (solid line), with physical residuals.*

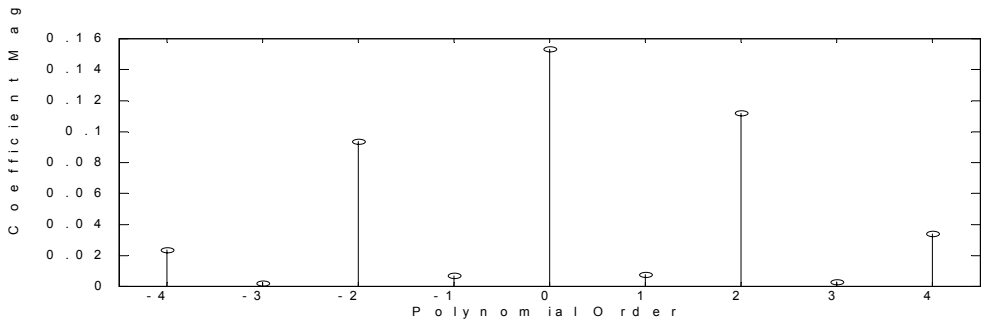

Figure 3-2(b). *Magnitude of residual polynomial coefficients for Figure 3-2(a).*

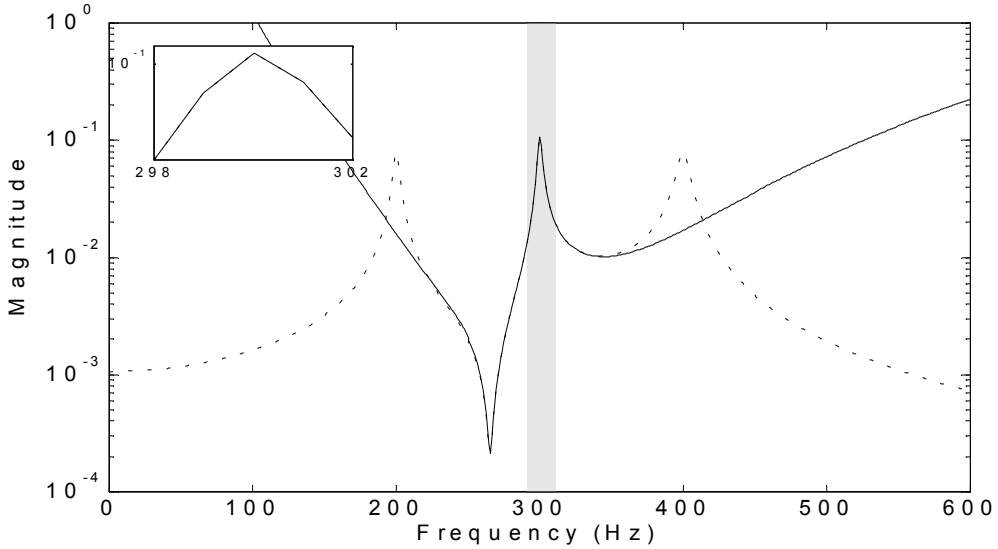

Figure 3-3(a). *Comparison of a 3-DOF analytical FRF (dashed line) and the FRF synthesized from estimated polynomial coefficients (solid line), with a generalized residual polynomial of orders -4:4.*

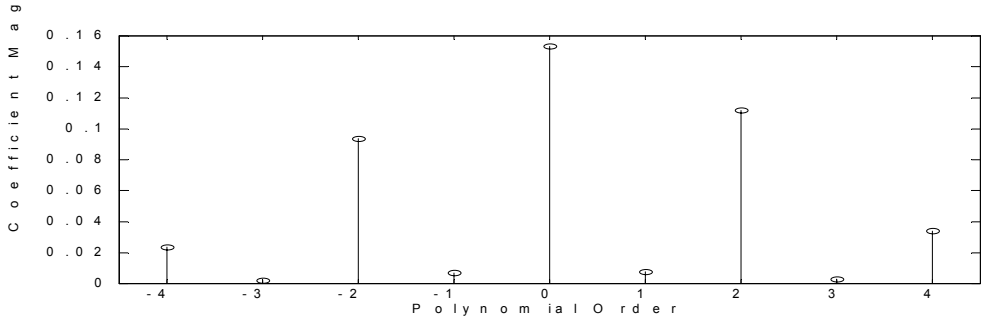

Figure 3-3(b). *Magnitude of residual polynomial coefficients for Figure 3-3(a).*

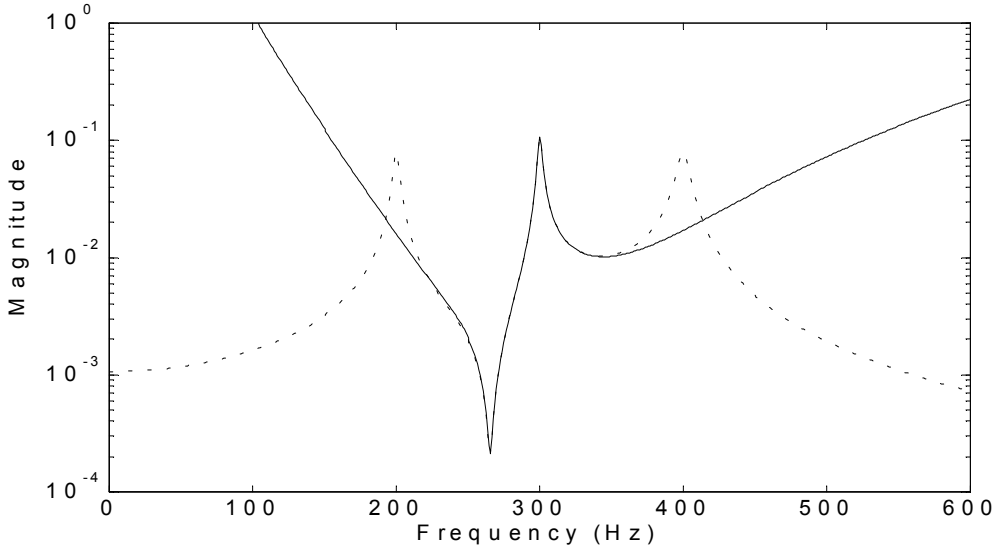

Figure 3-3(c). *Comparison of a 3-DOF analytical FRF (dashed line) and the FRF synthesized from estimated and deconvolved polynomial coefficients (solid line), with a generalized residual polynomial of orders -4:4.*

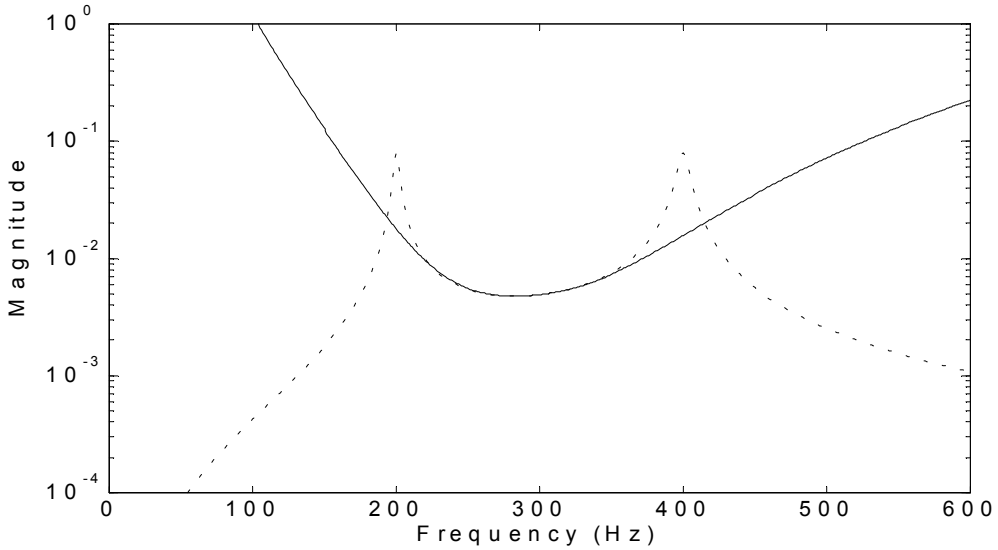

Figure 3-3(d). *Comparison of the generalized residual polynomial with orders -4:4 to the contribution of the residual modes.*

Residuals	Frequency	Damping	Residue
analytical system	300 Hz	0.5 %	$0 - j1.00$
$n_l = 0,\ n_u = -2$	300.2048 Hz	0.4880 %	$0.0000 - j0.9931$
$n_l = -2,\ n_u = 0$	300.0008 Hz	0.5000 %	$0.0000 - j1.0000$
$n_l = -4,\ n_u = 4$	300.0000 Hz	0.5000 %	$0.0000 - j1.0000$

Table 3-1. *Estimated modal parameters of 3-DOF system.*

The plots in Figures 3-1 through 3-3 and the results in Table 3-1 show that the greatest error in the estimated modal parameters is for the case with no residuals and the accuracy improves by including residuals in the parameter estimation model. In this case, the physical residuals were adequate to compensate for the out-of-band modes, but this system had relatively well-spaced modes.

The next system has more closely-spaced modes and again the modal parameters of the second mode are estimated with the SDOF frequency domain algorithm of Equation 3-1 for several residual polynomials. The FRF synthesized from Equation 2-12 with the estimated α_k and $\hat{\beta}_k$ coefficients is compared to the analytical function in Figure 3-4(a) for no residuals, in Figure 3-5(b) for the physical residuals and in Figure 3-6(a) for a general residual polynomial ($n_l = -12$ and $n_u = 12$). The magnitudes of the residual polynomial coefficients are also plotted in Figures 3-5(b) and 3-6(b). The inset plot in the (a) figures details the comparison of the original and synthesized functions in the region near the resonance peak. The estimated modal parameters are listed in Table 3-2.

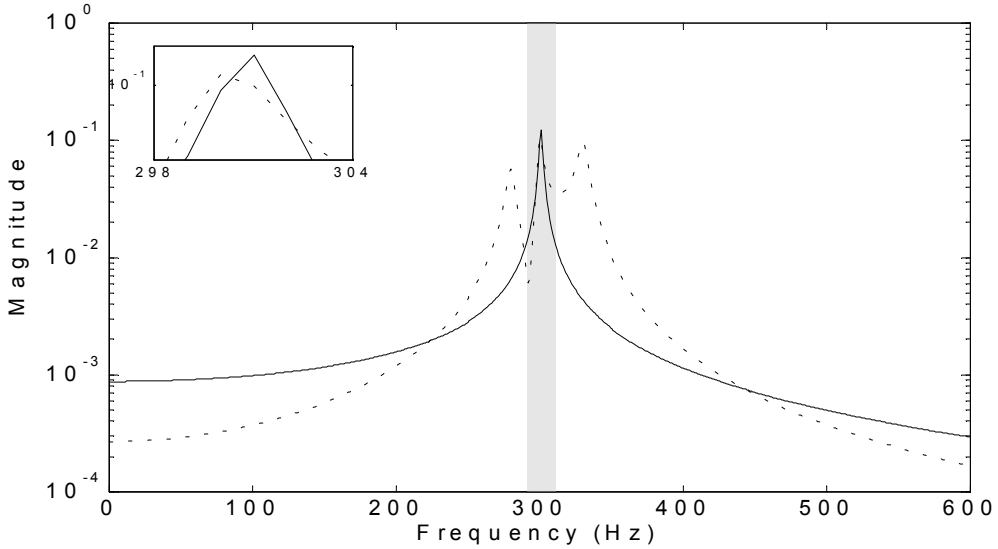

Figure 3-4(a). *Comparison of a 3-DOF analytical FRF (dashed line) and the FRF synthesized from estimated polynomial coefficients (solid line), with no residuals.*

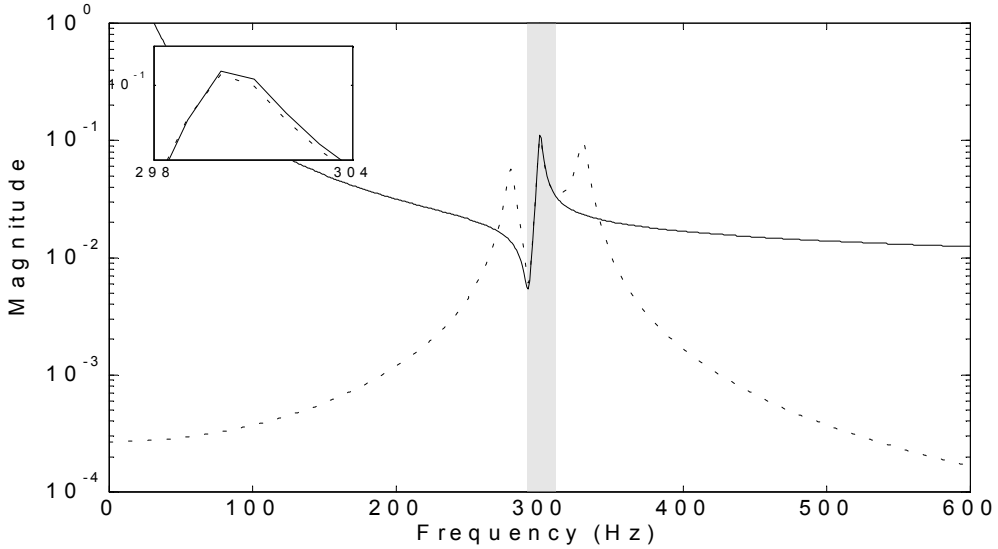

Figure 3-5(a). *Comparison of a 3-DOF analytical FRF (dashed line) and the FRF synthesized from estimated polynomial coefficients (solid line), with physical residuals.*

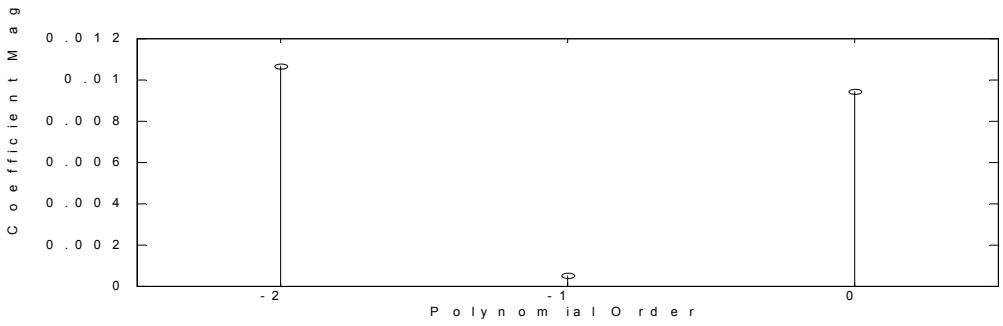

Figure 3-5(b). *Magnitude of residual polynomial coefficients for Figure 3-5(a).*

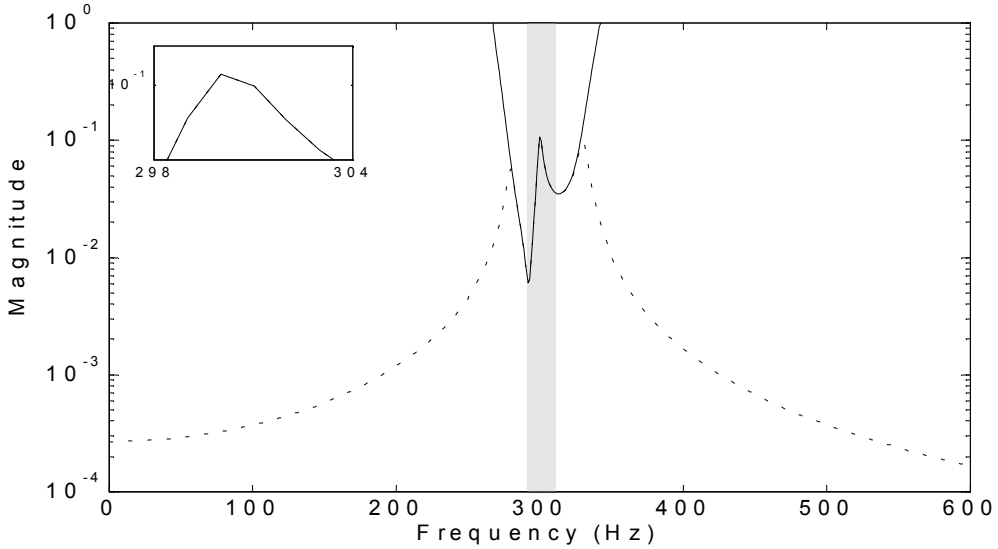

Figure 3-6(a). *Comparison of a 3-DOF analytical FRF (dashed line) and the FRF synthesized from estimated polynomial coefficients (solid line), with a generalized residual polynomial of orders -12:12.*

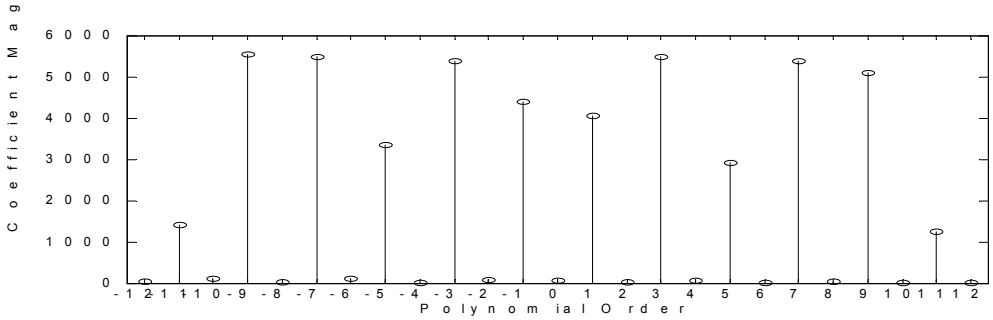

Figure 3-6(b). *Magnitude of residual polynomial coefficients for Figure 3-6(a).*

Residuals	Frequency	Damping	Residue
analytical system	300 Hz	0.5 %	$0 - j1.00$
$n_l = 0,\ n_u = -2$	300.8512 Hz	0.3545 %	$0.0000 - j\ 0.8265$
$n_l = -2,\ n_u = 0$	300.0603 Hz	0 .4923 %	$0.0000 - j\ 0.9936$
$n_l = -12,\ n_u = 12$	300.0000 Hz	0.5000 %	$0.0000 - j1.0004$

Table 3-2. *Estimated modal parameters of 3-DOF system.*

The plots in Figures 3-4 through 3-6 and the results in Table 3-2 show essentially the same results as the preceding example in that the greatest error in the estimated modal parameters is for the case with no residuals and the accuracy improves by including residuals in the parameter estimation model. However, there is much greater error with no residuals and still some error with the physical residuals. In this case, a generalized residual polynomial with more orders was needed to accurately estimate the modal parameters. This is typical, that is, the closer the out-of-band modes are to the frequency range of interest, the more residual terms that are required to completely account for their effects.

3.2 Complex Mode Indicator Function Parameter Estimation Method

The Complex Mode Indicator Function (CMIF) was originally developed as aid to model order determination for multiple reference datasets,[25] but has since become the basis for a spatial domain parameter estimation algorithm.[52,53] As stated previously in Section 1.2, the common approach in modal parameter estimation is a two-stage, linear process. The frequency domain algorithms considered thus far, as well as time domain algorithms, produce temporal information, the poles, in the first stage and scaled spatial information,

the modal vectors and modal scaling, in the second stage. Conversely, spatial domain algorithms produce unscaled spatial information, the modal vectors, in the first stage and temporal and scaling information, the poles and modal scaling, in the second stage. A spatial domain algorithm is classified as a zero-order UMPA model, which is an algorithm that is "programmed to process data at a single temporal condition (frequency or time)."[1]

The CMIF is formed by computing the economical singular value decomposition (SVD) of the FRF matrix at each spectral line,

$$\underset{(N_o \times N_i)}{[H(\omega_k)]} = \underset{(N_o \times N_i)(N_i \times N_i)}{[U_k]} \lceil \Sigma_k \rfloor \underset{(N_i \times N_i)}{[V_k]^H} \tag{3-6}$$

where $\lceil \Sigma_k \rfloor$ is a diagonal matrix of real, non-negative singular values in ascending order, $[U_k]$ is the matrix of left singular vectors and $[V_k]$ is the matrix of right singular vectors, for $N_o \geq N_i$, otherwise CMIF processes the transpose of the FRF matrix.

A CMIF is a plot of the singular values as a function of frequency, usually on a log-magnitude scale, with one curve for each singular value. Often the tracked CMIF is plotted to alleviate the singular value crossover effect.[54] The peaks in the CMIF curves coincide with the resonances of the system and locate the damped natural frequency of the modes to the nearest spectral line. The left singular vector associated with the significant singular value at a CMIF peak is an approximation of the mode shape, and the

right singular vector is an approximation of the modal participation factors. Figure 3-7 shows the CMIF of a measured dataset of FRFs for a system with N_o=145, N_i=3 and Δf=1 Hz.

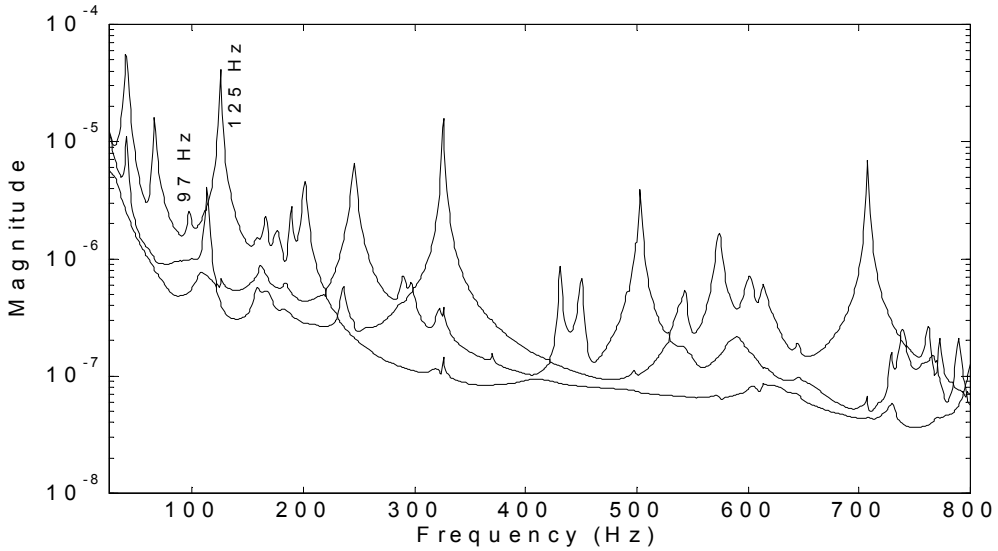

Figure 3-7. *Complex mode indicator function of a measured FRF dataset.*

To use the CMIF parameter estimation method, the peaks in the CMIF curves corresponding to modes of the system are selected by the operator. This is usually a straightforward task, but in some instances additional analysis techniques, such as MAC, mode tracking[1] and consistency diagrams, are needed to select a valid set of modes. If two CMIF curves have a peak at the same, or nearly the same, frequency, then there are two significant singular vectors, which indicates a repeated, or pseudo-repeated, mode of multiplicity two. This same reasoning also applies to modes of multiplicity greater than two.

Time and frequency domain algorithms utilize the poles obtained in the first stage to estimate the residues in the second stage. The approximate modal vectors and participation factors obtained in the first stage of the CMIF method are used to generate an Enhanced Frequency Response Function (eFRF) for each mode. The poles are then estimated from the eFRFs, which must be scaled correctly[54,55] to also be used to estimate the modal scaling[53]. The left and right singular vectors at the CMIF peaks create a spatial filter that transforms the measured FRF matrix from the physical space to the modal space and creates a virtual measurement that enhances the mode of interest. The eFRF for mode s, $eH_s(\omega_k)$, is a scalar function that is generated at each spectral line as,

$$\underset{(1\times1)}{eH_s(\omega_k)} = \underset{(1\times N_o)}{\{U_s\}^T} \underset{(N_o\times N_i)}{[H(\omega_k)]} \underset{(N_1\times1)}{\{V_s\}} = \{U_s\}^T \left[\sum_{r=1}^{2N} \frac{\{\psi_r\}\{L_r\}^T}{j\omega - \lambda_r} \right] \{V_s\} \tag{3-7}$$

The effect of this operation is to attenuate the contribution of all modes except mode s, thus enhancing this mode. The degree of enhancement is dependent on the inner-product of the left singular vector $\{U_s\}$ and the modal vectors $\{\psi_r\}$. If the spatial distribution of the DOFs is such that the mode shapes are sufficiently dissimilar, then inner-product will approach zero for $r \neq s$ and mode r will not contribute to the summation in Equation 3-7. Ideally the transformation uncouples the eFRF into an SDOF function in the region near the principal peak, such as in Figure 3-8. Then the pole can be estimated from the eFRF for each mode with a scalar, SDOF, frequency domain model.

$$\left[(j\omega)^2 a_2 + (j\omega) a_1 + a_o \right] eH(\omega) = \beta_o \tag{3-8}$$

The eFRF generated by Equation 3-7 of the CMIF peak marked at 125 Hz in Figure 3-7 is plotted in Figure 3-8, also plotted is the eFRF synthesized by Equation 3-8 with the estimated α_k and β_0 polynomial coefficients. The shaded region indicates the frequency band around the peak evaluated in the parameter estimation algorithm. The estimated frequency was 125.270 Hz and the damping ratio was 0.595 %. This example shows that if the eFRF is uncoupled into a SDOF function, at least near the principal peak, an SDOF algorithm is adequate to estimate the pole and residuals are not needed.

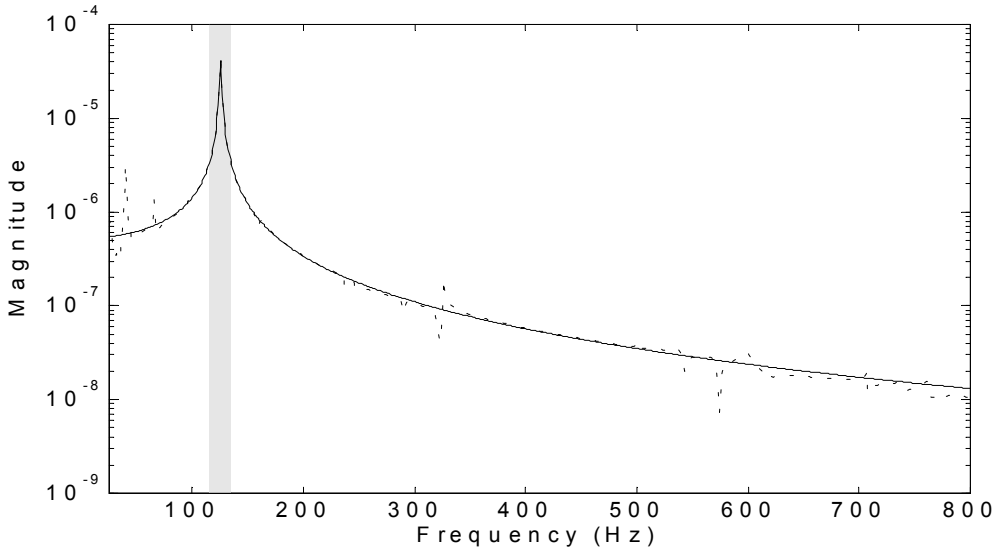

Figure 3-8. *Enhanced frequency response function for the mode at 125 Hz; generated from measured FRFs (dashed line) and synthesized from UMPA model (solid line).*

If the eFRF does not isolate the mode of interest, the surrounding modes will influence the estimation of pole and a simple SDOF algorithm is not sufficient. The basic idea of the CMIF parameter estimation method is to select peaks from the CMIF curves and obtain the mode shape and pole for that mode directly. Increasing the model α-order is not a preferable modification of the algorithm to account for the other modes present in

the eFRF, because to do so would introduce computational poles, which is contrary to the benefits of the CMIF method. Since these other modes in the eFRF are just residuals with respect to the mode of interest, an SDOF algorithm with a generalized residual polynomial, such as that in Section 3.1 with the FRF replaced with an eFRF, is appropriate for the CMIF method.

$$\sum_{k=0}^{2}\left[(j\omega)^k a_k\right] eH(\omega) = \sum_{k=n_l}^{n_u+2}(j\omega)^k \hat{\beta}_k \tag{3-9}$$

The eFRF of the CMIF peak marked at 97 Hz in Figure 3-7 is shown in Figure 3-9. It is not an SDOF function near the principal peak, but has significant contribution of some nearby modes which were not attenuated by the spatial filter. Some residuals are needed in the parameter estimation algorithm to account for the other modes in the eFRF. But which residual polynomial? Instead of trial and error with different residual polynomials, a consistency diagram can be generated with the indices of the residual polynomial (n_l and n_u) as the variable parameters in the UMPA model. In a traditional consistency diagram for model α-order, only the value of m, the upper order of the denominator polynomial, can be varied (e.g.,$m = 2, 3, \ldots, 10$). In a consistency diagram for residuals, the values of n_l, n_u or both can be varied. The indices n_l and n_u define the orders of the generalized residual polynomial $\sum_{k=n_l}^{n_u}(j\omega)^k R_k$, which multiplies with $\sum_{k=0}^{2}(j\omega)^k a_k$ and combines with β_o to form the numerator polynomial of $\sum_{k=n_l}^{n_u+2}(j\omega)^k \hat{\beta}_k$.

The consistency diagram for the peak at 97 Hz is shown in Figure 3-10(a) for varying n_l, in Figure 3-10(b) for varying n_u and in Figure 3-10(c) for varying both n_l and n_u. Table 3-3 lists the orders of the residual polynomial for the model variations of the consistency

diagrams in Figures 3-10(a-c). The consistency criteria are: 1% for frequency, 5% for damping, 1% for conjugates and 10^{-6} for reciprocal of the condition number. Figure 3-11 is the eFRF synthesized by Equation 3-9 for all model variations of the consistency diagram in Figure 3-10(c), the inset plot shows the region near the peak of interest. Figure 3-12 is the synthesized eFRF for model variation number 5, the first consistent pole. In Table 3-4 is a list of the poles estimated for the model variations of the consistency diagram in Figure 3-10(c).

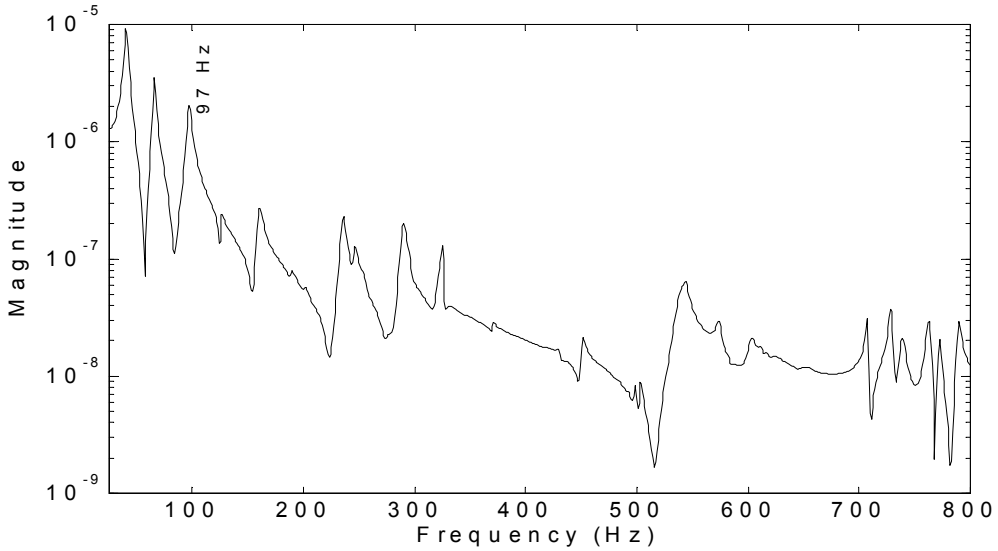

Figure 3-9. *Enhanced frequency response function for the mode at 97 Hz.*

	Figure 3-10(a)	Figure 3-10(b)	Figure 3-10(c)
1	$n_l = 0,\ n_u = -2$ (*no residuals*)	$n_l = 0,\ n_u = -2$ (*no residuals*)	$n_l = 0,\ n_u = -2$ (*no residuals*)
2	$n_l = 0,\ n_u = 1$	$n_l = -1,\ n_u = 0$	$n_l = 0,\ n_u = 0$
3	$n_l = 0,\ n_u = 2$	$n_l = -2,\ n_u = 0$	$n_l = -1,\ n_u = 1$
4	$n_l = 0,\ n_u = 3$	$n_l = -3,\ n_u = 0$	$n_l = -2,\ n_u = 2$
5	$n_l = 0,\ n_u = 4$	$n_l = -4,\ n_u = 0$	$n_l = -3,\ n_u = -3$

6			$n_l = -4,\ n_u = -4$

Table 3-3. *The lower and upper orders of the residual polynomial for the model variations of the consistency diagrams in Figures 3-10(a-c).*

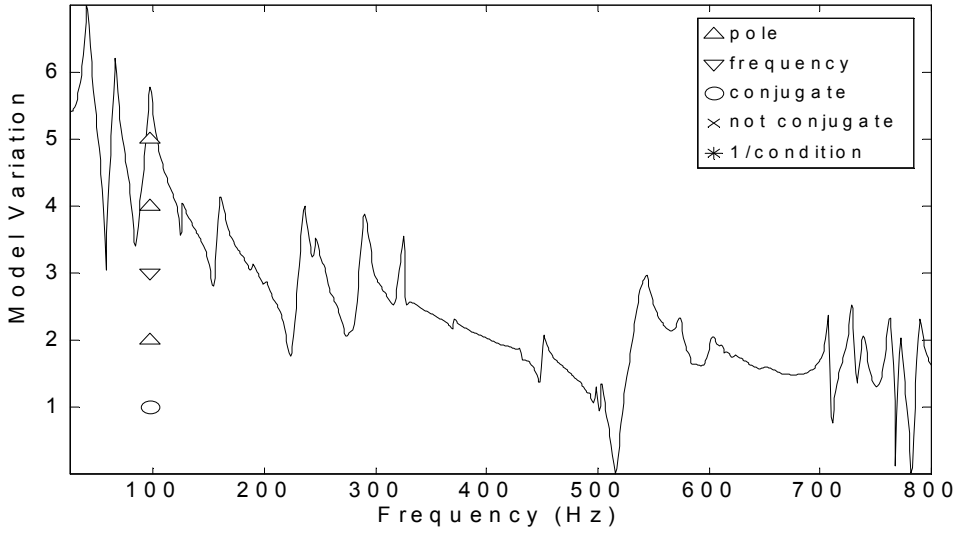

Figure 3-10(a). *CMIF method consistency diagram of the mode at 97 Hz, for varying the lower order of the residual polynomial.*

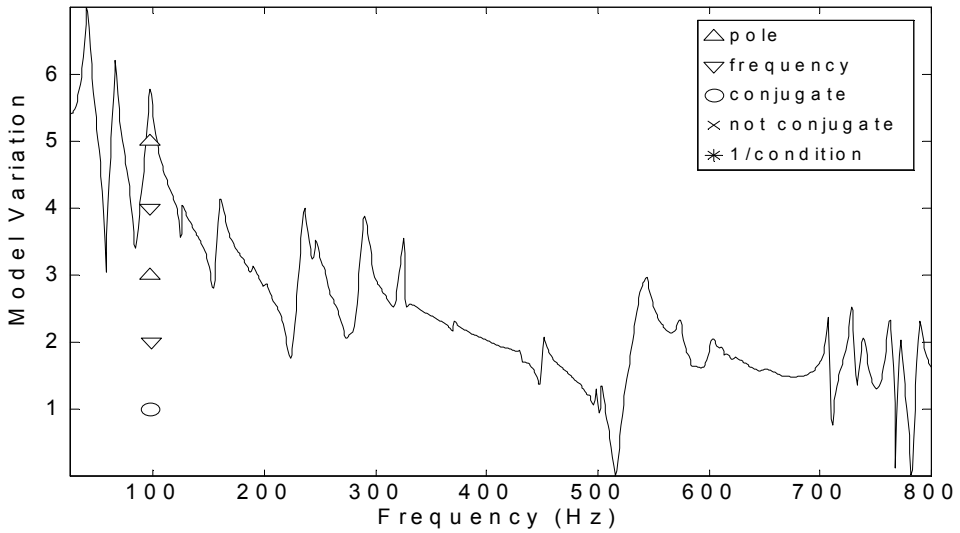

Figure 3-10(b). *CMIF method consistency diagram of the mode at 97 Hz, for varying the upper order of the residual polynomial.*

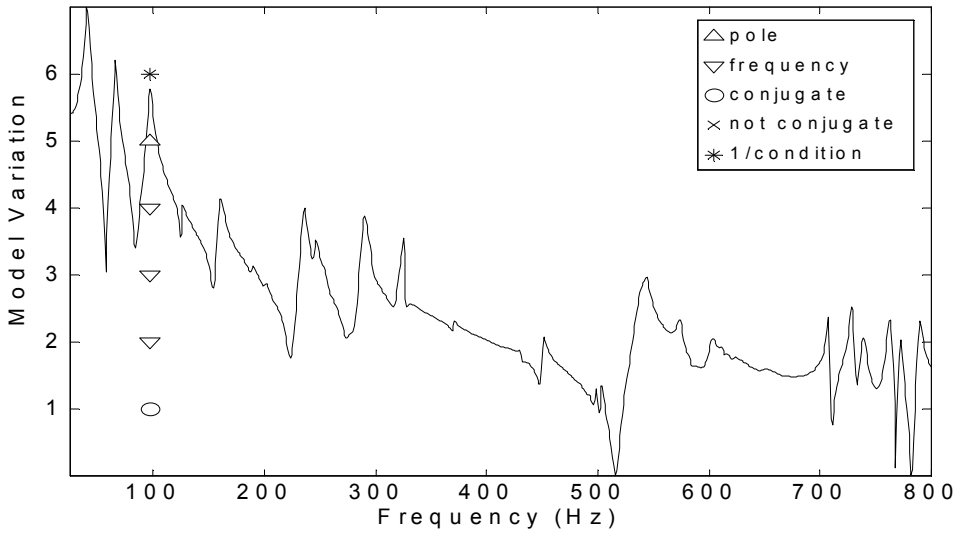

Figure 3-10(c). *CMIF method consistency diagram of the mode at 97 Hz, for varying the lower and upper orders of the residual polynomial*.

	Residuals	Frequency	Damping	Consistency	1/Condition
1	$n_l = 0,\ n_u = -2$	97.002 Hz	1.898 %	conjugate	3.777e-001
2	$n_l = 0,\ n_u = 0$	96.895 Hz	2.190 %	frequency	5.149e-002
3	$n_l = -1,\ n_u = 1$	96.929 Hz	1.903 %	frequency	2.645e-003
4	$n_l = -2,\ n_u = 2$	96.900 Hz	2.058 %	frequency	1.365e-004
5	$n_l = -3,\ n_u = 3$	96.880 Hz	2.052 %	pole	6.962e-006
6	$n_l = -4,\ n_u = 4$	96.880 Hz	2.070 %	1/condition	3.509e-007

Table 3-4. *The estimated poles for the model variations of the consistency diagram in Figure 3-10(c).*

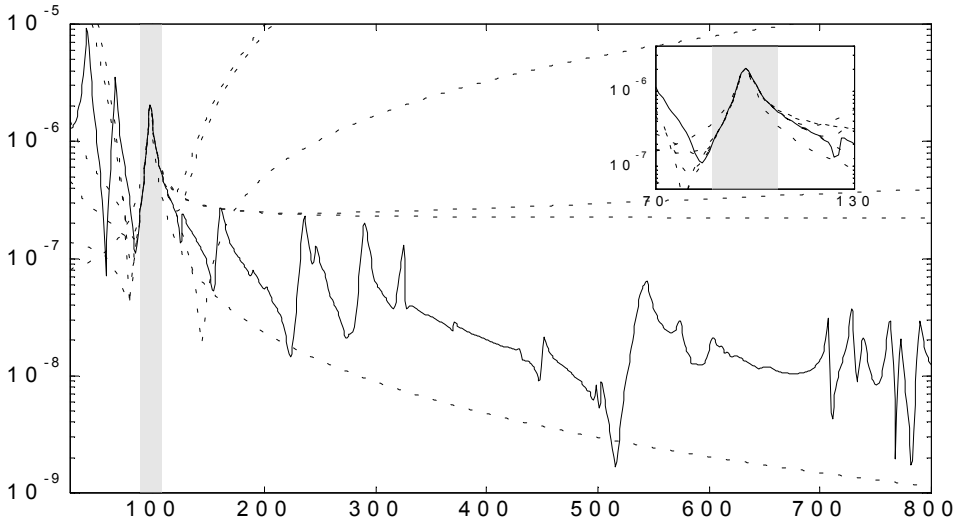

Figure 3-11. *Enhanced frequency response function for the mode at 97 Hz; generated from measured FRFs (solid line) and synthesized from UMPA model for all residual polynomials of the consistency diagram in Figure 3-10(c) (dashed lines).*

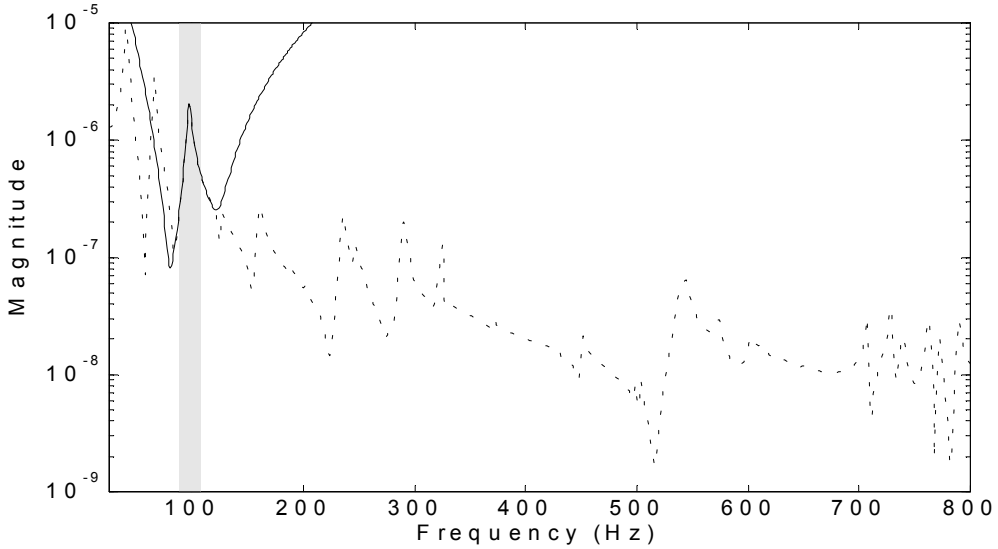

Figure 3-12. *Enhanced frequency response function for the mode at 97 Hz; generated from measured FRFs (dashed line) and synthesized from UMPA model variation 5 in Figure 3-10(c) (solid line).*

In Figure 3-13 is the consistency diagram for the earlier example of the mode at 125 Hz in Figure 3-8, the orders of the residual polynomial and the estimated poles for the model

variations are listed in Table 3-5 . In this case of an uncoupled eFRF, the pole is consistent for no residuals. The addition of residuals does not adversely affect the estimation of the pole, until the numerator polynomial orders become high enough to cause a poor condition number of the UMPA model solution. Table 3-5 is a list of the modal parameters estimated for the model variations of the consistency diagram in Figure 3-13.

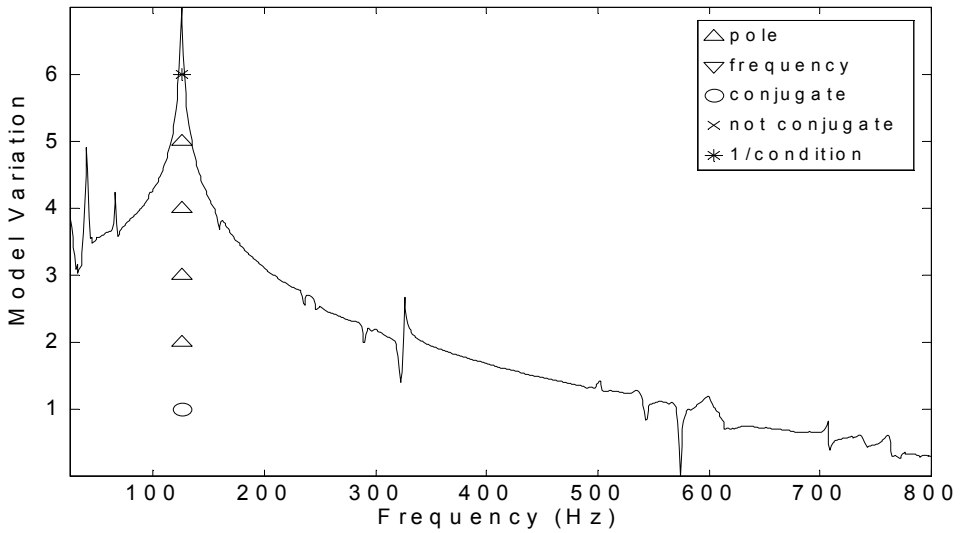

Figure 3-13. *CMIF method consistency diagram of the mode at 125 Hz.*

	Residuals	Frequency	Damping	Consistency	1/Condition
1	$n_l = 0,\ n_u = -2$	125.270 Hz	0.595 %	conjugate	3.220e-001
2	$n_l = 0,\ n_u = 0$	125.264 Hz	0.595 %	pole	4.476e-002
3	$n_l = -1,\ n_u = 1$	125.263 Hz	0.592 %	pole	1.826e-003
4	$n_l = -2,\ n_u = 2$	125.263 Hz	0.592 %	pole	7.292e-005
5	$n_l = -3,\ n_u = 3$	125.263 Hz	0.593 %	pole	2.887e-006
6	$n_l = -4,\ n_u = 4$	125.263 Hz	0.593 %	1/condition	1.137e-007

Table 3-5. *The lower and upper orders of the residual polynomial and the estimated poles for the model variations of the consistency diagram in Figure 3-13.*

3.3 Enhanced Mode Indicator Function Parameter Estimation Method

In regions of high modal density and for datasets with limited spatial resolution, the CMIF method may not be able to isolate individual modes in an uncoupled eFRF. The assumption that the singular vector is a good approximation of the mode shape may also be invalid in these regions. The Enhanced Mode Indicator Function (EMIF) parameter estimation method[56-59] is an MDOF extension of the CMIF method that has been developed for cases in which the SDOF techniques of the previous section are not sufficient to estimate the modal parameters. EMIF uses a low-order, frequency domain UMPA model with matrix coefficients to estimate the poles in a selected frequency band. The EMIF method relies on a transformation of the FRF matrix, similar to the eFRF for the CMIF method. But instead of condensing the FRF matrix to a scalar function for a single mode, only the response space is condensed to limit the number of poles of the second-order UMPA model.

The size of the UMPA model denominator polynomial coefficient matrices is equal to the number of active modes in a frequency band of interest (N_b), which is determined from the CMIF plot. It is not necessary to study the CMIF plot to track the curves and select peaks as in the CMIF method, but just to count the number of CMIF curves that rise to peaks in the frequency band. In general, with more references in the dataset, that is, with more CMIF curves, the number of modes active in a frequency band is more readily apparent. The SVD is computed on a matrix containing columns of the FRF matrix at spectral lines in that frequency band, as in Equation 3-11. The significant left singular

vectors, $[U_b]$, equal in number to the modes in the band, are used as spatial filters to condense the measured FRFs to a set of eFRFs.

$$\underset{(N_b \times N_i)}{[e\bar{H}(\omega_k)]} = \underset{(N_b \times N_o)}{[U_b]^T} \underset{(N_o \times N_i)}{[H(\omega_k)]} \tag{3-10}$$

where the overbar notation indicates that the eFRFs are condensed to the size of N_b.

The matrix from which the left singular vectors that condense the eFRFs are produced is formed by augmenting the FRF matrices at spectral lines in the frequency band.

$$[U][\Sigma][V]^H = \mathbf{svd}([[H(\omega_1)][H(\omega_2)]\cdots[H(\omega_{N_s})]])_{(N_o \times N_i N_s)} \tag{3-11}$$

The number of spectral lines and the references per spectral line can be decimated to reduce the size of the matrix. However, the number of columns can still be very large and computing the SVD can take a long time. The number of U-vectors is the lesser of N_o or $N_i N_s$ for the economical SVD, but only N_b of them will be used to generate the eFRFs, and N_b is typically much less than N_o or $N_i N_s$. An alternative approach is to the sum the 3-D FRF matrix along the temporal dimension instead of augmenting the matrices. In this case, the matrix for the SVD in Equation 3-11 is $N_o \times N_i$ and N_i U-vectors are produced. The rationale behind this approach is that the columns of the FRF matrix are a linear combination of the mode shapes and SVD extracts the basis vectors that comprise the columns of the FRF matrix into the left singular vectors. Summing the FRF matrix combines a linear combination of the mode shapes, which is still a linear combination of the mode shapes. This technique is essentially an averaging of the FRF matrix over a number of spectral lines.

The summation method has produced results that were nearly identical to the augmentation method in all test cases that have been examined, but there are potential limitations of this technique. One constraint is the that number of modes active in the frequency band can not exceed the number of references. Since the EMIF method is intended primarily for datasets with many references, this constraint should not be relevant in most cases. If it is, then a combination of augmentation and summation can be used. There may also be the possibility that the summation of particular modes could approach zero under certain conditions, and thus eliminate those modes. Although this phenomena has not been observed, it has not been fully examined yet either and is a proposed subject of further study.

A second-order, frequency domain model with generalized residuals is used to estimate the poles from the set of eFRFs.

$$\sum_{k=0}^{2}\left[(j\omega)^k[a_k]\right][e\bar{H}(\omega)] = \sum_{k=n_l}^{n_u+2}\left[(j\omega)^k\left[\hat{\beta}_k\right]\right] \tag{3-12}$$

The mode shapes are produced from the eigenvectors of the UMPA model in the condensed space by expanding back to the physical space with the inverse transformation of Equation 3-10. A second-order UMPA model with $[a_k]$ coefficient matrices of size $N_b \times N_b$ will have N_b pairs of conjugate poles. Thus, by condensing the response space to match the number of modes, the second-order model does not generate any computational poles. Residuals are included in the numerator polynomial to compensate for out-of-band modes and inconsistencies in the data without increasing the model α-order. But again, what residual polynomial should be included in the UMPA model? A consistency

diagram for residuals is applicable to the EMIF method as for the CMIF method, since the model α-order is fixed and only the β-order is a variable of the UMPA model. The EMIF method is illustrated in the following examples.

The CMIF of a measured FRF dataset with $N_o = 35$, $N_i = 14$ and $\Delta f = 0.0625$ Hz is shown in Figure 3-14. There is a group a four modes in the frequency band of interest marked with the vertical lines, that is, $N_b = 4$. The consistency diagram for this frequency band is shown in Figure 3-15. The consistency criteria are: 1% for frequency, 5% for damping, 1% for conjugates and 10^{-6} for reciprocal of the condition number. The indicator functions plotted on the consistency diagram are a summation of the $N_b \times N_i$ eFRF matrix across the references, there are four curves since $N_b = 4$. In Table 3-6 is a list of the residual polynomial orders and the estimated poles for the model variations of the consistency diagram in Figure 3-15. The CMIF synthesized from the EMIF model is compared to the CMIF of the measured dataset in Figure 3-16 to show the global fit of the estimated parameters for model variation number 3. The eFRF matrix is synthesized from the estimated $[a_k]$ and $\left[\hat{\beta}_k\right]$ coefficient matrices by Equation 3-12, then expanded back into the physical space with the inverse transformation of Equation 3-10 to reconstruct the entire FRF matrix for the CMIF computation. Again, evaluating the UMPA model with this type of consistency diagram improves the estimates of the poles in the frequency band, without generating any computational poles.

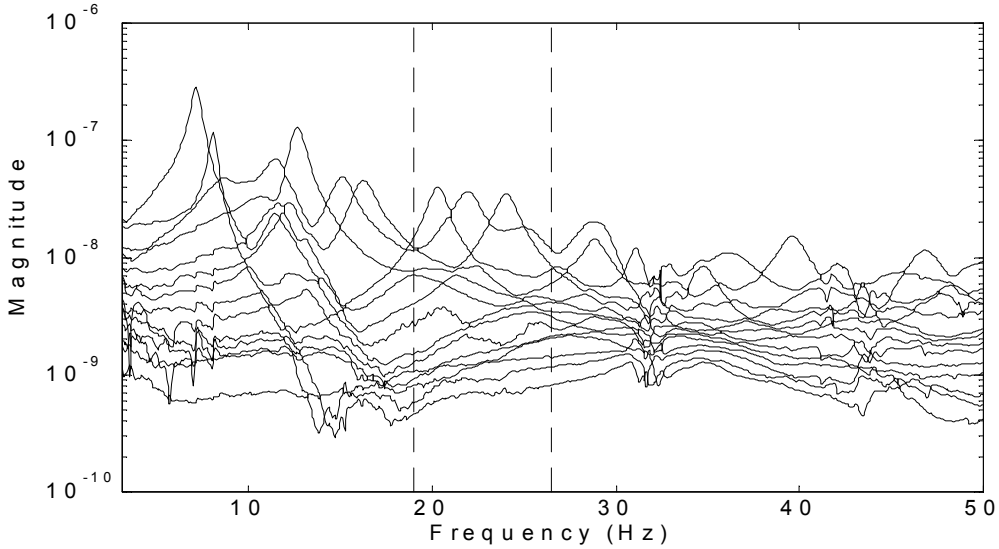

Figure 3-14. *Complex mode indicator function of a measured FRF dataset with a frequency band of interest.*

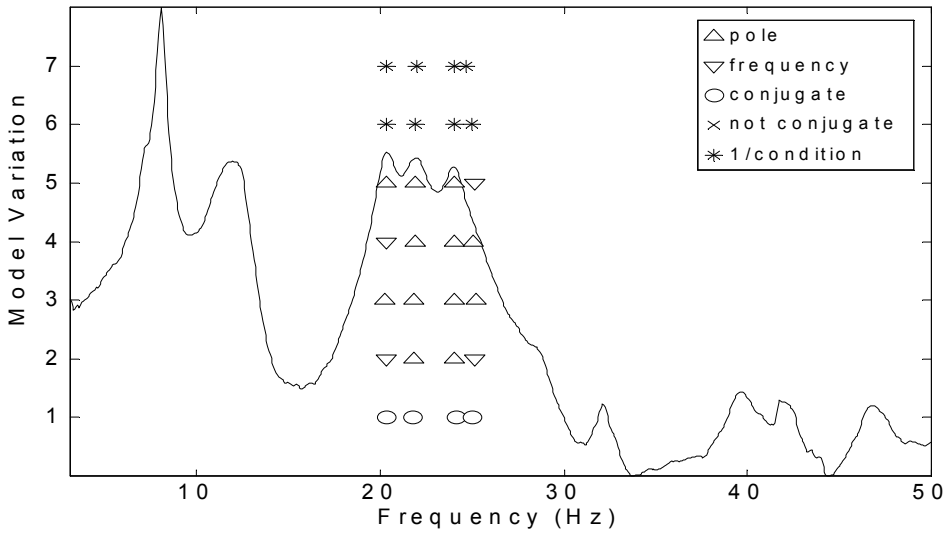

Figure 3-15. *EMIF method consistency diagram for the frequency band in Figure 3-14.*

	Residuals	Frequency (Hz)	Damping (%)	Consistency	1/Condition
1	$n_l = 0,\ n_u = -2$	20.290 21.775 24.098 24.961	2.743 3.504 2.596 5.600	conjugate conjugate conjugate conjugate	2.657e-001
2	$n_l = -1,\ n_u = 1$	20.289 21.795 24.011 25.110	2.397 3.405 2.572 5.281	frequency pole pole frequency	4.832e-003
3	$n_l = -2,\ n_u = 2$	20.278 21.839 24.043 25.251	2.370 3.406 2.640 5.025	pole pole pole pole	4.130e-004
4	$n_l = -3,\ n_u = 3$	20.304 21.876 24.020 25.100	2.507 3.350 2.581 4.827	frequency pole pole pole	3.529e-005
5	$n_l = -4,\ n_u = 4$	20.298 21.921 24.028 25.104	2.494 3.290 2.573 4.198	pole pole pole frequency	2.942e-006
6	$n_l = -5,\ n_u = 5$	20.291 21.944 24.027 25.022	2.447 3.241 2.586 3.082	1/condition 1/condition 1/condition 1/condition	2.422e-007
7	$n_l = -6,\ n_u = 6$	20.308 21.968 24.035 24.637	2.353 3.173 2.557 1.879	1/condition 1/condition 1/condition 1/condition	1.955e-008

Table 3-6. *The residual polynomial orders and estimated poles for the model variations of the consistency diagram in Figure 3-15.*

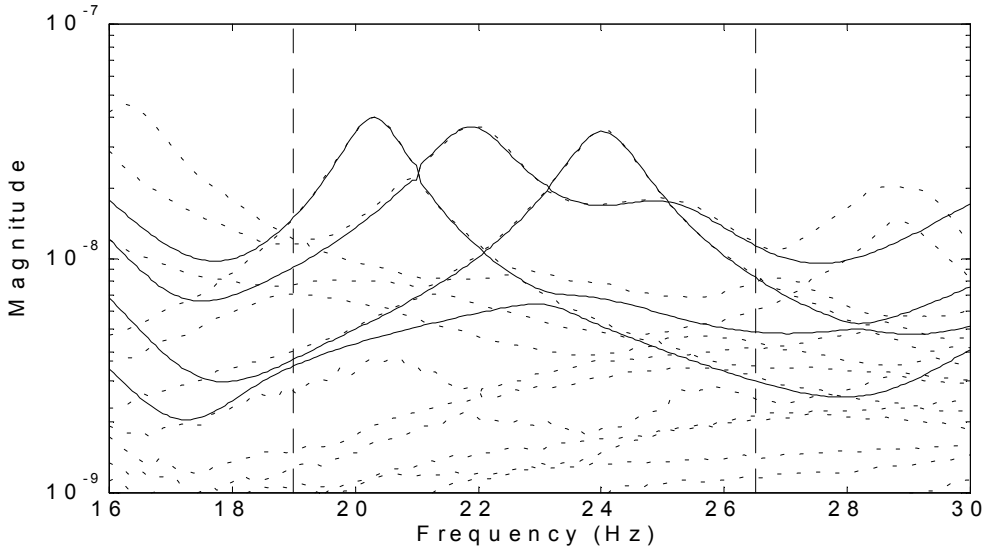

Figure 3-16. *Complex mode indicator function reconstructed from the EMIF model (solid lines) and of the measured FRF dataset (dashed lines).*

Typically there are as many unique, significant vectors in the frequency band of interest as there are modes, and a low-order UMPA model is appropriate for the EMIF method. There are rare occurrences, however, in which there are fewer vectors than modes, and a high-order UMPA model must be used. In this case, the $[a_k]$ coefficient matrices are $N_v \times N_v$ and not $N_b \times N_b$, where N_v is the number of vectors in the frequency band of interest. The order of the denominator must then be greater than two so that the UMPA model yields enough poles. This leads to the possibility of computational poles for certain combinations of N_b, N_v and m. For example, if $N_b = 4$ and $N_v = 3$, m must be 3 to yield 9 poles, of which 8 are 4 conjugate pairs and 1 is an extra computational pole.

Consider the following example of the two modes (i.e., $N_b = 2$) in the frequency band marked in Figure 3-17, which is the CMIF of a measured FRF dataset with $N_o = 180$, $N_i = 3$ and $\Delta f = 1$Hz. The MAC value between the left singular vectors associated with

these two CMIF peaks is 0.9932, which means that these two mode shapes are essentially identical. If the FRF matrix is condensed with two left singular vectors (i.e., $N_v = 2$), the resulting eFRFs are as shown in Figure 3-18. The highest peak in the eFRFs is the mode at 670 Hz, which is outside the frequency band of interest. Of the two left singular vectors used to generate the eFRFs, one is of the two modes in the frequency band, but the other is of the out-of-band mode. The consistency diagram for $N_b = 2$ and $N_v = 2$ is shown in Figure 3-19. A pole for the out-of-band mode and one between the two modes of interest are identified, until enough residuals are added, but then the condition number consistency criteria is exceeded.

Now if the FRF matrix is condensed with just one left singular vector (i.e., $N_v = 1$), the resulting eFRFs are as shown in Figure 3-20. The 670 Hz out-of-band mode is now suppressed and the two modes of interest dominate the eFRFs in the frequency band. For this case with $N_b = 2$ and $N_v = 1$, $m = 4$ and $[a_k]$ is 1×1. The UMPA model yields two pairs of conjugate poles and no computational poles. The consistency diagram for $N_b = 2$ and $N_v = 1$ is shown in Figure 3-21, which now identifies both modes in the frequency band. The reconstructed CMIF for model variation number 3 is compared to the CMIF of the measurements in Figure 3-22.

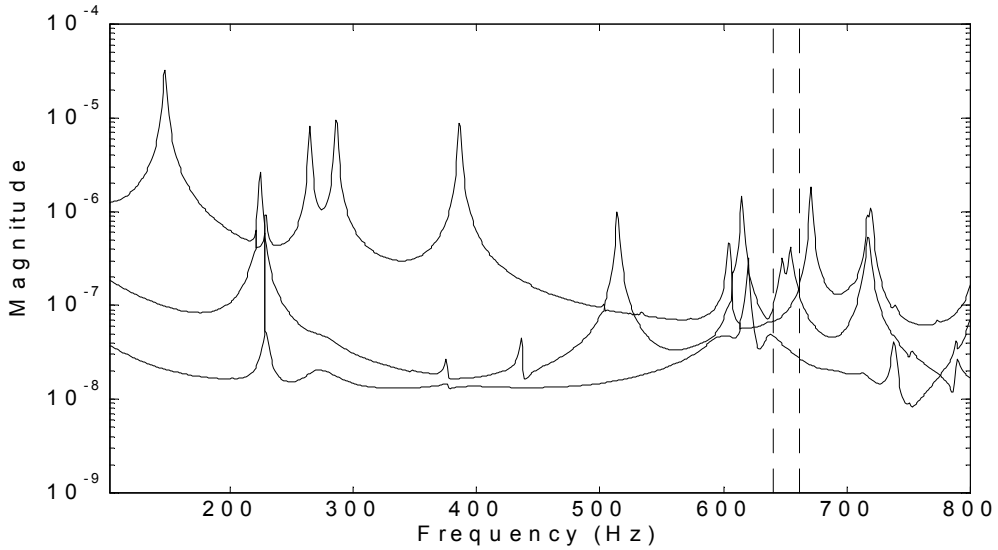

Figure 3-17. *Complex mode indicator function of a measured FRF dataset with a frequency band of interest.*

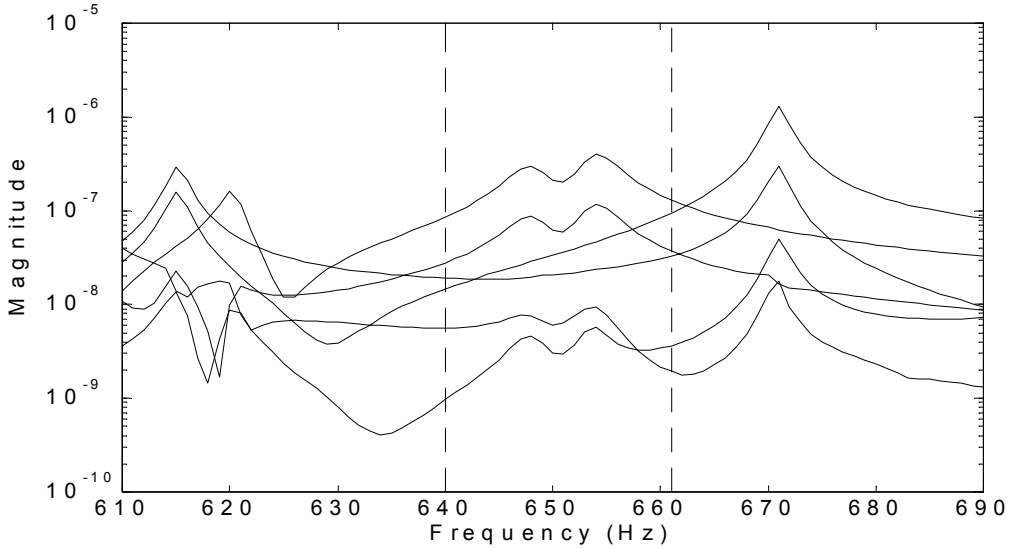

Figure 3-18. *EMIF method enhanced frequency response functions for condensation with two left singular vectors.*

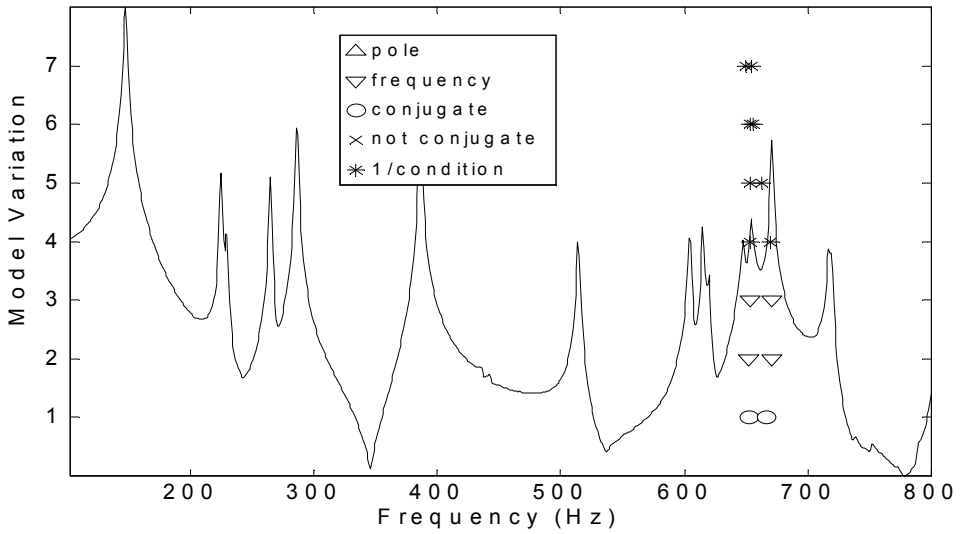

Figure 3-19. *EMIF method consistency diagram for the frequency band in Figure 3-17 for condensation with two left singular vectors.*

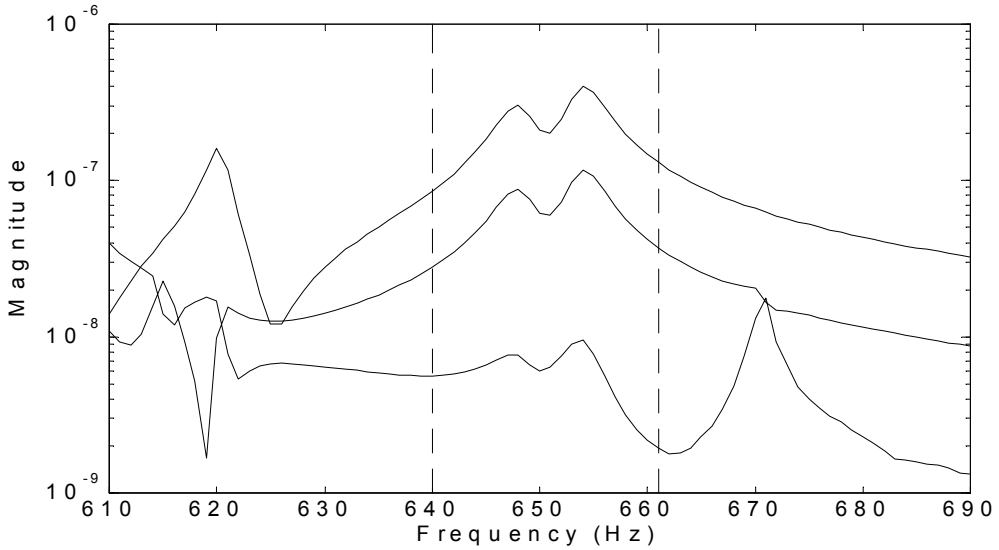

Figure 3-20. *EMIF method enhanced frequency response functions for condensation with one left singular vector.*

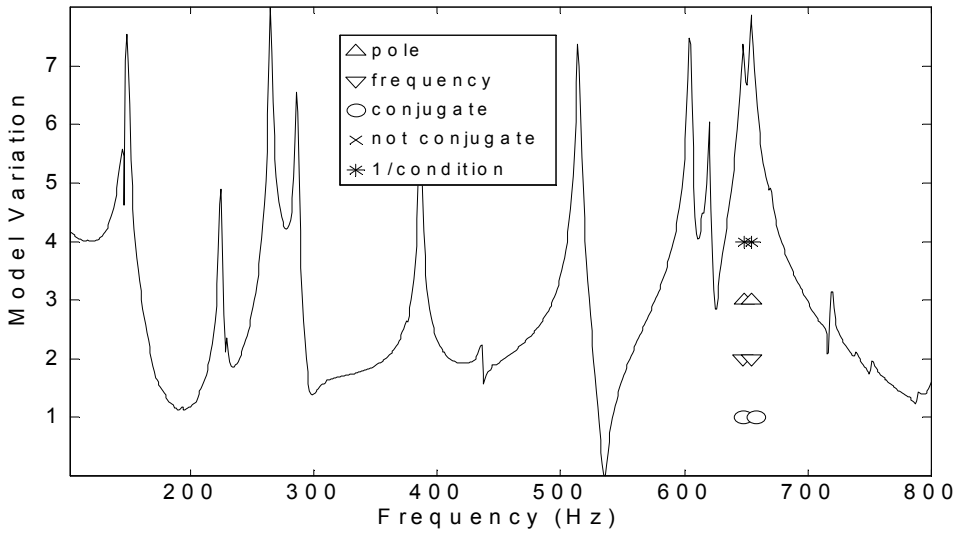

Figure 3-21. *EMIF method consistency diagram for the frequency band in Figure 3-17 for condensation with one left singular vector.*

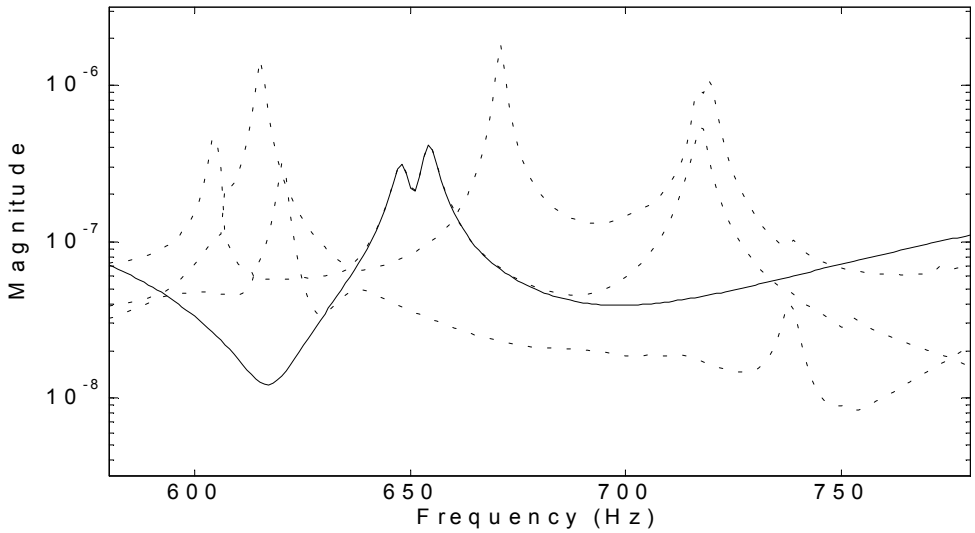

Figure 3-22. *Complex mode indicator function reconstructed from the EMIF model (solid line) and of the measured FRF dataset (dashed lines).*

3.4 Unified Matrix Polynomial Approach Parameter Estimation Method

For the methods in the preceding sections, the UMPA model α-order was fixed and only the β-order (i.e., the order of the generalized residual polynomial) could be varied to generate a consistency diagram. This was because the number of modes was known, either one mode for the SDOF and CMIF algorithms or a limited number of enhanced modes for the EMIF algorithm. In general, the number of modes is not known and varying the model α-order is also necessary to produce consistent estimates of the poles. The examples in this section illustrate the application of the general, frequency domain UMPA model with variations of both the α-order and the β-order. The measured dataset has $N_o = 27$, $N_i = 3$ and $\Delta f = 0.5$ Hz and the frequency band of interest is 73.5 to 87.5 Hz. The orders of the denominator (m) and of the generalized residual polynomial (n_l, n_u) for the model variations of the consistency diagrams in Figures 3-23 through 3-25 are listed in Table 3-7. For the UMPA model solutions in the following examples, α_m is identity.

For a low-order UMPA model, the α-order is fixed at two (or one) and a consistency diagram can be generated by varying the β-order. This is similar to the EMIF method, but without condensation of the FRF matrix response space to match the number of modes. A consistency diagram for a low-order UMPA model algorithm is shown in Figure 3-23. The algorithm yields $2N_o$ poles, but there are only four modes in the frequency band of interest. Some of the extra poles may help to describe the out-of-band modes, while others are purely computational poles. Without varying the β-order, only one set of poles can be estimated and a consistency diagram can not be evaluated.

	Figure 3-23			Figure 3-24			Figure 3-25(a)			Figures 3-25(b,c)		
	m	n_l	n_u	m	n_l	n_u	m	n_l	n_u	m	n_l	n_u
1	2	0	-2	2	0	-2	2	0	-2	2	0	-2
2	2	-1	1	3	0	-2	2	-1	1	3	0	-2
3	2	-2	2	4	0	-2	2	-2	2	4	0	-2
4	2	-3	3	5	0	-2	2	-3	3	5	0	-2
5	2	-4	4	6	0	-2	2	-4	4	6	0	-2
6							3	0	-2	2	-1	1
7							3	-1	1	3	-1	1
8							3	-2	2	4	-1	1
9							3	-3	3	5	-1	1
10							3	-4	4	6	-1	1
11							4	0	-2	2	-2	2
12							4	-1	1	3	-2	2
13							4	-2	2	4	-2	2
14							4	-3	3	5	-2	2
15							4	-4	4	6	-2	2
16							5	0	-2	2	-3	3
17							5	-1	1	3	-3	3
18							5	-2	2	4	-3	3
19							5	-3	3	5	-3	3
20							5	-4	4	6	-3	3
21							6	0	-2	2	-4	4
22							6	-1	1	3	-4	4
23							6	-2	2	4	-4	4
24							6	-3	3	5	-4	4
25							6	-4	4	6	-4	4

Table 3-7. *The UMPA model denominator order and the generalized residual polynomial lower and upper orders for the model variations of the consistency diagrams in Figures 3-23 through 3-25.*

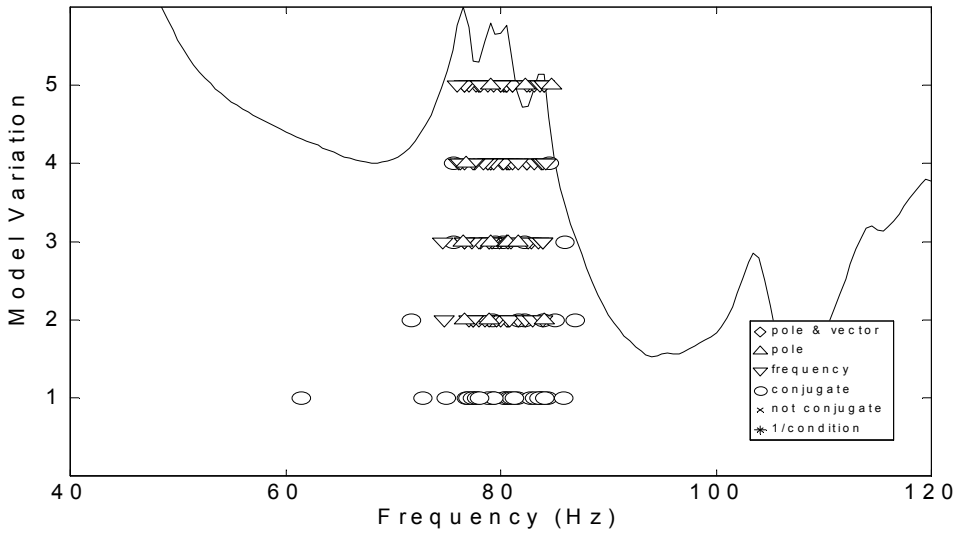

Figure 3-23. *Consistency diagram of a low-order UMPA model, for varying the β-order.*

For a high-order UMPA model, both the α-order and β-order can be varied to generate a consistency diagram. Figure 3-24 is a traditional consistency diagram in which only the α-order is varied, with no residuals for this example. Residuals could have been included, but only a fixed set for the variations of the α-order. A consistency diagram that varies both the α-order and β-order can be generated in several ways. The β-order can be varied for a fixed α-order, then repeated for another α-order, as in Figure 3-25(a), or the α-order can be varied for a fixed β-order, as in Figure 3-25(b). When the β-order is changed, the consistency evaluation can continue, as in Figure 3-25(b), or can be reset, as in Figure 3-25(c), which is really a set of traditional consistency diagrams for fixed residuals appended together.

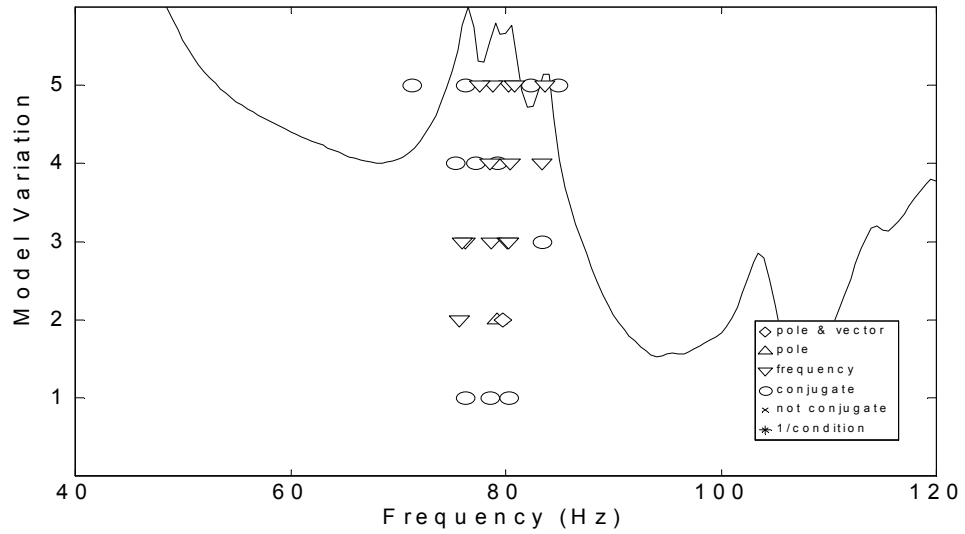

Figure 3-24. *Consistency diagram of a high-order UMPA model, for varying the α-order, with no residuals.*

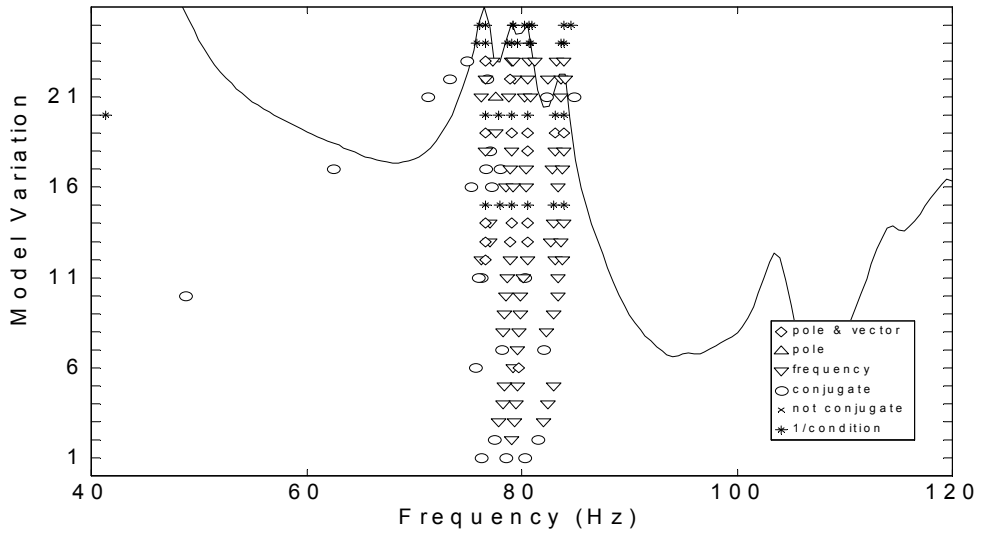

Figure 3-25(a). *Consistency diagram of a high-order UMPA model, for varying the β-order then the α-order.*

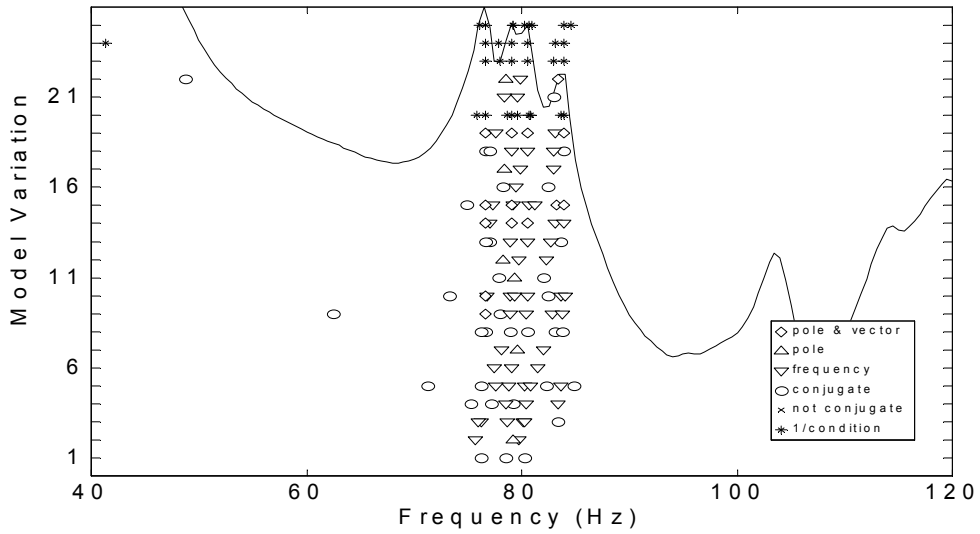

Figure 3-25(b). *Consistency diagram of a high-order UMPA model, for varying the α-order then the β-order.*

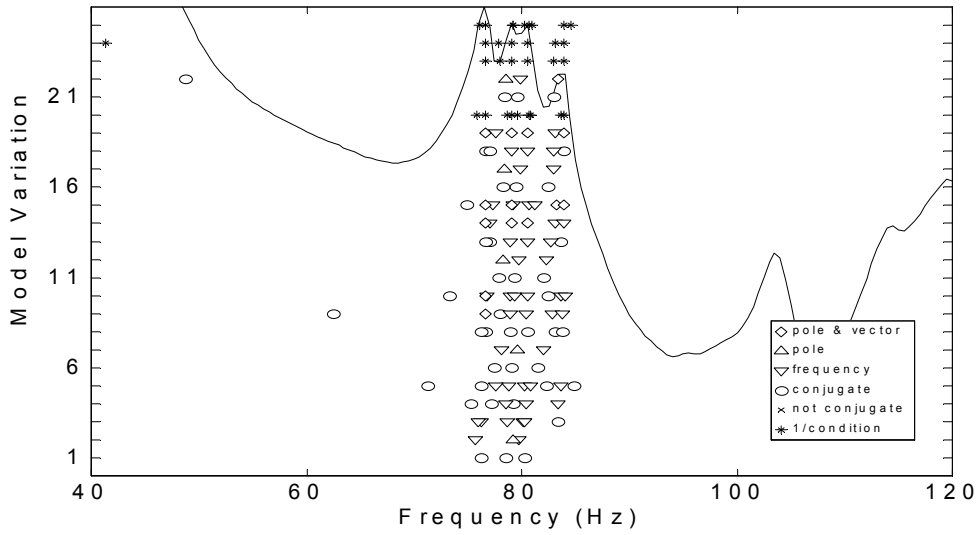

Figure 3-25(c). *Consistency diagram of a high-order UMPA model, for varying the α-order then the β-order, with resetting the consistency evaluation.*

As an alternative to a consistency diagram, all of the poles from all of the model variations can be plotted on a pole surface diagram, in which the consistent poles will form

clusters.[60] The pole surface can be plotted for consistency, as in Figure 3-26(a), or for pole density, as in Figure 3-26(b). The pole density is indicated by the color of the marker and is equal to the number of poles within a circular region around the pole, which is defined by a pole density criterion (typically, a percentage of the undamped natural frequency). The pole nearest the centroid of a cluster can be selected or an average pole can be created at the centroid of the cluster.

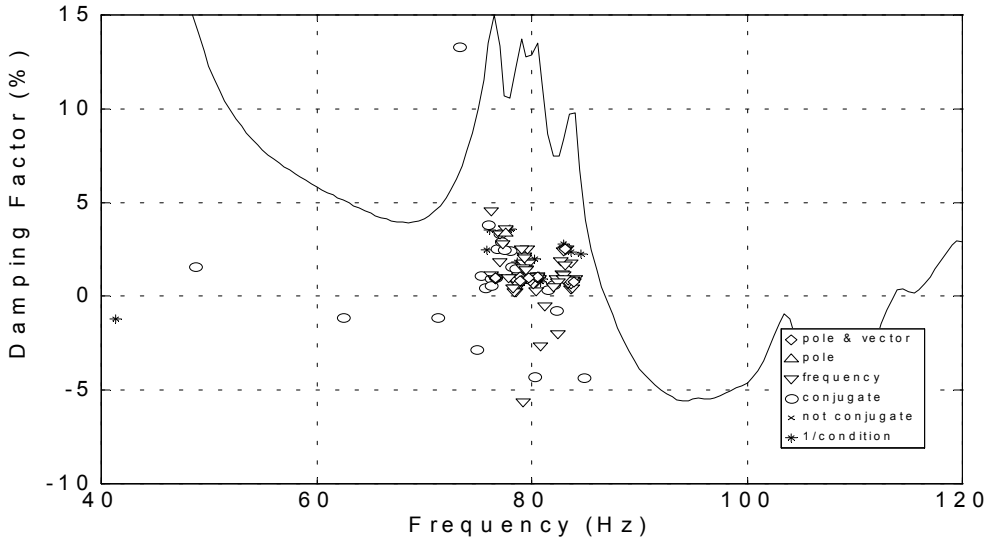

Figure 3-26(a). *Pole surface consistency for the model variations of the consistency diagram in Figure 3-25(a).*

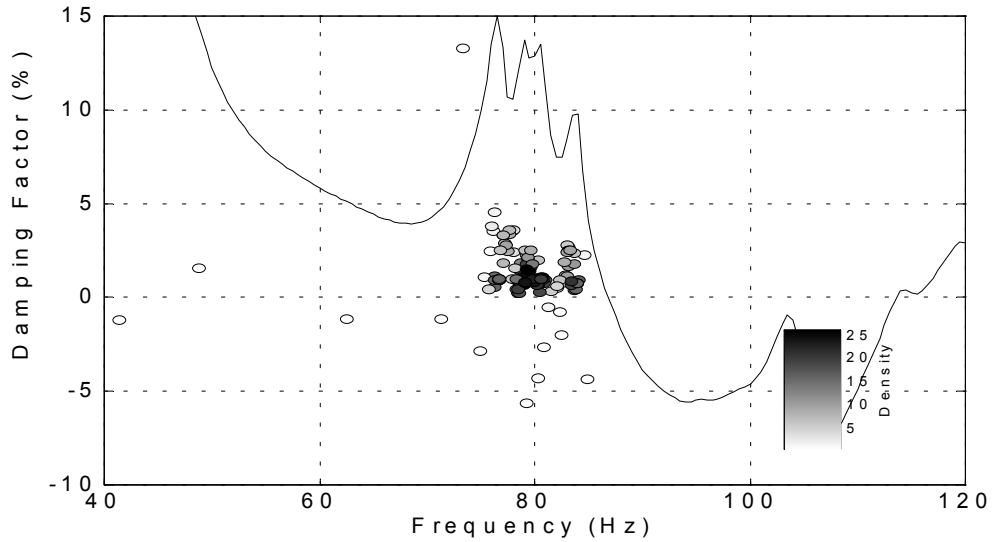

Figure 3-26(b). *Pole surface density for the high-order UMPA model variations in Figures 3-25(a-c).*

CHAPTER FOUR

4 Conclusion

The applications presented in the preceding chapter have illustrated the implementation of a generalized residual polynomial in frequency domain modal parameter estimation. Since the earliest appearance of residuals in modal parameter estimation, the development of most frequency domain algorithms have included some consideration of residuals. If the variety of opinions concerning residuals described in the literature review of Chapter One seemed disjointed, this is because there has been no general agreement on the role of residuals in the parameter estimation process. For the most part, residuals have either been just some extra numerator terms thrown in to get a better fit or an overly complicated derivation to model the physical aspects of out-of-band modes. This dissertation has attempted to approach frequency domain parameter estimation residuals in a systematic and generalized manner.

4.1 Summary of Dissertation

The basic idea of "adding extra numerator terms" is not new, as the citations from the references will attest, but only as a fixed set of terms. Most of the emphasis in the many modal parameter estimation algorithms that have been developed over the years has been on determining the proper model α-order. However, the model β-order can also be considered as a variable condition in the modal parameter estimation process, as has been demonstrated in the applications in Chapter 3. In most of the earlier residual models, only the upper bound of the numerator order was increased, but the lower bound remained at zero. As has been shown, positive and negative residual polynomial orders can both be used in the rational fraction polynomial model. The approach of the techniques developed in this dissertation has been to consider the numerator and denominator polynomial coefficients equally in the parameter estimation process.

The single-term, physical residual model, a constant upper residual representing the flexibility of the upper modes as stiffness line and a $1/\omega^2$ lower residual representing inertia of the lower modes the mass line, is based on the asymptotic behavior an SDOF mode. The physical residuals have always been used with the implicit assumption that the out-of-band modes are "well-separated" from the in-band modes. The limits of this assumption were established by examining the relative error between the asymptotes of an SDOF FRF and the constant and $1/\omega^2$ residuals. The residual modes must be separated from the frequency range of interest by a factor of ten for a one-percent agreement. This is typically not the case, especially when processing a narrow sub-band of frequency; the residual modes are usually just outside of the band. If the out-of-band modes are not

sufficiently separated from the in-band modes, their effects cannot be adequately described by the simple, physical residual model. Typically, the closer the out-of-band modes are to the frequency range of interest, the greater the number of residual terms that are needed to fully account for their influence.

A power polynomial of frequency of the form $\sum_{k=n_l}^{n_u} (j\omega)^k R_k$, with both positive and negative orders, was proposed and developed as a generalized residual model. This generalized frequency domain power polynomial residual model is a purely mathematical construct. It does not have direct physical significance to the FRF model, but can more completely describe the contributions of the residual modes that are not well separated from the frequency range of interest. The lower and upper residual terms are combined into one expression to form the generalized residual polynomial. The negative polynomial orders represent the lower residuals and the positive (and zero) polynomial orders represent the upper residuals. The zero-order term was included with the positive orders as a matter of notational convenience and since it is the physical, upper residual. Comparison of the positive- and negative-order polynomial functions to the low- and high-frequency asymptotic shape an the FRF, respectively, confirmed that the power polynomial of frequency is the proper choice for a generalized residual model.

An MDOF FRF is a superposition of SDOF modes, but with respect to any mode or band of modes, all other modes can be considered residuals. It was verified that a power polynomial function can be curve-fit to any segment of an FRF away from resonance, and consequently model the residual effects. At the resonance peaks, the power polynomial function is unable to describe the $1/(j\omega - \lambda)$ characteristics of the modal model. The

$1/(j\omega - \lambda)$ functions describe the modal model for all frequency, but away from resonance, a power polynomial of frequency can also approximate the functional behavior. Together the modal model and the generalized residual model account for all of the contributions to the FRF in a frequency band.

The rational fraction polynomial FRF model that includes generalized residuals is formed by combining the generalized residual and numerator polynomials over a common denominator. The result is essentially a change of the numerator polynomial order indices from $k = 0, ..., m-2$ to $k = n_l, ..., m + n_u$, where n_l and n_u are the lower and upper limits of the generalized residual polynomial orders indices, respectively. All of the properties of the original frequency domain UMPA model apply, there are just more numerator terms in the solution.

The generalized residual polynomial is necessarily assumed to be a complete polynomial and defined by n_l and n_u, because in most cases any omitted orders will be produced by convolution with the rational fraction polynomial model denominator. A complete polynomial is also required so that the numerator polynomial coefficients ($\hat{\beta}_k$) can be deconvolved into the generalized residual polynomial coefficients (R_k) and the original numerator polynomial coefficients (β_k). The $\hat{\beta}_k$ coefficients are linear combinations of the β_k, a_k and R_k coefficients. An algorithm for deconvolving the β_k and R_k coefficients from the a_k and $\hat{\beta}_k$ coefficients of the UMPA model solution was developed in Section 2.3.2. The original β_k coefficients are needed to determine the residues from the UMPA model solution, as derived in Section A.2.

The principal application of residuals is to compute better estimates of poles and residues. This dissertation has dealt primarily with the first stage of the modal parameter estimation process, estimating the poles and participation factors from the UMPA model. However, the generalized residual polynomial is also applicable to frequency domain residue estimation algorithms, as described in Appendix A. Previously, only the physical residuals were included in residue estimation algorithms, but including additional terms in a generalized residual polynomial for residue estimation has the same benefits as for pole estimation. The single- and multiple-reference residue estimation algorithms that include a generalized residual polynomial were outlined in Section A.1 and are a natural extension of the traditional algorithms. By realizing the equivalence of the partial fraction model and the rational fraction polynomial model of the FRF to represent the same system, the residue information contained in the UMPA model numerator was discovered. The residue of a SISO SDOF system can be found directly from the β_0 coefficient. A matrix solution was also developed for a SISO MDOF system.

The consistency diagram is the most widely used aid in model order determination for modal parameter estimation. The traditional consistency diagram is generated by sequentially evaluating the UMPA model for increasing model α-order. The concept of a consistency diagram has been extended by allowing the model β-order (or residuals) to also be varied. This technique is well-suited for methods in which the α-order is fixed, such as CMIF and EMIF. This basic principle was demonstrated and implemented in the applications presented in Chapter 3.

The number of modes is not usually known and varying the α-order is necessary for a consistency diagram to produce valid estimates of the poles. The α-order typically has to be over-specified to compensate for out-of-band modes, but by including residuals in the parameter estimation algorithm, the α-order does not have to be over-specified as much. A consistency diagram can be generated by varying the α-order, the β-order, or a combination of both. In the traditional consistency diagram, only the α-order is varied, from a minimum to a maximum, but in a consistency diagram for residuals, n_l, n_u or both can be varied. Varying the β-orders allows a consistency diagram to be generated for a low-order model the same as for a high-order model. For a high-order model, the α-order and β-order can be varied in different permutations to generate a consistency diagram.

The idea of a consistency diagram for residuals was first conceived and implemented for the CMIF method as a systematic procedure to evaluate a number of SDOF UMPA model solutions to obtain a valid estimate of the pole. Ideally the eFRF transformation uncouples the mode of interest from the other modes, but if it does not, residuals are needed in the eFRF model. Since CMIF uses an SDOF algorithm, the α-order is fixed and the only means to compensate for other modes in the eFRF, without introducing computational poles, is with residuals. A trial-and-error procedure of selecting a set of numerator terms was not efficient. A more generalized and systematic methodology was needed. The technique was next naturally incorporated into the EMIF method since it too has an algorithm with a fixed α-order. The EMIF method has been improved from its earlier

form with the summation method of assembling the SVD matrix and by allowing the number of vectors to be less than the number of modes.

A consistency diagram for residuals improves the estimates of the poles in the frequency band of interest without generating more computational poles. For an SDOF algorithm without condensation, residuals are certainly necessary since the model α-order is fixed. For the general UMPA model with no condensation, the α-order can be increased to account for out-of-band modes, which introduces computational poles that must be sorted, or residuals can be used. Applied to general frequency domain UMPA algorithms, varying the β-order yields multiple estimates for low-order models and more variations for high-order models.

4.2 Recommendations for Future Work

While the primary focus of this dissertation has been a generalized residual model for frequency domain modal parameter estimation, the broader view of the methodology introduced is to consider the order of the denominator polynomial as only one of the variable conditions in the parameter estimation process. There are several other conditions of the UMPA model, such as the order of the numerator polynomial and the a_k identity coefficient, that can be varied to estimate consistent poles. Additionally, pre-processing criteria such as the DOF sieve, condensation, spectral filtering and over-determination have an effect on the estimation of the poles.[61] Even estimates from different types of algorithms (e.g., high-order or low-order, time or frequency domain) could be evaluated together.

The prospect of these different model variations will yield numerous estimates of the system poles. One of the challenges of this new approach will be visualization and utilization of the results. Many permutations of the consistency diagram ordinate will be possible and the pole surface density may prove to be the preferred format to present all of this modal information. The next area of study is exploring the other variable conditions in the UMPA model solution listed above as well as the distribution and statistics of the multiple modal parameter estimates.[60,62]

Only frequency domain algorithms have been considered in this dissertation because residuals are not readily formulated in the time domain. This is not to say that time domain residuals have been completely disregarded. In a recent publication, a new technique that includes a residual flexibility term in the residue estimation of a time domain system realization algorithm has been developed.[63] The time domain residual model is the numerical values of the inverse discrete Fourier transform of a frequency domain polynomial term (a constant for displacement, s for velocity or s^2 for acceleration). It would be worthwhile to investigate if this method could be generalized and applied to the time domain UMPA model algorithms.

There does not appear to be a solution for determining the residues from the UMPA model coefficients for the general MIMO MDOF system, because of mathematical restrictions of the matrix sizes and computational difficulties concerning the adjoint of a matrix polynomial. This is a somewhat troubling curiosity that has not yet been resolved. If some clever mathematics and programming do happen to reveal a solution, this technique may still have only limited practical utility. The restriction is that all of the

poles and residues must be for a complete UMPA model, not a selected subset from different model variations.

The summation method of assembling the SVD matrix greatly reduces the computational load for the EMIF condensation. It has performed comparably to augmentation method in all of the cases that have been tested. However, the possibility of the summation eliminating modes in the frequency band should be more fully examined to determine the limitations of this approach.

REFERENCES

[1] R.J. Allemang, D.L. Brown, "A Unified Matrix Polynomial Approach to Modal Identification", *Journal of Sound and Vibration*, Vol. 211, No. 3, Apr. 1998, p. 301-322.

[2] R.L. Allemang, D.L. Brown, W.A. Fladung, "Modal Parameter Estimation: A Unified Matrix Polynomial Approach", *Proceedings of the Twelfth International Modal Analysis Conference*, 1994, p. 501-504.

[3] A.W. Phillips, R.L. Allemang, "Numerical Considerations in Modal Parameter Estimation", *Proceedings of the Twenty-First International Seminar on Modal Analysis*, 1996, p. 1097-1108.

[4] M.H. Richardson, D.L. Formenti, "Parameter Estimation from Frequency Response Measurements Using Rational Fraction Polynomials", *Proceedings of the First International Modal Analysis Conference*, 1982, p. 167-181.

[5] J.M. Leuridan, J.A. Kundrat, "Advanced Matrix Methods for Experimental Modal Analysis: A Multi-Matrix Method for Direct Parameter Estimation", *Proceedings of the First International Modal Analysis Conference*, 1982, p. 192-200.

[6] J.G. Gimenez, L.I. Carrascosa, "Global Fitting: An Efficient Method of Experimental Modal Analysis of Mechanical Systems", *Proceedings of the First International Modal Analysis Conference*, 1982, p. 528-533.

[7] L. Petrick, "Obtaining Global Frequency and Damping Estimates Using Single Degree-of-Freedom Real Mode Methods", *Proceedings of the Second International Modal Analysis Conference*, 1984, p. 425-431.

[8] M.H. Richardson, D.L. Formenti, "Global Curve Fitting of Frequency Response Measurements Using the Rational Fraction Polynomial Method", *Proceedings of the Third International Modal Analysis Conference*, 1985, p. 390-397.

[9] M.H. Richardson, “Global Frequency & Damping Estimates from Frequency Response Measurements, *Proceedings of the Fourth International Modal Analysis Conference*, 1986, p. 465-470.

[10] H. Van der Auweraer, J. Leuridan, “Multiple Input Orthogonal Polynomial Parameter Estimation”, *Proceedings of the Fifth International Modal Analysis Conference*, 1987, p. 986-994.

[11] D.K. Gustaveson, “Direct Parameter Identification from Frequency Response Measurements”, *Proceedings of the Fifth International Modal Analysis Conference*, 1987, p. 1352-1356.

[12] K. Shye, C. Van Karsen, M. Richardson, “Modal Testing Using Multiple References”, *Proceedings of the Fifth International Modal Analysis Conference*, 1987, p. 1407-1416.

[13] P. Ebersbach, H. Irretier, “On the Application of Modal Parameter Estimation Using Frequency Domain Algorithms”, *The International Journal of Analytical and Experimental Modal Analysis*, Vol. 4, No. 4, 1989, p. 109-116.

[14] C.Y. Shih, Y.G. Tsuei, R.J. Allemang, D.L. Brown, “A Frequency Domain Global Parameter Estimation Method for Multiple Reference Frequency Response Measurements”, *Proceedings of the Sixth International Modal Analysis Conference*, 1988, p. 389-396.

[15] Y.S. Wei, R.G. Smiley, R.C. Sohaney, “A Global Frequency Domain Rational Fraction Orthogonal Polynomial Curve Fit”, *Proceedings of the Sixth International Modal Analysis Conference*, 1988, p. 1648-1654.

[16] F. Lembregts, J. Leuridan, “Frequency Domain Direct Parameter Identification for Modal Analysis: State Space Formulation”, *Proceedings of the Seventh International Modal Analysis Conference*, 1989, p. 1271-1277.

[17] W.B. Jeong, A. Nagamatsu, “A New Method for Poly-Reference Identification of Modal Parameters in Modal Testing”, *Proceedings of the Tenth International Modal Analysis Conference*, 1992, p. 153-158.

[18] K. Kochersberger, L.D. Mitchell, “A Method for Determining Modal Parameters Using FRF Curve-Fitting and Off-Resonance Sine Dwell”, *Proceedings of the Tenth International Modal Analysis Conference*, 1992, p. 757-763.

[19] X. Keqin, “Using the Imaginary-Part of FRF for Modal Identification and IRF Estimation”, *Proceedings of the Tenth International Modal Analysis Conference*, 1992, p. 1431-1437.

[20] E. Chatelet, J. Piranda, "Modal Identification by Squared Amplitude Fitting Methods", *Proceedings of the Thirteenth International Modal Analysis Conference*, 1995, p. 40-46.

[21] E. Balmes, "Frequency Domain Identification of Structural Dynamics Using the Pole/Residue Parametrization", *Proceedings of the Fourteenth International Modal Analysis Conference*, 1996, p. 540-546.

[22] T.M. Dahling, R.J. Allemang, A.W. Phillips, "Application of Differencing to Frequency Domain Parameter Estimation Algorithms", *Proceedings of the Seventeenth International Modal Analysis Conference*, 1999, p. 833-839.

[23] S. Braun, Y. Ram, "Time and Frequency Identification Methods in Overdetermined Systems", *Mechanical Systems and Signal Processing*, Vol. 1, No. 3, 1987, p. 245-257.

[24] H. Van der Auweraer, J. Leuridan, "Multiple Input Orthogonal Polynomial Parameter Estimation", *Mechanical Systems and Signal Processing*, Vol. 1, No. 3, 1987, p. 259-272.

[25] C.Y. Shih, Y.G. Tsuei, R.J. Allemang, D.L. Brown, "A Frequency Domain Global Parameter Estimation Method for Multiple Reference Frequency Response Measurements", *Mechanical Systems and Signal Processing*, Vol. 2, No. 4, 1988, p. 349-366.

[26] D.L. Brown, R.J. Allemang, R.J. Zimmerman, M. Mergeay, "Parameter Estimation Techniques for Modal Analysis", *SAE Paper Number 790221, SAE Transactions*, Volume 88, 1979, p. 828-846.

[27] F. Deblauwe, C.Y. Shih, R.W. Rost, D.L. Brown, "Survey of Modal Parameter Estimation Algorithms Applicable to Spatial Domain Sine Testing", *Proceeding of the Twelfth International Seminar on Modal Analysis*, Katholieke Universiteit of Leuven, 1987, 15 pp.

[28] H. Van der Auweraer, R. Snoeys, J.M. Leuridan, "A Global Frequency Domain Parameter Estimation Technique for Mini-computers", *Proceedings of the Tenth International Seminar on Modal Analysis*, 1985.

[29] S.M Crowley, D.L. Brown, R.J. Allemang, "The Extraction of Valid Residue Terms Using the Polyreference Technique", *Proceedings of the Third International Modal Analysis Conference*, 1985, p. 80-87.

[30] J. Leuridan, J. Lipkens, H. Van der Auweraer, F. Lembgrets, "Global Modal Parameter Estimation Methods: An Assessment of Time Versus Frequency Domain

Implementation", *Proceedings of the Fourth International Modal Analysis Conference*, 1986, p. 1586-1595.

[31] R.L. Mayes, "A Multi-Degree-of-Freedom Mode Shape Estimation Algorithm Using Quadrature Response", *Proceedings of the Eleventh International Modal Analysis Conference*, 1993, p. 1026-1034.

[32] K. Kochersberger, L.D. Mithcell, "The Use of an Improved Residual Model and Sine Excitation to Iteratively Determine Mode Vectors", *Proceedings of the Twelfth International Modal Analysis Conference*, 1994, p. 356-262.

[33] M.A. Lamontia, "On the Determination and Use of Residual Flexibilities, Inertia Restraints and Rigid Body Modes", *Proceedings of the First International Modal Analysis Conference*, 1982, p. 152-159.

[34] B.A. Brinkman, "Generating Modal Parameters that Compensate for Residual Energy", *Proceedings of the Fourth International Modal Analysis Conference*, 1986, p. 119-122.

[35] B.A. Brinkman, "A Quantitative Study Using Residual Modes to Improve Dynamic Models", *Proceedings of the Fifth International Modal Analysis Conference*, 1987, p. 671-678.

[36] M.L.M. Duarte, D.J. Ewins, "High-Frequency Pseudo-Mode Approximation for High Frequency Residual Terms", *Proceedings of the Fourteenth International Modal Analysis Conference*, 1996, p. 261-266.

[37] M.L.M. Duarte, D.J. Ewins, "Mass-Residual Approach for the Compensation of High-Frequency Residual Terms, *Proceedings of the Fifteenth International Modal Analysis Conference*, 1997, p. 2038-2043.

[38] N. Okubo, T. Matsuzaki, "The Effect of Inertia Restraint and Residual Flexibility on the Accuracy of Structural Modification", *Proceedings of the Thirteenth International Seminar on Modal Analysis*, 1988.

[39] M.L.M. Duarte, D.J. Ewins, "Experimental Estimation of High-Frequency Residual Term Based on Two Extra Parameters", *Proceedings of the Twenty-First International Seminar on Modal Analysis*, 1996, p. 1277-1286.

[40] I. Ahmed, G.R. Tomlinson, "Reducing the Effects of Residual Modes in Measured Frequency-Response Data", *The International Journal of Analytical and Experimental Modal Analysis*, Vol. 2, No. 3, 1987, p. 113-120.

[41] A. Klosterman, **On the Experimental Determination and Use of Modal Representations of Dynamic Characteristics**, *Doctoral Dissertation, University of Cincinnati*, 1971, 184 pp.

[42] P. Van Loon, **Modal Parameters of Mechanical Structures**, *Doctoral Dissertation, Katholieke Universiteit of Leuven*, Leuven Belgium, 1974.

[43] M. Mergeay, "Theoretical Background of Curve Fitting Methods used by Modal Analysis", *Proceedings of the Sixth International Seminar on Modal Analysis*, 1979.

[44] R.J. Allemang, **Vibrations: Analytical and Experimental Modal Analysis, Chapter 6 - Modal Parameter Estimation**, UC-SDRL-CN-20-263-662, *University of Cincinnati*, Feb. 1998, 96 pp.

[45] D. Weng, P.E. Nikravesh, E.Y. Kuo, W.J. Jung, S. Li, "An Optimization Method for Selecting Physical Modes in Poly-Reference Modal Analysis of Vehicle Systems", *SAE Paper No. 1999-01-1782*, *SAE Noise and Vibration Conference*, 1999, p. 1019-1025.

[46] R.J. Allemang, D.L. Brown, "A Review of Modal Parameter Estimation Concepts", *Proceedings of the Eleventh International Seminar on Modal Analysis*, 1986.

[47] R.N. Coppolino, "A Simultaneous Frequency Domain Technique for Estimation of Modal Parameters", *SAE Paper No. 811046*, 1981, 12 pp.

[48] J.N. Juang, **Applied System Identification**, Prentice Hall, 1994.

[49] J.V. Beck, K.J. Arnold, **Parameter Estimation in Engineering and Science**, John Wiley & Sons, 1977.

[50] R.B. Randall, Y. Gao, A. Settieri, "Phantom Zeros in Curve-Fitted Frequency Response Functions", *Mechanical Systems and Signal Processing*, Vol. 8, No. 6, 1994, p. 607-622.

[51] Y. Gao, R.B. Randall, "Zeros vs Residues", *Proceedings of the Seventeenth International Seminar on Modal Analysis*, 1992, p. 1643-1654.

[52] C.Y. Shih, Y.G. Tsuei, R.J. Allemang, D.L. Brown, "Complex Mode Indication Function and Its Applications to Spatial Domain Parameter Estimation", *Mechanical Systems and Signal Processing*, Vol. 2, No. 4, 1988, p. 367-377.

[53] W.A. Fladung, "The Development and Implementation of Multiple Reference Impact Testing", *Masters Thesis*, University of Cincinnati, 1994, 191 pp.

[54] A.W. Phillips, R.L. Allemang, W.A. Fladung, "The Complex Mode Indicator Function (CMIF) as a Parameter Estimation Method", *Proceedings of the Sixteenth International Modal Analysis Conference*, 1991, p. 705-710.

[55] A.W. Phillips, R.J. Allemang, "The Enhanced Frequency Response Function (eFRF): Scaling and Other Issues", *Proceedings of the Twenty-Third International Seminar on Modal Analysis*, 1998, p. 385-392.

[56] W.A. Fladung, A.W. Phillips, D.L. Brown, "The Development of an Enhanced Mode Indicator Function Parameter Estimation Algorithm", *Proceedings of the Japanese Modal Analysis Conference*, 1997.

[57] W.A. Fladung, A.W. Phillips, D.L. Brown, "The Development of an Enhanced Mode Indicator Function Parameter Estimation Algorithm", *Proceedings of the ASME Design Engineering Technical Conferences*, 1997.

[58] W.A. Fladung, A.W. Phillips, D.L. Brown, "Specialized Parameter Estimation Algorithms for Multiple Reference Testing", *Proceedings of the Fifteenth International Modal Analysis Conference*, 1997, p. 1078-1087.

[59] S. Li, W.A. Fladung, A.W. Phillips, D.L. Brown, "Automotive Applications of the Enhanced Mode Indicator Function Parameter Estimation Method", *Proceedings of the Sixteenth International Modal Analysis Conference*, 1998, p. 36-44.

[60] A.W. Phillips, R.J. Allemang, C.R. Pickrel, "Clustering of Modal Frequency Estimates from Difference Solution Sets", *Proceedings of the Fifteenth International Modal Analysis Conference*, 1997, p. 1053-1063.

[61] K.D. Dippery, "Methods of Reducing the Size of the Low Order Matrix Polynomial Frequency Domain Parameter Estimation Problem in Modal Analysis", *Masters Thesis*, University of Cincinnati, 1993, 219 pp.

[62] A.W. Phillips, R.J. Allemang, C.R. Pickrel, "Estimating Modal Parameters from Different Solution Sets", *Proceedings of the Sixteenth International Modal Analysis Conference*, 1998, p. 1014-1021.

[63] K.F. Alvin, L.D. Peterson, "Determination of Modal Residues and Residual Flexibility for Time-Domain System Realization", *Journal of Guidance, Control and Dynamics*, Vol. 21, No. 4, 1998, pp. 588-594.

[64] R. Bronson, **Matrix Methods : An Introduction**, Academic Press, Inc., 1970.

[65] C.W. Groetsch, J.T. King, **Matrix Methods & Applications**, Prentice Hall, 1988.

APPENDIX A

A Residue Estimation

The first stage of time and frequency domain modal parameter estimation is to produce the poles and modal participation factors from the UMPA model. The second stage of the parameter estimation process is to determine the residues, which contain the modal vector and modal scaling information. Regardless of their source (e.g., the domain or order of the UMPA model), a set of poles and participation factors can be used in the residue estimation. Although there are both time and frequency domain residue estimation algorithms, the frequency domain formulation is usually implemented because residuals can be included in the model. In this appendix, frequency domain, partial fraction FRF model residue algorithms that include a generalized residual polynomial are presented. In addition, it is shown that the residues can be determined directly from the UMPA model poles and numerator polynomial coefficients. An algorithm is developed for a single-input, single-output system, but for the general case of a multiple-input, multiple-output system, there are some mathematical restrictions and computational difficulties that have as yet not been resolved.

A.1 Residue Estimation from the Partial Fraction Model

As mentioned previously in Section 1.2, once the poles and participation factors are known, the solution of the partial fraction FRF model in Equation A-1 for the residues (A_{pqr}) is linear.

$$H_{pq}(\omega) = \sum_{r=1}^{2N} \frac{A_{pqr}}{j\omega - \lambda_r} \tag{A-1}$$

where the upper index on the summation of $2N$ implies conjugate pairs of poles, p denotes the output DOF ($1 \le p \le N_o$), q denotes the input DOF ($1 \le q \le N_i$) and r denotes the mode number ($1 \le r \le 2N$).

For the single-reference case, the summation in Equation A-1 in matrix form becomes[2]

$$H_{pq}(\omega) = \begin{bmatrix} \frac{1}{j\omega - \lambda_1} & \frac{1}{j\omega - \lambda_2} & \cdots & \frac{1}{j\omega - \lambda_{2N}} \end{bmatrix} \begin{Bmatrix} A_{pq1} \\ A_{pq2} \\ \vdots \\ A_{pq2N} \end{Bmatrix} \tag{A-2}$$

An overdetermined, least-squares solution for the residues is generated by evaluating Equation A-2 at a number of frequencies ($N_s \ge 2N$), both positive and negative for the conjugate pair poles.

$$\begin{Bmatrix} H_{pq}(\omega_1) \\ H_{pq}(\omega_2) \\ \vdots \\ H_{pq}(\omega_{N_s}) \end{Bmatrix} = \begin{bmatrix} \frac{1}{j\omega_1 - \lambda_1} & \frac{1}{j\omega_1 - \lambda_2} & \cdots & \frac{1}{j\omega_1 - \lambda_{2N}} \\ \frac{1}{j\omega_2 - \lambda_1} & \frac{1}{j\omega_2 - \lambda_2} & \cdots & \frac{1}{j\omega_2 - \lambda_{2N}} \\ \vdots & \vdots & & \vdots \\ \frac{1}{j\omega_{N_s} - \lambda_1} & \frac{1}{j\omega_{N_s} - \lambda_2} & \cdots & \frac{1}{j\omega_{N_s} - \lambda_{2N}} \end{bmatrix} \begin{Bmatrix} A_{pq1} \\ A_{pq2} \\ \vdots \\ A_{pq2N} \end{Bmatrix} \tag{A-3}$$

If a generalized residual polynomial of orders $n_l < 0$ to $n_u \geq 0$ is added to the partial fraction FRF model in Equation A-1, the residue estimation model is

$$H_{pq}(\omega) = \sum_{r=1}^{2N} \frac{A_{pqr}}{j\omega - \lambda_r} + \sum_{k=n_l}^{n_u} (j\omega)^k R_{pqk} \tag{A-4}$$

or in matrix form,

$$H_{pq}(\omega) = \begin{bmatrix} \frac{1}{j\omega - \lambda_1} & \cdots & \frac{1}{j\omega - \lambda_{2N}} & (j\omega)^{n_l} & \cdots & (j\omega)^{n_u} \end{bmatrix} \begin{Bmatrix} A_{pq1} \\ \vdots \\ A_{pq2N} \\ R_{pqn_l} \\ \vdots \\ R_{pqn_u} \end{Bmatrix} \tag{A-5}$$

and the residual coefficients ($R_{pqn_l}, \ldots, R_{pqn_u}$) are estimated along with the residues from Equation A-6.

$$\begin{Bmatrix} H_{pq}(\omega_1) \\ H_{pq}(\omega_2) \\ \vdots \\ H_{pq}(\omega_{N_s}) \end{Bmatrix} = \begin{bmatrix} \frac{1}{j\omega_1 - \lambda_1} & \cdots & \frac{1}{j\omega_1 - \lambda_{2N}} & (j\omega_1)^{n_l} & \cdots & (j\omega_1)^{n_u} \\ \frac{1}{j\omega_2 - \lambda_1} & \cdots & \frac{1}{j\omega_2 - \lambda_{2N}} & (j\omega_2)^{n_l} & \cdots & (j\omega_2)^{n_u} \\ \vdots & & \vdots & & & \vdots \\ \frac{1}{j\omega_{N_s} - \lambda_1} & \cdots & \frac{1}{j\omega_{N_s} - \lambda_{2N}} & (j\omega_{N_s})^{n_l} & \cdots & (j\omega_{N_s})^{n_u} \end{bmatrix} \begin{Bmatrix} A_{pq1} \\ \vdots \\ A_{pq2N} \\ R_{pqn_l} \\ \vdots \\ R_{pqn_u} \end{Bmatrix} \tag{A-6}$$

For the multiple-reference case, the residue (A_{pqr}) is written as the product of the modal participation factor (L_{qr}) and the modal coefficient (ψ_{pr}).[2]

$$A_{pqr} = L_{qr}\psi_{pr} \tag{A-7}$$

where, $\{\psi_p\} = \left\{ \begin{array}{ccc} \psi_{p1} & \cdots & \psi_{p2N} \end{array} \right\}$ and $[L] = \left[\begin{array}{cccc} L_{11} & L_{12} & \cdots & L_{12N} \\ L_{21} & L_{22} & \cdots & L_{22N} \\ \vdots & \vdots & & \vdots \\ L_{N_i1} & L_{N_i2} & \cdots & L_{N_i2N} \end{array} \right]$

Equation A-1 is written for the row of the FRF matrix that corresponds to output p and all the inputs as

$$\underset{(1\times N_i)}{\{H_p(\omega)\}} = \sum_{r=1}^{2N} \frac{\psi_{pr}}{j\omega - \lambda_r} \underset{(1\times N_i)}{\{L_r\}^T} \tag{A-8}$$

and the transpose of Equation A-8 in matrix from is

$$\underset{(N_i\times 1)}{\{H_p(\omega)\}^T} = \underset{(N_i\times 2N)}{[L]} \underset{(2N\times 2N)}{\left[\begin{array}{cccc} \frac{1}{j\omega - \lambda_1} & & & \\ & \frac{1}{j\omega - \lambda_2} & & \\ & & \ddots & \\ & & & \frac{1}{j\omega - \lambda_{2N}} \end{array} \right]} \underset{(2N\times 1)}{\{\psi_p\}^T} \tag{A-9}$$

Again, an overdetermined set of equations for the solution of the residues is formed by evaluating Equation A-9 at a number of frequencies and augmenting the matrices.

The multiple-reference residue model that includes a generalized residual polynomial is

$$\underset{(1\times N_i)}{\{H_p(\omega)\}} = \sum_{r=1}^{2N} \frac{\psi_{pr}}{j\omega - \lambda_r} \underset{(1\times N_i)}{\{L_r\}^T} + \sum_{k=n_l}^{n_u} (j\omega)^k \underset{(1\times N_i)}{\{R_{pk}\}} \tag{A-10}$$

or in matrix form, where I_{N_i} is an $N_i \times N_i$ identity matrix,

$$\{H_p(\omega)\}^T = \begin{bmatrix} L & I_{N_i} & \cdots & I_{N_i} \end{bmatrix} \begin{bmatrix} \frac{1}{j\omega - \lambda_1} & & & & & \\ & \ddots & & & & \\ & & \frac{1}{j\omega - \lambda_{2N}} & & & \\ & & & (j\omega)^{n_l} I_{N_i} & & \\ & & & & \ddots & \\ & & & & & (j\omega)^{n_u} I_{N_i} \end{bmatrix} \begin{Bmatrix} \{\psi_p\}^T \\ \{R_{pn_l}\}^T \\ \vdots \\ \{R_{pn_u}\}^T \end{Bmatrix} \tag{A-11}$$

A.2 Residue Estimation from the Rational Fraction Polynomial Model

The partial fraction model of Equation A-12 and the rational fraction polynomial model of Equation A-13 both represent the frequency response matrix of a system.

$$[H(\omega)] = \sum_{r=1}^{2N} \frac{[A_r]}{j\omega - \lambda_r} \tag{A-12}$$

$$[H(\omega)] = \frac{\sum_{k=0}^{m-2} (j\omega)^k [\beta_k]}{\sum_{k=0}^{m} (j\omega)^k [a_k]} \text{ , where } m \geq 2 \tag{A-13}$$

Once the residues have been estimated with the algorithms in the preceding section, FRFs can be synthesized by Equation A-12 with the estimated poles and residues. However, FRFs can also be synthesized by Equation A-13 with the $[a_k]$ and $[\beta_k]$ polynomial coefficients from the UMPA model solution, such as in Figures 3-1 through 3-6.† The poles of the UMPA model are computed from the $[a_k]$ polynomial coefficients and are then used

---

† Note that the FRFs in Figure 3-1 through 3-6 were synthesized by Equation 2-12, with the $\hat{\beta}_k$ coefficients of the numerator polynomial that contained residuals. For the equations developed in this section, the β_k coefficients of the original numerator polynomial (without residuals) must be used in the solution for the residues. The β_k coefficients can separated from $\hat{\beta}_k$ coefficients by the process outlined in Section 2.3.2.

to estimation the residues. Since the rational fraction polynomials can synthesize an FRF that replicates both its resonance and magnitude characteristics, it stands to reason that the residue information must also be contained in the $[\beta_k]$ polynomial.

To reveal the relationship between the residues and $[\beta_k]$ polynomial, first consider a single-input, single-output, single degree-of-freedom system and expand the partial fraction model as†

$$H(s) = \frac{A_1}{s-\lambda_1} + \frac{A_2}{s-\lambda_2}$$

$$= \frac{(s-\lambda_2)A_1 + (s-\lambda_1)A_2}{(s-\lambda_1)(s-\lambda_2)}$$

$$= \frac{(A_1+A_2)s - \lambda_2 A_1 - \lambda_1 A_2}{s^2 - (\lambda_1+\lambda_2)s + \lambda_1\lambda_2}$$

$$= \frac{\beta_0 + \beta_1 s}{a_2 s^2 + a_1 s + a_0} \tag{A-14}$$

which is now in the form of a rational fraction polynomial model. By equating the like terms in the third and fourth lines of Equation A-14, with $\beta_1 = 0$, and arranging into a matrix equation, the residues can be computed as

$$\begin{bmatrix} 1 & 1 \\ -\lambda_2 & -\lambda_1 \end{bmatrix} \begin{Bmatrix} A_1 \\ A_2 \end{Bmatrix} = \begin{Bmatrix} 0 \\ \beta_0 \end{Bmatrix} \tag{A-15}$$

---

† Note that the following derivations are presented in terms of the Laplace domain variable s rather than the frequency variable $j\omega$ for notational conciseness.

Equation A-15 can be further simplified by using the relations

$$\lambda_1 = \sigma_1 + j\omega_1 \,, \quad \lambda_2 = \lambda_1^* = \sigma_1 - j\omega_1 \quad \text{and} \quad A_2 = -A_1 \tag{A-16}$$

which gives the direct solution of the residue (A_1) of a SISO, SDOF system from the β_0 coefficient of the UMPA model numerator polynomial as

$$A_1 = \frac{\beta_0}{2j\omega_1} \tag{A-17}$$

This procedure can be extended to a single-input, single-output, multiple degree-of-freedom system. Next consider a 2-DOF system, the partial fraction model expands as

$$\begin{aligned} H(s) &= \sum_{r=1}^{4} \frac{A_r}{s-\lambda_r} \\ &= \frac{(s-\lambda_2)A_1 + (s-\lambda_1)A_2}{(s-\lambda_1)(s-\lambda_2)} + \frac{(s-\lambda_4)A_3 + (s-\lambda_3)A_4}{(s-\lambda_3)(s-\lambda_4)} \\ &= \frac{[(s-\lambda_2)A_1 + (s-\lambda_1)A_2](s-\lambda_3)(s-\lambda_4) + [(s-\lambda_4)A_3 + (s-\lambda_3)A_4](s-\lambda_1)(s-\lambda_2)}{(s-\lambda_1)(s-\lambda_2)(s-\lambda_3)(s-\lambda_4)} \\ &\vdots \\ &= \frac{\beta_3 s^3 + \beta_2 s^2 + \beta_1 s + \beta_0}{\alpha_4 s^4 + \alpha_3 s^3 + \alpha_2 s^2 + \alpha_1 s + \alpha_0} \end{aligned} \tag{A-18}$$

The set of poles included in the residue estimation algorithms in Section A.1 could be combined from different UMPA model solutions. The poles included in Equation A-18 must be the complete set of poles computed for the same UMPA model from which the β_k coefficients were estimated, so that the entire partial fraction and rational fraction

polynomial models can be compared. Again, equating like terms in Equation A-18, with $\beta_3 = 0$, the matrix solution is

$$\begin{bmatrix} 1 & 1 & 1 & 1 \\ -(\lambda_2+\lambda_3+\lambda_4) & -(\lambda_1+\lambda_3+\lambda_4) & -(\lambda_1+\lambda_2+\lambda_4) & -(\lambda_1+\lambda_2+\lambda_3) \\ \lambda_2\lambda_3+\lambda_2\lambda_4+\lambda_3\lambda_4 & \lambda_1\lambda_3+\lambda_1\lambda_4+\lambda_3\lambda_4 & \lambda_1\lambda_2+\lambda_1\lambda_4+\lambda_2\lambda_4 & \lambda_1\lambda_2+\lambda_1\lambda_3+\lambda_2\lambda_3 \\ -\lambda_2\lambda_3\lambda_4 & -\lambda_1\lambda_3\lambda_4 & -\lambda_1\lambda_2\lambda_4 & -\lambda_1\lambda_2\lambda_3 \end{bmatrix} \begin{Bmatrix} A_1 \\ A_2 \\ A_3 \\ A_4 \end{Bmatrix} = \begin{Bmatrix} 0 \\ \beta_2 \\ \beta_1 \\ \beta_0 \end{Bmatrix} \quad \text{(A-19)}$$

Note the pattern of the λ-terms in Equation A-19. The second row is permutations of sums of the λ's, the third row is permutations of double-products of the λ's and the fourth row is permutations of triple-products of the λ's. There is an alternating sign on the rows and for each column k, λ_k is omitted from that column. It can be shown that this pattern continues for higher DOF systems, with $\beta_{m-1} = 0$ as in Equation 2-16. Also, Equation A-19 reduces to Equation A-14 for an SDOF system if the third and fourth rows and columns are deleted and λ_3 and λ_4 are omitted.

For a multiple-input, multiple-output system, the partial fraction model expands as

$$[H(s)] = \sum_{r=1}^{mN_a} \frac{[A_r]}{s-\lambda_r}$$

$$= \frac{[A_1]}{s-\lambda_1} + \frac{[A_2]}{s-\lambda_2} + \sum_{r=3}^{mN_a} \frac{[A_r]}{s-\lambda_r}$$

$$= \frac{(s-\lambda_2)[I][A_1] + (s-\lambda_1)[I][A_2]}{(s-\lambda_1)(s-\lambda_2)} + \sum_{r=3}^{mN_a} \frac{[A_r]}{s-\lambda_r}$$

$$= \frac{([A_1]+[A_2])s - \lceil\Lambda_2\rfloor[A_1] - \lceil\Lambda_1\rfloor[A_2]}{s^2 - (\lambda_1+\lambda_2)s + \lambda_1\lambda_2} + \sum_{r=3}^{mN_a} \frac{[A_r]}{s-\lambda_r}$$

$$= \frac{\sum_{k=1}^{mN_a-1}\left[\tilde{\beta}_k\right]s^k}{characterstic\ equation} \tag{A-20}$$

where N_a is the size of the $[a_k]$ coefficient matrices and m is the order of the $[a_k]$ polynomial. The $\left[\tilde{\beta}_k\right]$ numerator polynomial coefficients in Equation A-20 are not the same as those of the UMPA model numerator because the characteristic equation is a scalar polynomial but the UMPA model denominator is a matrix polynomial. The UMPA model of Equation A-21 can be manipulated into a form comparable to that of Equation A-20, by using the formula for the inverse of a matrix, $\mathbf{A}^{-1} = \mathbf{adj}(\mathbf{A}) / \mathbf{det}(\mathbf{A})$,†

$$\left[\sum_{k=0}^{m}[a_k]s^k\right][H(s)] = \sum_{k=0}^{m-1}[\beta_k]s^k \tag{A-21}$$

or

$$[H(s)] = \left[\sum_{k=0}^{m}[a_k]s^k\right]^{-1}\sum_{k=0}^{m-1}[\beta_k]s^k$$

$$= \frac{\mathbf{adj}\left(\sum_{k=0}^{m}[a_k]s^k\right)\sum_{k=0}^{m-1}[\beta_k]s^k}{\mathbf{det}\left(\sum_{k=0}^{m}[a_k]s^k\right)}$$

$$= \frac{\sum_{k=1}^{2m-1}\left[\tilde{\beta}_k\right]s^k}{characterstic\ equation} \tag{A-22}$$

---

† The *adjoint*[64] of a matrix **A**, which is also known as the *adjugate*[65] and denoted as **adj**(**A**), is the transpose of the matrix of cofactors of **A**. The *determinate* of a matrix **A** is denoted as **det**(**A**). The *characteristic equation* of a rational fraction polynomial model is the determinate of the denominator.

The mathematical restriction mentioned in the introduction of this chapter is imposed by the upper limits of the indices on the numerator polynomials in Equation A-20, which is $mN_a - 1$, and in Equation A-22, which is $2m - 1$. These two polynomials can only be equated if $N_a = 2$, which means that this algorithm is only applicable to the special case of an UMPA model with 2×2 denominator coefficient matrices.

If the $\left[\tilde{\beta}_k\right]$ polynomial can be constructed from the $[\alpha_k]$ and $\left[\tilde{\beta}_k\right]$ polynomials, then a solution for the residues similar to Equation A-18 could be formulated for an MDOF system. However, there are computational difficulties in producing the $\left[\tilde{\beta}_k\right]$ polynomial because, in general,

$$\mathbf{adj}\left(\sum_k [\alpha_k]\right) \neq \sum_k \mathbf{adj}([\alpha_k]) \tag{A-22}$$

Thus, computing the adjoint of the $[\alpha_k]$ polynomial is unfortunately not a practically implementable solution. Coincidentally however, for a matrix polynomial with 2×2 coefficients, the adjoint of the summation does equal the summation of the adjoints, that is, the inequality in Equation A-22 becomes an equality. In this case, the adjoint of each $[\alpha_k]$ can be computed as $\mathbf{adj}(\mathbf{A}) = \mathbf{det}(\mathbf{A}) \cdot \mathbf{inv}(\mathbf{A})$ (where the $\mathbf{det}(\mathbf{A})$ is equal to the product of the eigenvalues a $\mathbf{A}$). Then $\sum_{k=0}^{m} \mathbf{adj}([\alpha_k]) s^k$ is convolved with $\sum_{k=0}^{m-1} [\beta_k] s^k$ to produce $\sum_{k=0}^{2m-1} \left[\tilde{\beta}_k\right] s^k$.

To construct an MDOF solution for the residues, the scalar λ_r terms in Equation A-19 are replaced with diagonal $\lceil \Lambda_r \rfloor$ matrices, as in Equation A-20. For the case of a high-order

UMPA model of order m, with $N_o \geq N_i$, $N_a = N_i$, $[A_r]$ is $N_i \times N_o$, $\left[\tilde{\beta}_k\right]$ is $N_i \times N_o$ and $\lceil \Lambda_r \rfloor$ is $N_i \times N_i$, Equation A-19 then becomes, for the MDOF case,

$$\underset{(2mN_i \times mN_i^2)}{\begin{bmatrix} [I_{N_i}] & \cdots & [I_{N_i}] \\ \lceil \bar{\Lambda}_1 \rfloor & \cdots & \lceil \bar{\Lambda}_{mN_i} \rfloor \\ \lceil \bar{\Lambda}_1 \rfloor^2 & \cdots & \lceil \bar{\Lambda}_{mN_i} \rfloor^2 \\ \vdots & & \vdots \\ \lceil \bar{\Lambda}_1 \rfloor^{2m-1} & \cdots & \lceil \bar{\Lambda}_{mN_i} \rfloor^{2m-1} \end{bmatrix}} \underset{(mN_i^2 \times N_o)}{\begin{Bmatrix} [A_1] \\ \vdots \\ [A_{mN_i}] \end{Bmatrix}} = \underset{(2mN_i \times N_o)}{\begin{Bmatrix} \left[\tilde{\beta}_{2m-1}\right] \\ \left[\tilde{\beta}_{2m-2}\right] \\ \left[\tilde{\beta}_{2m-3}\right] \\ \vdots \\ \left[\tilde{\beta}_0\right] \end{Bmatrix}} \tag{A-24}$$

where $\left[\tilde{\beta}_{2m-1}\right] = [0]$ and $\lceil \bar{\Lambda}_i \rfloor^k$ is a diagonal matrix of permutations of products of the poles with the pattern in Equation A-19. This 2×2 curiosity appears here again in that the matrix in Equation A-24 is square, and invertible, only if $2mN_i = mN_i^2$, or $N_i = 2$.

Equation A-24 can also be written in terms of the modal vectors and participation factors as

$$\underset{(2mN_i \times mN_i^2)}{\begin{bmatrix} [I_{N_i}] & \cdots & [I_{N_i}] \\ \lceil \bar{\Lambda}_1 \rfloor & \cdots & \lceil \bar{\Lambda}_{mN_i} \rfloor \\ \lceil \bar{\Lambda}_1 \rfloor^2 & \cdots & \lceil \bar{\Lambda}_{mN_i} \rfloor^2 \\ \vdots & & \vdots \\ \lceil \bar{\Lambda}_1 \rfloor^{2m-1} & \cdots & \lceil \bar{\Lambda}_1 \rfloor^{2m-1} \end{bmatrix}} \underset{(mN_i^2 \times mN_i)}{\begin{bmatrix} \{L_1\} & & \\ & \ddots & \\ & & \{L_{mN_i}\} \end{bmatrix}} \underset{(mN_i \times N_o)}{\begin{Bmatrix} \{\psi_1\}^T \\ \vdots \\ \{\psi_{mN_i}\}^T \end{Bmatrix}} = \underset{(2mN_i \times N_o)}{\begin{Bmatrix} \left[\tilde{\beta}_{2m-1}\right] \\ \left[\tilde{\beta}_{2m-2}\right] \\ \left[\tilde{\beta}_{2m-3}\right] \\ \vdots \\ \left[\tilde{\beta}_0\right] \end{Bmatrix}} \tag{A-25}$$

$$\text{where , } \quad [A_r] = \{L_r\}\{\psi_r\}^T, \quad \{L_r\} = \begin{Bmatrix} L_{1r} \\ \vdots \\ L_{N_i r} \end{Bmatrix}, \quad \{\psi_r\} = \begin{Bmatrix} \psi_{1r} \\ \vdots \\ \psi_{N_o r} \end{Bmatrix} \tag{A-26}$$

and

$$\underset{(mN_i^2 \times N_o)}{\begin{Bmatrix} [A_1] \\ \vdots \\ [A_{mN_i}] \end{Bmatrix}} = \underset{(mN_i^2 \times N_o)}{\begin{Bmatrix} \{L_1\}\{\psi_1\}^T \\ \vdots \\ \{L_{mN_i}\}\{\psi_{mN_i}\}^T \end{Bmatrix}} = \underset{(mN_i^2 \times mN_i)}{\begin{bmatrix} \{L_1\} & & \\ & \ddots & \\ & & \{L_{mN_i}\} \end{bmatrix}} \underset{(mN_i \times N_o)}{\begin{Bmatrix} \{\psi_1\}^T \\ \vdots \\ \{\psi_{mN_i}\}^T \end{Bmatrix}} \tag{A-27}$$

A.3 Residue Estimation with Scaled Frequency

Frequency scaling is necessary in the implementation of frequency domain modal parameter estimation algorithms for better numerical conditioning of the UMPA model solution.[3] Scaled frequency and poles should also be used in the partial fraction model residue estimation algorithms of Section A-1, especially when a generalized residual polynomial is included in the model. Scaled poles should also be used in the rational fraction polynomial residue estimation algorithms of Section A-2 because of the multiple products of poles in Equation A-19, A-24 and A-25.

If the frequency ω, or equivalently the Laplace variable s, is scaled by $\bar{\omega}$, such that

$$\omega' = \frac{\omega}{\bar{\omega}} \quad \text{or} \quad s' = \frac{s}{\bar{\omega}}, \tag{A-28}$$

where the tick ($'$) notation denotes a parameter associated with the scaled-frequency domain, the relationship between the original and scaled-frequency domains is

$$H(s) = \sum_r \frac{A_r}{s - \lambda_r} = \sum_r \frac{A_r}{\bar{\omega}s' - \lambda_r} = \sum_r \frac{\frac{A_r}{\bar{\omega}}}{s' - \frac{\lambda_r}{\bar{\omega}}} = \sum_r \frac{A_r'}{s' - \lambda_r'} = H(s') \tag{A-29}$$

The true system pole (λ_r) is related to the pole estimated with scaled frequency (λ_r') by

$$\lambda_r = \bar{\omega}\lambda_r' \tag{A-30}$$

and the true residue (A_r) is related to the estimated residue (A_r') by

$$A_r = \bar{\omega}A_r' \tag{A-31}$$

APPENDIX B

B Polynomial Curve-Fit Plots

The plots in this appendix are associated with Figures 2-4 through 2-10, as noted in the figure captions. The shaded region in the plots indicates the segment of the data that was used in Equation 2-2 to estimate the polynomial coefficients. The magnitude is plotted in the (a) figures, the phase is plotted in the (b) figures, the real part is plotted in the (d) figures and the imaginary part is plotted in the (e) figures. The (f) figures are Nyquist (i.e., real vs. imaginary) plots, the inset plot shows the region near the estimation interval. The magnitude of the polynomial coefficients are plotted in the (c) figures.

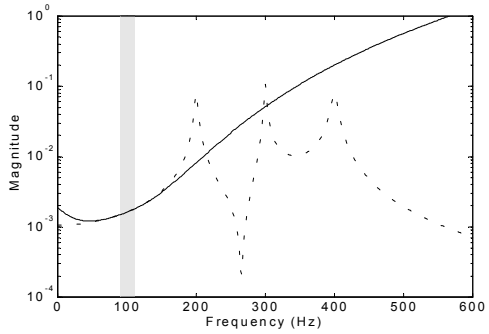

(a) Magnitude

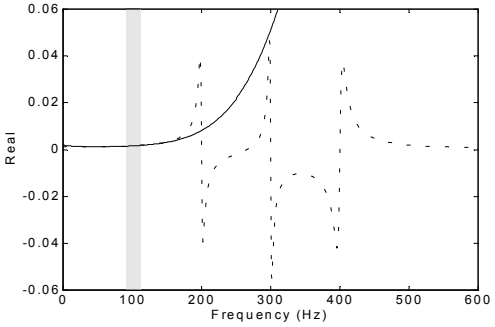

(d) Real Part

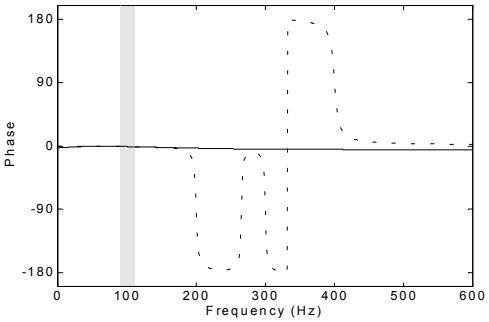

(b) Phase

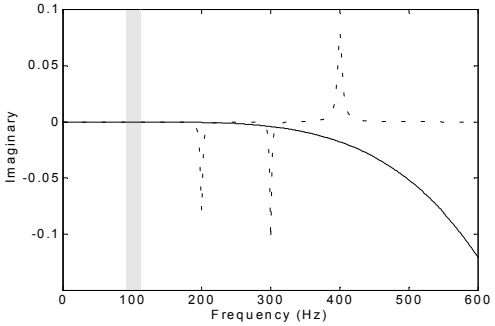

(e) Imaginary Part

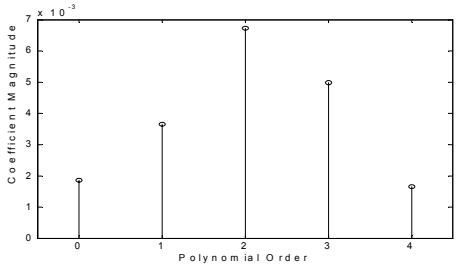

(c) Polynomial Coefficients

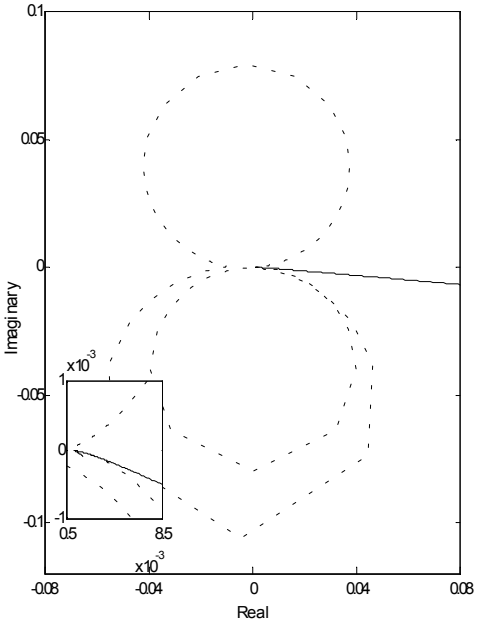

(f) Nyquist

Figure B-1. *Polynomial curve-fit with orders 0:4 of the upper residual segment of an FRF away from resonance, ref. Figure 2-4.*

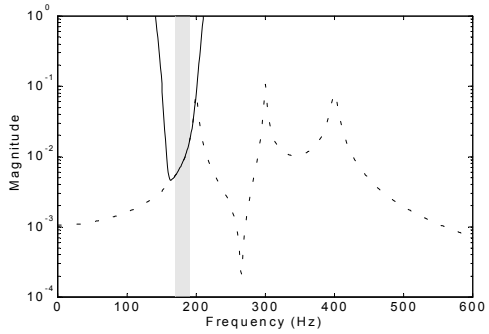

(a) Magnitude

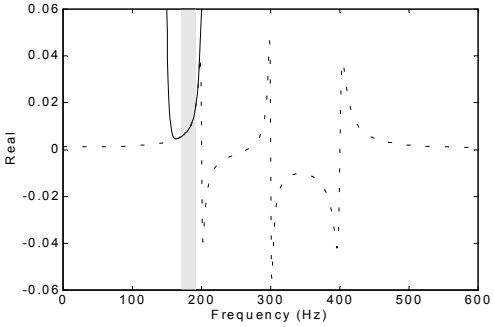

(d) Real Part

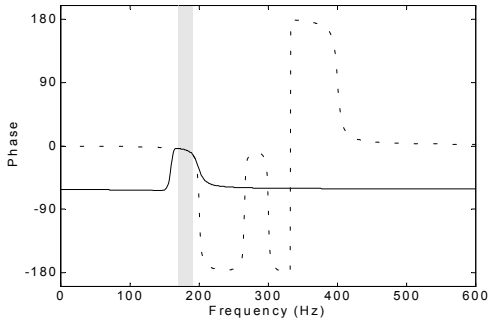

(b) Phase

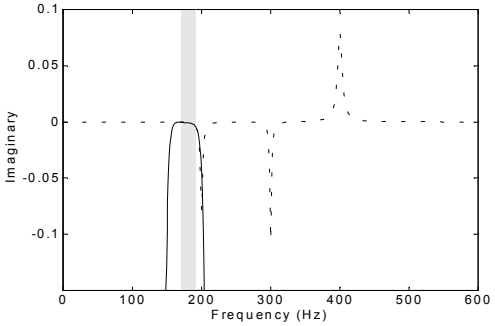

(e) Imaginary Part

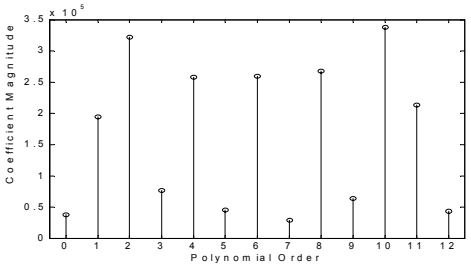

(c) Polynomial Coefficients

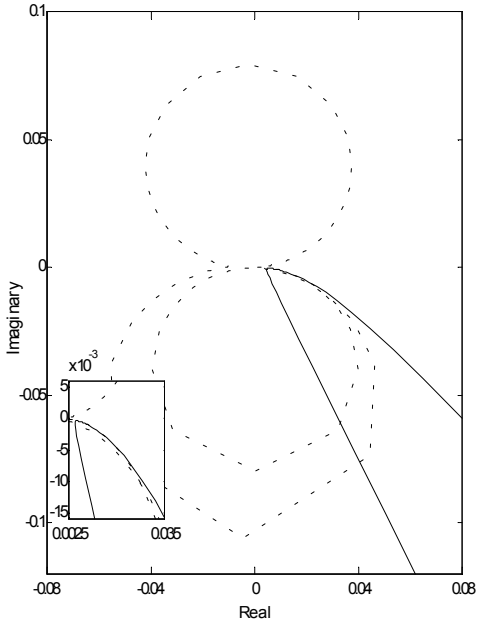

(f) Nyquist

Figure B-2. *Polynomial curve-fit with orders 0:12 of the upper residual segment of an FRF near resonance, ref. Figure 2-5.*

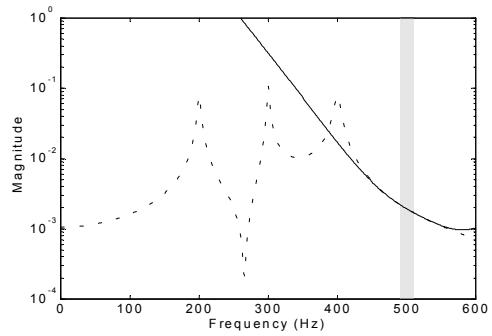

(a) Magnitude

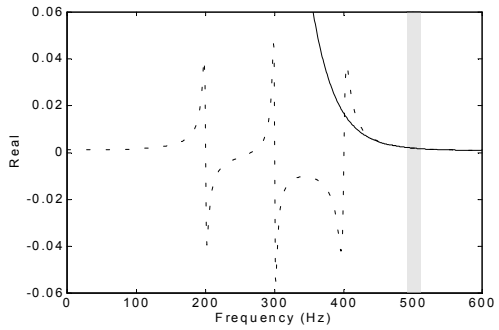

(d) Real Part

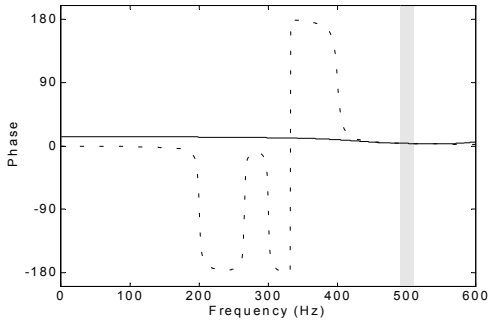

(b) Phase

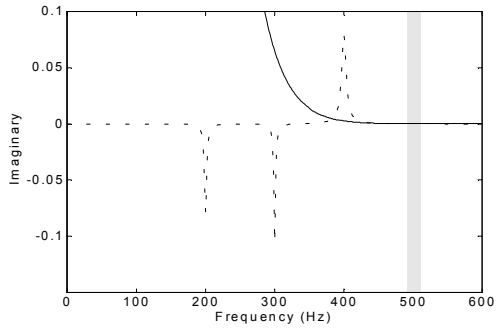

(e) Imaginary Part

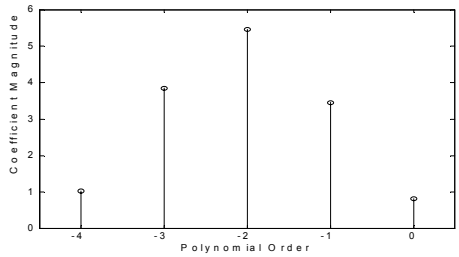

(c) Polynomial Coefficients

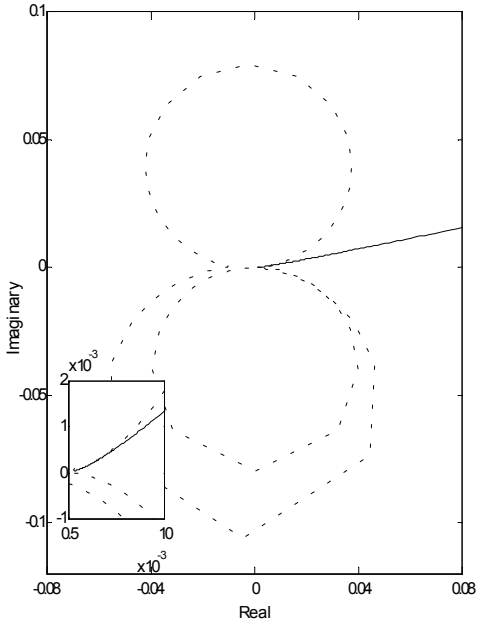

(f) Nyquist

Figure B-3. *Polynomial curve-fit with orders -4:0 of the lower residual segment of an FRF away from resonance, ref. Figure 2-6.*

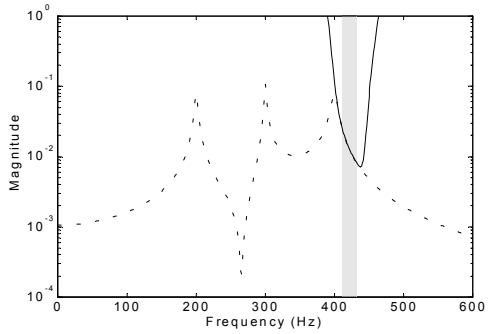

(a) Magnitude

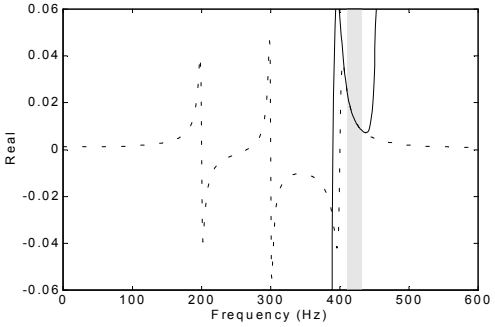

(d) Real Part

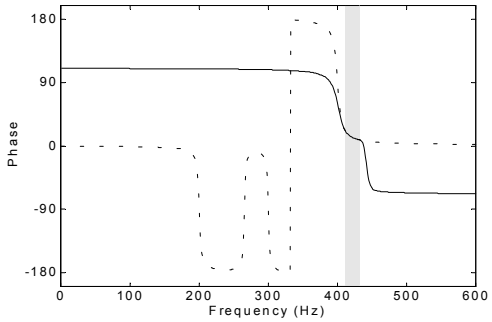

(b) Phase

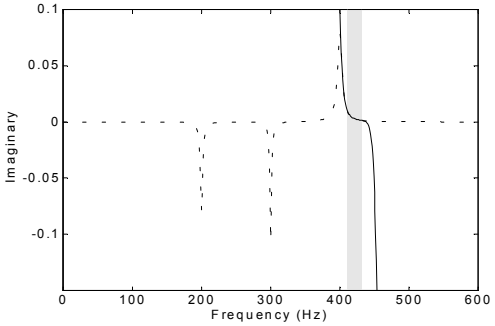

(e) Imaginary Part

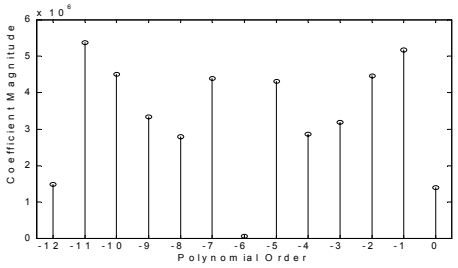

(c) Polynomial Coefficients

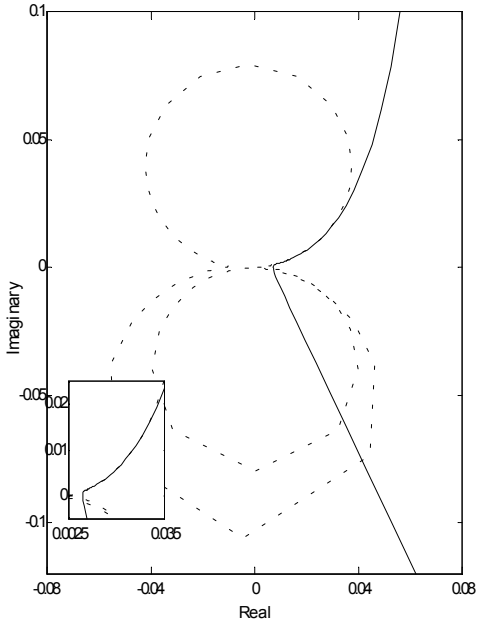

(f) Nyquist

Figure B-4. *Polynomial curve-fit with orders -12:0 of the lower residual segment of an FRF near resonance, ref. Figure 2-7.*

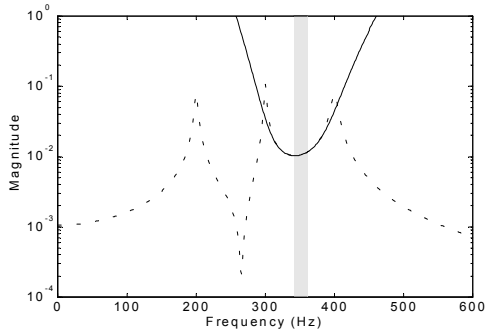

(a) Magnitude

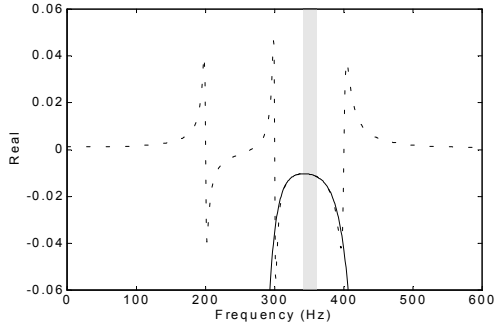

(d) Real Part

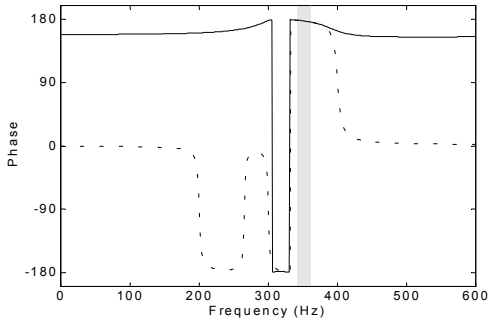

(b) Phase

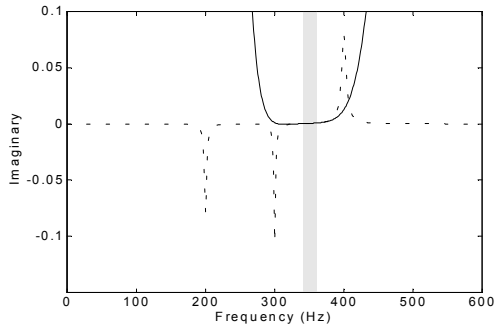

(e) Imaginary Part

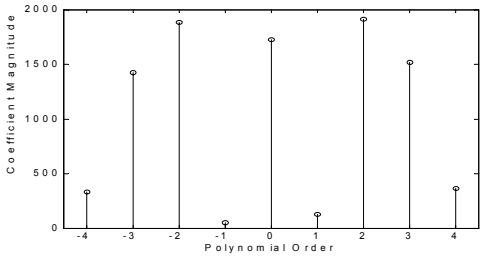

(c) Polynomial Coefficients

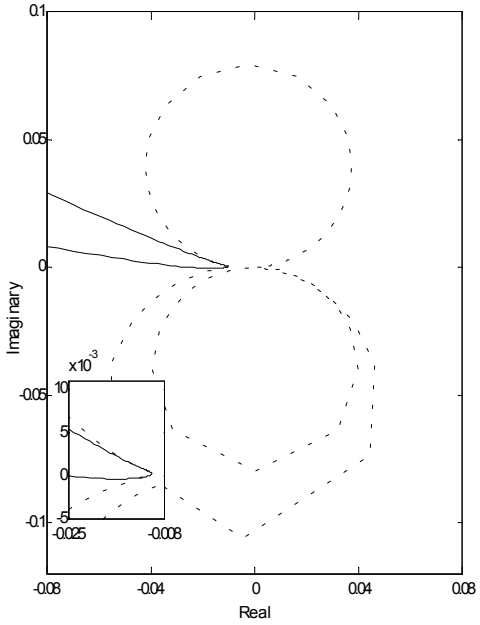

(f) Nyquist

Figure B-5. *Polynomial curve-fit with orders -4:4 of the FRF segment between two resonances without an antiresonance, ref. Figure 2-8.*

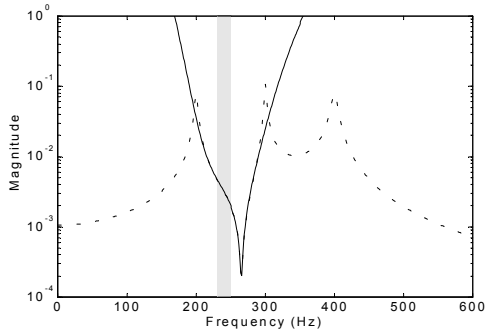

(a) Magnitude

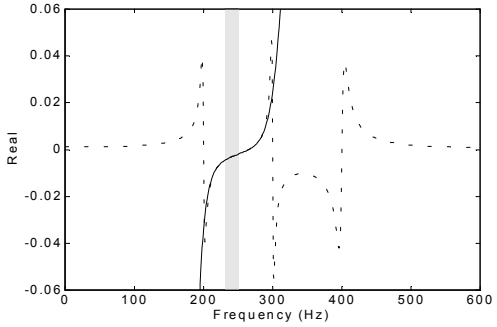

(d) Real Part

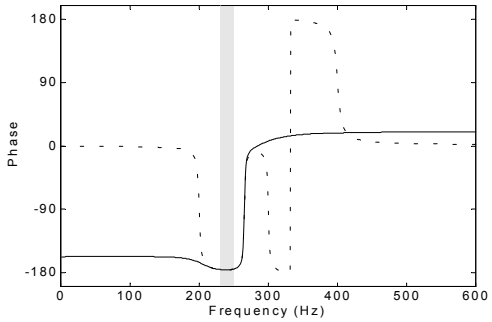

(b) Phase

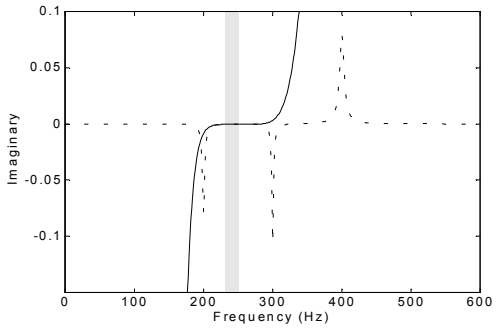

(e) Imaginary Part

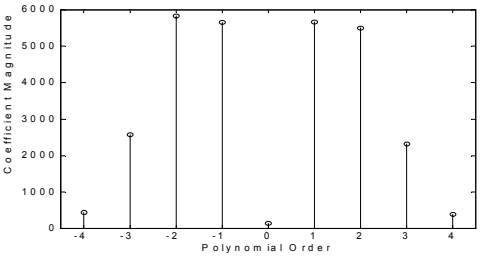

(c) Polynomial Coefficients

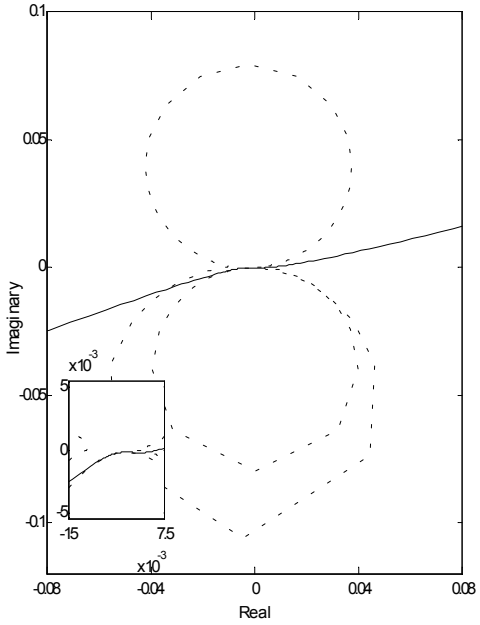

(f) Nyquist

Figure B-6. *Polynomial curve-fit with orders -4:4 of the FRF segment between two resonances with an antiresonance, ref. Figure 2-9.*

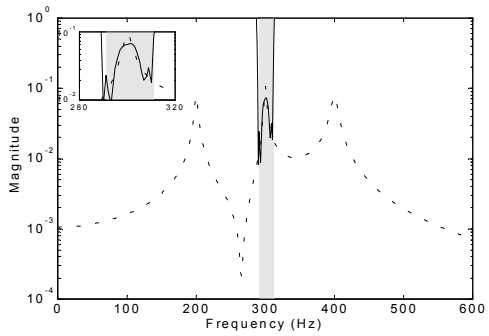

(a) Magnitude

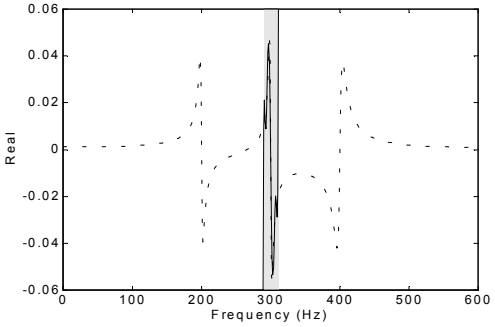

(d) Real Part

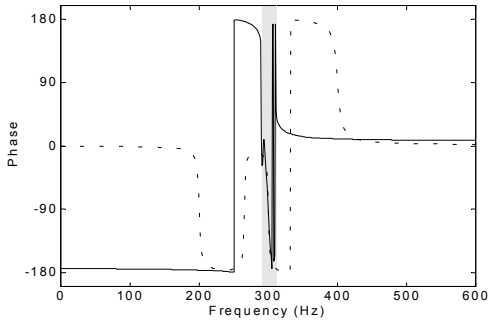

(b) Phase

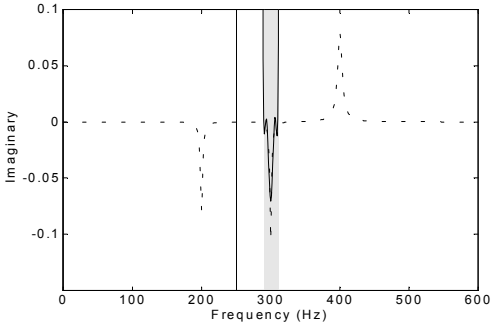

(e) Imaginary Part

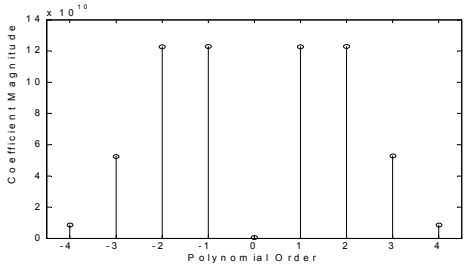

(c) Polynomial Coefficients

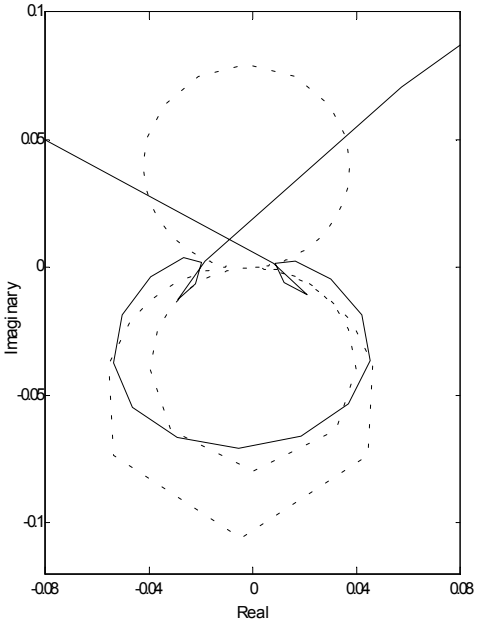

(f) Nyquist

Figure B-7. *Polynomial curve-fit with orders -4:4 of an FRF segment at a resonance, ref. Figure 2-10.*

APPENDIX C

C MATLAB Functions

Listed in this appendix are several Matlab functions that implement some of the algorithms presented in this dissertation or were used to produce some of the figures.

synth_siso_frf.m

This function synthesizes a SISO, MDOF FRF from the partial fraction model.

$$H(\omega) = \sum_{r=1}^{N} \left(\frac{A_r}{j\omega - \lambda_r} + \frac{A_r^*}{j\omega - \lambda_r^*} \right) \tag{C-1}$$

fd is an $N \times 1$ array of damped natural frequencies, in Hertz.
zeta is an $N \times 1$ array of damping ratios, $0 \le \zeta \le 1$.
A is an $N \times 1$ array of residues.
freq is an $1 \times N_s$ array of the frequency variable, in Hertz.
H is an $N+1 \times N_s$ array of the synthesized FRFs. Rows $1{:}N$ contain the FRFs of each SDOF mode and row N contains the summation of rows $1{:}N$.

```
function H = synth_siso_frf(fd,zeta,A,freq)

omegad = 2*pi*fd;   % damped natural frequency (rad/sec),  ωd = 2πfd
sigma  = -zeta.*omegad./sqrt(1-zeta.^2); % damping factor, σ = -ζωd/√(1-ζ²)
lambda = sigma+j*omegad;   % pole, λ = σ + jωd
w  = 2*pi*freq(:).';       % frequency variable (rad/sec)
N  = length(lambda);       % number of modes
Ns = length(freq);         % number of spectral lines
H  = zeros(N+1,Ns);        % allocate FRF array

% evaluate Equation C-1 for each SDOF mode
for rr=1:N
   H(rr,:) = A(rr)./(j*w-lambda(rr)) + A(rr)'./(j*w-lambda(rr)');
end
H(end,:) = sum(H);   % the last row is the summation of the SDOF modes
```

umpa_sdof.m

This function solves the SDOF UMPA model with generalized residuals

$$[j\omega a_1 + a_o]H(\omega) - \sum_{k=n_l}^{n_u+2} (j\omega)^k \hat{\beta}_k = -(j\omega)^2 H(\omega) \tag{C-2}$$

H is a $1 \times N_s$ frequency response function.
w is a $1 \times N_s$ array of the scaled frequency.
Border is the array of numerator polynomial orders, $(n_l, \ldots, n_u + 2)$.
A is the array of denominator coefficients, $\begin{bmatrix} a_1 & a_0 \end{bmatrix}$.
B is the array of numerator coefficients, $\begin{bmatrix} \beta_{n_l} & \cdots & \beta_{n_u+2} \end{bmatrix}$.
RCOND is the reciprocal of the condition number of the UMPA model solution.

```
function [A,B,RCOND] = umpa_sdof(H,w,Border)

Ns = length(w);          % number of spectral lines
NB = length(Border);     % number of numerator polynomial orders
w  = [w,-w];             % positive and negative frequencies for conjugate poles
H  = [H,conj(H)];        % positive and negative frequency FRF
HW = zeros(2*Ns,NB+2);   % allocate matrix
Bscale = max(H).^2;      % numerator polynomial coefficient scaling

for kk = 1:2*Ns
   HW(kk,1:2  ) = [ j*w(kk),1]*H(kk);          % left-hand side α-terms
   HW(kk,3:end) = -(j*w(kk)).^Border*Bscale; % left-hand side β-terms
end
w2H = [w.*w.*H].';  % right-hand side of Equation C-2

AB = pinv(HW)*w2H;         % pseudo-inverse solution
A = AB(1:2).';             % denominator polynomial coefficients
B = Bscale*AB(3:end).';    % numerator polynomial coefficient, corrected for scaling

RCOND = 1/cond(HW);  % reciprocal of condition number of pseudo-inverse solution
```

synth_siso_ab.m

This function synthesizes an SISO, MDOF FRF from the UMPA model numerator and denominator polynomial coefficients.

$$H(\omega) = \frac{\sum_{k=n_l}^{n_u+2} (j\omega)^k \hat{\beta}_k}{\sum_{k=0}^{2} \left[(j\omega)^k a_k \right]} \tag{C-3}$$

A is the array denominator coefficients, $\left[\begin{array}{cccc} a_{m-1} & \cdots & a_1 & a_0 \end{array} \right]$, $a_m = 1$.
B is the array numerator coefficients, $\left[\begin{array}{ccc} \beta_{n_l} & \cdots & \beta_{n_u+2} \end{array} \right]$.
w is a $1 \times N_s$ array of the scaled frequency.
Border is the array of numerator polynomial orders, $(n_l, \ldots, n_u + 2)$.
Hw is a $1 \times N_s$ frequency response function.
Aw is an $m + 1 \times N_s$ array of denominator polynomial functions.
Bw is an $n_u + n_l + 3 \times N_s$ array of numerator polynomial functions.

```
function [Hw,Aw,Bw] = synth_siso_ab(A,B,w,Border)

Ns = length(w);    % number of spectral lines
NA = length(A);    % number of denominator polynomial orders
NB = length(B);    % number of numerator polynomial orders

Aw = zeros(NA+1,Ns); mm=0;      % allocate denominator matrix, initialize index
Bw = zeros(NB  ,Ns); nn=0;      % allocate numerator matrix, initialize index

Aw(1,:) = (j*w).^NA;                    % evaluate a_m = 1 term
for kk=NA-1:-1:0, mm=mm+1;
   Aw(mm+1,:) = (j*w).^kk*A(mm);        % evaluate denominator of Equation C-3
end

for kk=Border, nn=nn+1;
   Bw(nn,:) = (j*w).^kk*B(nn);          % evaluate numerator of Equation C-3
end

Hw = sum(Bw)./sum(Aw);          % divide Equation C-3 numerator by denominator
```

synth_siso_r.m

This function synthesizes a SISO generalized residual polynomial.

$$R(\omega) = \sum_k (j\omega)^k R_k \tag{C-4}$$

R is the array numerator residual coefficients, $\begin{bmatrix} R_{n_l} & \cdots & R_{n_u} \end{bmatrix}$.
w is a $1 \times N_s$ array of the scaled frequency.
Rorder is the array of residual polynomial orders, $(n_l, \ldots, n_u)$.
Rw is an $n_u + n_l + 1$ array of residual polynomial functions.

```
function Rw = synth_siso_r(R,w,Rorder)

Ns = length(w);          % number of spectral lines
NR = length(Rorder);     % number of generalized residual polynomial orders
Rw = zeros(NR,Ns);       % allocate generalized residual matrix
nn = 0;                  % initialize index

for kk=Rorder, nn=nn+1;
   Rw(nn,:) = (j*w).^kk*R(nn);   % evaluate Equation C-4 for each polynomial order
end
```

fit_siso_r.m

This function fits the generalized residual polynomial to an SISO FRF.

$$H(\omega) = \sum_k (j\omega)^k R_k \tag{C-5}$$

H is a $1 \times N_s$ frequency response function.
w is a $1 \times N_s$ array of the scaled frequency.
Rorder is an array of residual polynomial orders, $(n_l, \ldots, n_u)$.
R is the array of residual polynomial coefficients, $\begin{bmatrix} R_{n_l} & \cdots & R_{n_u} \end{bmatrix}$.

```
function R = fit_siso_r(H,w,Rorder)

Ns = length(w);          % number of spectral lines
NR = length(Rorder);     % number of generalized residual polynomial orders
WR = zeros(Ns,NR);       % allocate matrix

for kk=1:NR
   WR(:,kk) = (j*w(:)).^Rorder(kk);   % right-hand side of Equation C-5
end

R = pinv(WR)*H.';   % pseudo-inverse solution
```

numer_poly_orders.m

This function convolves the denominator polynomial (α_k) orders and the residual polynomial (R_k) orders and combines with the numerator polynomial (β_k) orders to form the numerator polynomial with residuals ($\hat{\beta}_k$) orders.

$$\sum_k (j\omega)^k \left[\hat{\beta}_k\right] = \sum_{k=0}^{m-2} (j\omega)^k [\beta_k] + \sum_{k=0}^{m} (j\omega)^k [\alpha_k] \sum_k (j\omega)^k [R_k] \tag{C-6}$$

A is an array of denominator polynomial orders, $[0, \ldots, m]$
R is an array of residual polynomial orders
B is an array of numerator polynomial with residuals orders

```
function B = numer_poly_orders(A,R)

if isempty(R)
   B = [0:max(A)-2]; return  % no residuals
end

CA = ismember([min(A):max(A)],sort(A));   % index of denominator polynomial orders
CR = ismember([min(R):max(R)],sort(R));   % index of residual polynomial orders

B = find(conv(CA,CR))+(min(A)+min(R))-1; % convolve α_k and R_k
B = unique([B,[0:max(A)-2]]);            % combine with β_k
```

deconv_numer.m

This function deconvolves the UMPA model numerator polynomial coefficients ($\hat{\beta}_k$) into the original numerator polynomial coefficients (β_k) and the generalized residual polynomial coefficients (R_k), as in Equation 2-17.

A is an array of denominator polynomial coefficients, $[a_o, \ldots, a_m]$.
Bhat is an array of the UMPA model numerator polynomial coefficients, $\left[\hat{\beta}_{n_l}, \ldots, \hat{\beta}_{n_u+m}\right]$.
Bhatorder is an array of numerator polynomial with residuals orders , $(n_l, \ldots, n_u + m)$.
Rorder is an array of residual polynomial orders, $(n_l, \ldots, n_u)$.
R is an array of residual polynomial coefficients, $[R_{n_l}, \ldots, R_{n_u}]$.
B is an array of original numerator polynomial coefficients, $[\beta_0, \ldots, \beta_{m-1}]$.

```
function [R,B] = deconv_numer(A,Bhat,Bhatorder,Rorder)

NR = length(Rorder);   % number of generalized residual polynomial orders
if(NR==0)
   R = []; B = [Bhat;0]; return  % no residuals, βk = β̂k with βm−1 = 0
end

M  = length(A)-1;             % denominator polynomial order
AA = zeros(length(Bhat));     % allocate matrix

for kk=1:size(AA,1)-M
   AA(kk+[0:M],kk) = A(:);    % fill first nu − nl + 1 columns
end

bb = 0;
for kk=size(AA,1)-M+1:size(AA,1)
   AA(find(Border==bb),kk) = 1;   % fill last m columns
   bb = bb+1;
end

RB = AA\Bhat(:);      % pseudo-inverse solution
R  = RB(1:NR);        % residual polynomial coefficients
B  = RB(NR+1:end);    % original numerator polynomial coefficients
```

lambda_combo_prods.m

This function evaluates permutations of multiple-products of λ's to fill the rows of a matrix of the form in Equation A-19, from which the residues can be determined from the rational fraction polynomial model. Note that because of restrictions of the **nchoosek** function, this implementation is only usable for cases with less than sixteen λ's.

S is an array of λ's.
N is the number of the row.

```
function A = lambda_combo_prod(S,N)

A = zeros(size(S));  % allocate row

for kk=1:length(A)   % fill row column by column
   idx = [1:length(S)];
   idx(kk) = [];              % remove k^th pole for permutations
   idx = nchoosek(idx,N-1);   % all combinations of λ's
   for nn=1:size(idx,1)
      A(kk) = A(kk)+prod(S(idx(nn,:)));   % sum multiple-products of λ's
  end
end

A = (-1)^(N-1)*A;   % alternating sign on the row
```